AN EXPERIMENTAL
INVESTIGATION OF LARGE-
AMPLITUDE WAVE...

W. Liddell, Jr., 1973

DTIC
ELECTE
NOV 2 7 1995
F

19951121 024

This is an authorized facsimile and was produced
by microfilm-xerography in 1974 by Xerox University
Microfilms, Ann Arbor, Michigan, U.S.A.

74-5474

LIDDELL, Jr., Will Lithgow, 1937-
AN EXPERIMENTAL INVESTIGATION OF LARGE-
AMPLITUDE WAVE PROPAGATION AND DYNAMIC ELASTIC
PROPERTIES IN LONGITUDINALLY-IMPACTED
POLYCARBONATE RODS.

North Carolina State University at Raleigh,
Ph.D., 1973
Engineering Mechanics

University Microfilms, A XEROX Company, Ann Arbor, Michigan

Accesion For		
NTIS CRA&I	☑	
DTIC TAB	☐	
Unannounced	☐	
Justification		
By ADD 423227		
Distribution /		
Availability Codes		
Dist	Avail and / or Special	
A-1		

AN EXPERIMENTAL INVESTIGATION OF LARGE-AMPLITUDE WAVE PROPAGATION

AND DYNAMIC ELASTIC PROPERTIES IN LONGITUDINALLY-IMPACTED

POLYCARBONATE RODS

by

WILL LITHGOW LIDDELL, JR.
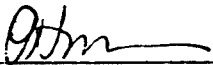
A thesis submitted to the Graduate Faculty of
North Carolina State University at Raleigh
in partial fulfillment of the
requirements for the Degree of
Doctor of Philosophy

DEPARTMENT OF ENGINEERING MECHANICS

RALEIGH

1 9 7 3

APPROVED BY:

Co-Chairman of Advisory Committee   Co-Chairman of Advisory Committee

BIOGRAPHY

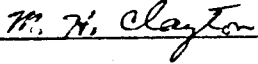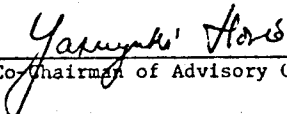Will L. Liddell, Jr., son of Will and Viola Liddell, was born February 21, 1937, in Camden, Alabama. He received his elementary and secondary education in Camden, graduating from Wilcox County High School in 1955.

He entered Auburn University in 1955, receiving the Bachelor of Science degree with Honor in Mechanical Engineering in 1959, and the Master of Science in Mechanical Engineering in 1963.

From 1959 to 1963, he was a teaching assistant in the Mechanical Engineering Department at Auburn University, approximately three years of which were on full-time appointment.

From 1963 to 1964, he was an Instructor in the Engineering Mechanics Department at Louisiana State University.

From 1964 to 1966, he was an Assistant Professor in the Mechanical Engineering Department at Auburn University.

In 1966, he was awarded a fourteen-month National Science Foundation Science Faculty Fellowship for study in the Department of Engineering Mechanics at North Carolina State University at Raleigh. From 1968 to 1971, he was a research assistant on Project Themis in that department. In 1971, he was appointed Instructor in the Department of Engineering Mechanics, in which he has been teaching since that time.

He is married to the former Mary Ethel Carr of Dothan, Alabama. They have one daughter, Mary Elizabeth.

ACKNOWLEDGMENTS

TABLE OF CONTENTS

TABLE OF CONTENTS (continued)

LIST OF TABLES

LIST OF TABLES (continued)

LIST OF FIGURES

Page

<u>Text</u>

LIST OF FIGURES (continued)

LIST OF FIGURES (continued)

1 INTRODUCTION

1.1 Motivation for and Synopsis of the Investigation

Engineering materials have long been known to exhibit marked differences in their mechanical behavior under conditions of impact and high rates of loading as compared to their behavior under quasi-static loading conditions. Thus, the proper utilization of these materials in dynamic environments requires a knowledge of their behavior under dynamic conditions.

Lexan, a polycarbonate material developed by the General Electric Company, is becoming widely employed where high impact resistance is required. Lexan's applications range from baby bottles to astronaut helmets; thus, its mechanical properties - quasi-static as well as dynamic - are of considerable interest in design. In another application, Lexan is being employed as a photoelastoplastic material in experimental studies. In all these static and quasi-static studies, easily-determined material constants such as Young's modulus and Poisson's ratio must be known; under dynamic conditions, those quantities no longer may be considered constants and must be determined as functions of stress, strain, strain rate, etc., so that experimental data can be correctly interpreted. There is a relative abundance of information in the literature concerning the quasi-static properties of polycarbonates as a class or of Lexan in particular, but little information concerning the behavior or properties of Lexan under dynamic loading conditions. This investigation is undertaken to add to the information concerning the dynamic behavior and dynamic properties of Lexan.

The matters concerning the dynamic mechanical behavior of Lexan which motivate this investigation and the manner in which they are addressed are discussed below; other matters concerning its dynamic behavior are left unanswered and are offered as possibilities for future investigation. The matters of major importance which are considered are:

1. At least one group of investigators (30) has obtained stress-strain curves for Lexan at strain rates ranging up to 0.2 min^{-1}. These curves show higher stresses for given strains on curves run at the higher strain rates, even for these very, very low rates of loading. In dynamic situations, where strain rates 10^6 times higher may be encountered, no valid constitutive relationship is known. In this investigation, a constitutive relationship will be developed for strains up to approximately 7 percent at strain rates on the order of 300 sec^{-1} to 2000 sec^{-1}. This will be accomplished by subjecting Lexan rods to high-speed axial impact. During propagation of the resulting large-amplitude strain waves, data will be recorded which will enable the strain wave speeds to be determined. The constitutive relationship will be developed using this wave speed data and results of von Karman's rate-independent theory of one-dimensional wave propagation in rods (65).

2. Preliminary studies using approximate strain wave speed data for Lexan indicated that it might be possible to use an approximate procedure to predict fairly accurately the propagation of large-amplitude strain waves along Lexan rods. This procedure uses the strain-time history at some point in the rod as input data and assumes strain level superposition and constant strain wave speeds. In this investigation, accurate strain wave speed data will be

experimentally determined and will be used to predict strain-time histories during large-amplitude strain wave propagation in situations which involve wave reflection from both free and fixed boundaries. These predicted strain-time histories will be compared to experimentally-observed histories to verify or disprove the validity of the procedure.

3. The variation in Poisson's ratio with strain and strain rate must be known to correctly interpret data from photoelastoplastic investigations. Such information is also useful in other static and dynamic applications. The known and reported variations of Poisson's ratio with strain for Lexan differ widely (16, 30), and are for quasi-static situations. In this investigation, the relation between Poisson's ratio and strain for Lexan will be determined for strains up to approximately 7 percent at strain rates on the order of 300 sec^{-1} to 2000 sec^{-1}. This relation will be determined using a procedure employed by Bell (5, 6) which utilizes the strain-time histories, the surface rotation-time histories, and the strain wave speeds in rods subjected to axial impact.

Matters of lesser importance which are considered are:

4. In an earlier series of tests in which Lexan rods were subjected to high-speed axial impact (48), the strain wave speeds were observed to be much higher than the wave speeds predicted by calculations based on quasi-static material properties. This suggested that the material properties are considerably different under static and dynamic conditions. In this investigation, Young's modulus and Poisson's ratio will be determined at strain rates on

the order of 300 sec^{-1} to 2000 sec^{-1} by using the experimentally-determined dilatational and rod wave speeds and the appropriate equations of linear elasticity.

5. Lexan is often employed in situations where the material is subjected to repeated impacts; thus, the effect of repeated elastic impacts on its dynamic behavior is of interest in design. In this investigation, this effect will be investigated by subjecting previously-impacted specimens to a second impact under essentially identical conditions. The strain-time behavior observed during the two impacts - which produce elastic compressive strains above 8 percent - will be compared to determine the effect - if any - of repeated elastic impact.

6. In previous tests which utilized Lexan rods subjected to axial impact, it was observed that some rods exhibited elastic behavior at impact velocities which should have produced - based on quasi-static material behavior - permanent plastic deformation in the rods. In this investigation, the yield point strain in Lexan subjected to compressive short-duration (approximately 120 μsec) loading-unloading pulses will be determined by subjecting Lexan rods to axial impacts at impact velocities which increase until permanent plastic deformation results. The maximum strain suffered by the material will be determined from a strain-time history recorded during the impact, while the permanent plastic strain will be determined from post-test measurements.

The experimental investigation to resolve the matters just discussed is carried out by subjecting Lexan rods to high-velocity axial impact. During propagation of the resulting large-amplitude strain waves in the

rods, high-speed streak cameras record axial surface strain-dependent
and surface rotation-dependent diffraction patterns from in-surface
diffraction grating strain transducers which are illuminated by a pulsed
ruby laser. To interpret this recorded diffraction data, diffraction-
strain relationships are developed and utilized to compute axial surface
strain-time and surface rotation-time histories at various locations
along the rods. The experimental data obtained in these tests are
analyzed to resolve the matters just discussed concerning the dynamic
mechanical behavior of Lexan. The results of this analysis are discussed
in detail in Chapter 4, and are summarized in Section 4.10.

1.2   Review of the Literature Concerning Mechanical Properties of Lexan

There is a relative abundance of information in the literature
concerning the quasi-static properties of polycarbonates as a class or
of Lexan in particular, but little information concerning the behavior
or properties under dynamic loading conditions. Some of this literature
is discussed in the following paragraphs.

Various investigators have reported quasi-static mechanical
properties of polycarbonates as a class or of Lexan in particular.
Christopher and Fox (21) describe the chemistry, application
characterization, and fabrication of polycarbonate. Gurtman *et al.*
(30) investigated Lexan in order to characterize it for use as a
photoplastic material. They report - among other things - creep and
relaxation data, tensile stress-strain curves run at various load rates
and strain rates from "static" to 50 lb/min and 0.2 min^{-1}, respectively,
and the variation of Poisson's ratio with strain. From their tests,
they develop a stress-strain-strain rate relation and a stress-stress

rate-strain-strain rate relation for Lexan covering the ranges of stress

rate and strain rate mentioned above. Brill (16) investigated the

mechanical behavior of Lexan for the same purpose as did Gurtman. He

performed stress relaxation tests, tensile stress-strain tests at strain

rates up to 0.025 min^{-1}, and determined the variation of Poisson's ratio

with strain. Brill found that Poisson's ratio increased gradually from

an initial value of 0.32 to a value of approximately 0.42 at 8 percent

strain, while Gurtman found that Poisson's ratio increased rather rapidly

from an initial value of 0.38 to a value of 0.5 at approximately 3.3

percent strain. Thus, there seems to be little agreement on this point.

Whitfield and Smith (68) also investigated Lexan as a potential

photoelastoplastic material. They repeated some of the constant strain

rate tensile tests performed by Gurtman, and obtained somewhat different

stress-strain curves; the difference was attributed to the fact that

Gurtman apparently did not account for strain outside the gage length.

Brinson (17) and Stormont et al. (62) have studied the fracture

characteristics of Lexan. As part of their investigation, Stormont's

group induced orthotropic behavior in Lexan sheet by cold-rolling it to

a 50 percent reduction in thickness. As a result, quite large variations

in yield strength, Young's modulus, and Poisson's ratio were observed

between tensile specimens cut parallel to and perpendicular to the

rolling direction. The General Electric Company - in their various

brochures - provides data which describe the application characterization

and fabrication of Lexan.

Investigations dealing with the dynamic mechanical behavior and

properties of Lexan are less prevalent in the literature than those

dealing with quasi-static properties. Asay and Guenther (2) - using an

acoustic technique - measured the dilatational and shear wave speeds

through 1-10 mm thick large Lexan sheets as a function of temperature,

and computed Young's modulus and the shearing modulus using the equations

of linear elasticity. Watson (66) has studied the viscoelastic properties

of Lexan in conjunction with an investigation of gage-length errors in

electrical resistance strain gages. Using experimentally-determined

viscoelastic parameters and one-dimensional viscoelastic theory, he was

successful in predicting strain-time histories for the case of a strain

pulse of 0.1 percent amplitude propagating along a slender Lexan rod.

The author and others have experimentally investigated large-amplitude

strain wave propagation in longitudinally-impacted Lexan rods (13, 26,

48, 49), and have used some of the results of these investigations to

examine aspects of the dynamic mechanical behavior of Lexan and to

determine some of its dynamic elastic properties (46).

1.3 Review of the Literature Concerning Testing of Materials to Determine Dynamic Material Behavior

The experimental determination of dynamic mechanical properties

of materials presents several major problems. (1) A specimen must be

loaded so as to produce a desired characteristic stress-strain state

in the material being investigated. (2) Precise, quantitative

measurements must be made of transient parameters as a function of

time. (3) The data obtained from the experimental investigation must

be correctly interpreted to yield the sought-after material properties.

Many different approaches have been used to surmount these problems;

some of these are briefly discussed in the following paragraphs, which

make no pretense of being an exhaustive review of the subject.

Conventional or modified testing machines have been used to obtain stress-strain data at low strain rates, but are limited by wave propagation in the machine and specimen as strain rates are increased. An upper limit for the strain rate imposed on the specimen depends on the accuracy required and on the specimen material and geometry; an upper limit based on plastic wave propagation in the material might be as low as 10-20 sec^{-1} (45, 52). Krafft (44) provides a good discussion of instrumentation for high-speed strain measurement.

Several experimental configurations have been employed which provide for dynamic deformation of materials under essentially wave-free conditions. Impulsively-loaded diaphragms have been used to determine stress-strain relationships for aluminum alloy at strain rates of 2-3 sec^{-1}, where the stress-strain data are deduced from measurements of diaphragm pressure and deflection (28). Symmetrical expansion of thin rings, tubes, or spherical shells offers a means to produce uniform deformation in a specimen, avoiding the problem of wave propagation. Johnson *et al.* (37) and later Hoggatt and Recht (33) devised means to symmetrically expand thin rings at high strain rates - to 8000 sec^{-1}; observation of the diameter of the freely-expanding ring as a function of time provides data sufficient to determine uniaxial stress-strain data for the ring. However, the method suffers from uncertainties introduced by the double differentiation of experimental displacement-time data necessary to compute stress. Perrone (55) discusses how the ring test may be utilized to determine the uniaxial flow laws of rate-sensitive perflectly plastic and strain-hardening materials.

The impact of flat plates at high velocities produces an initial one-dimensional strain state in the plate material; experiments of this

type are commonly used to determine the stress-volume Hugoniot curves
for materials (38). They are also used to investigate the applicability
of constitutive equations developed for materials (18), and to determine
mechanical properties of materials at high strain rates (39).

Some investigators have determined dynamic stress-strain
relationships for metals from impact tests using hard balls (54).

The split-Hopkinson-pressure bar technique has become a widely used
means of determining dynamic mechanical properties of materials. This
technique is most commonly used in the form introduced by Kolsky (41)
and developed by Hauser *et al.* (32), in which a stress pulse travels
through an elastic input bar, through a short specimen, and into an
elastic output bar. The elastic bars are instrumented with resistance
strain gages; the recorded strain pulses can be used to compute a dynamic
stress-strain curve for the specimen. This technique has been applied
by Lindholm (50) and Lindholm and Yeakley (51) at strain rates to 1000
sec^{-1}, by Maiden and Green (52) at strain rates to 10,000 sec^{-1}, and by
many others. The technique has been criticized on the basis of some of
the assumptions made in its use; Sharpe and Hoge (61) have discussed
these criticisms in a recent work and have shown that the technique,
if properly applied, gives valid results for strains above 1 percent.
A variation of this technique has been used by Duffy *et al.* (27) to
develop stress-strain relations for 1100-0 aluminum rods loaded by
torsional pulses; strain rates on the order of 800 sec^{-1} were achieved.

Wave propagation in impacted bars has been studied by numerous
investigators as a means either of directly determining the constitutive
equation for a material, or of verifying the validity of a proposed
constitutive equation. Donnell (23) introduced the first scheme for

treating longitudinal wave propagation in a medium with a stress-strain

relation deviating from Hooke's law. Stress waves in a long bar made of

a material which had a bilinear static stress-strain curve were analyzed

by a superposition technique in which the stress wave was treated as

a succession of incremental steps in stress. Each stress increment was

assumed to propagate at a velocity determined by the slope of the

material static stress-strain curve at the stress level of the increment.

After Donnell's paper, the subject of elastic-plastic wave propagation

appears to have received little further attention until the Second World

War. During that time, the problem was treated independently in the

United States, in Great Britian, and in the Soviet Union by von Karman

(64), von Karman and Duwez (65), Taylor (63), and Rakhmatulin (56),

respectively. These treatments were concerned with a material which

has - for the first deformation of the material beyond the elastic

limit - a single-valued rate-independent stress-strain curve in the form

$\sigma = \sigma(e)$, which is concave toward the strain axis. It is not specified

that the dynamic stress-strain curve is necessarily the same as the

static stress-strain curve. One-dimensional stress conditions are

assumed and radial inertia effects are neglected. A prediction of the

theory is that each increment in strain from e to e + de propagates at

a constant speed c given by

$$c^2 = \frac{1}{\rho_o} \frac{d\sigma}{de} \quad ,$$

where ρ_o is the initial material density and $d\sigma/de$ is the slope of the

stress-strain curve at strain e. The first experimentalist to consider

the possibility of a dynamic stress-strain relation differing from the

static stress-strain relation was Campbell (19), who made an effort
to determine dynamic stress-strain curves for copper from the study of
non-linear wave propagation in long rods. Since that time, numerous
investigators have studied wave propagation in rods as a means of
determining constitutive equations for a material or of verifying the
validity of a proposed constitutive equation. Investigations in this
area have been made by Bell (3, 5, 6, 7, 8, 9), Kolsky (43), Malvern
(53), Ripperberger (58), and many others - including the author and
associates (46, 49). Bell (9) gives a good review of work that has
been done in this area and provides an extensive bibliography; for
other sources which have extensive bibliographies on this subject, see
(1, 22, 29) and the volumes from which (8, 9, 39, 44) were taken.

With the advent of high-speed electronic computers, numerical
solutions have been obtained for two-dimensional axisymmetric wave
propagation in bars (10, 11, 12, 20, 31, 40). These solutions predict
and explain behavior which cannot be represented by one-dimensional
analysis. It is hoped that these techniques will be able to resolve
the apparent differences in material behavior as observed in long rod
experiments, short rod experiments with the Hopkinson pressure bar and
its modifications, and plate impact experiments. In addition, they
should provide a more rigorous means for testing proposed constitutive
equations, as well as aiding in the design and interpretation of
experimental studies made to examine dynamic behavior of materials. One
of these investigations (40) has indicated that a constitutive equation
proposed by Bell (8) for annealed 1100-0 aluminum - which was developed
from one-dimensional analysis of wave propagation in impacted rods - is
inaccurate, in that the proposed constitutive equation, when used in the

two-dimensional numerical solution, does not predict well the experimental

data from which it was derived. Another of these investigations (20)

shows that a condition of uniform one-dimensional stress in impacted

elastic rods is essentially attained after the stress wave has traveled

approximately four to five diameters from the impact site. A numerical

investigation of one-dimensional wave propagation in rods by Ripperberger

and Watson (59) leads them to conclude that measurements of wave front

shapes and strain propagation velocities are not reliable as indicators

of the constitutive relationship for a material, in that a given

propagating wave front may be produced by various combinations of

constitutive equation forms and input at the impact site.

1.4   Outline of the Thesis Organization

In this investigation, some of the aspects of the dynamic mechanical

behavior of Lexan are examined and some of its dynamic elastic properties

are determined through a study of the propagation of large-amplitude

strain waves in axially-impacted Lexan rods. The investigation is

presented in this thesis as follows: Chapter 2 discusses the diffraction

grating strain transducer which is used in the investigation, and derives

diffraction-strain relationships for measurements of axial surface strain

and surface rotation. Chapter 3 describes the experimental system and

the experimental procedures employed in the investigation. Chapter 4

gives the analysis of the surface strain-time and surface rotation-time

data, the results and conclusions obtained from this analysis, and some

tentative recommendations for future investigations. Chapter 5 gives

a list of the references cited in this thesis. Chapter 6 contains

Appendix 6.1, the computer printouts of tests (Appendix Tables 6.1

through 6.27); Appendix 6.2, summary of experimental conditions

(Appendix Table 6.28 and Appendix Figures 6.1 through 6.13); and,

Appendix 6.3, the list of symbols used throughout the thesis.

2 THE DIFFRACTION GRATING STRAIN TRANSDUCER

2.1 Introduction

The study made here of the propagation of large-amplitude strain waves in Lexan rods involves the use of the diffraction grating strain transducer, first introduced by Bell in 1956 (3), and used successfully by him over a period of years. A diffraction grating strain transducer consists of a number of equi-spaced and parallel shallow grooves formed into the surface of the material to be tested, as shown in Figure 2.1.
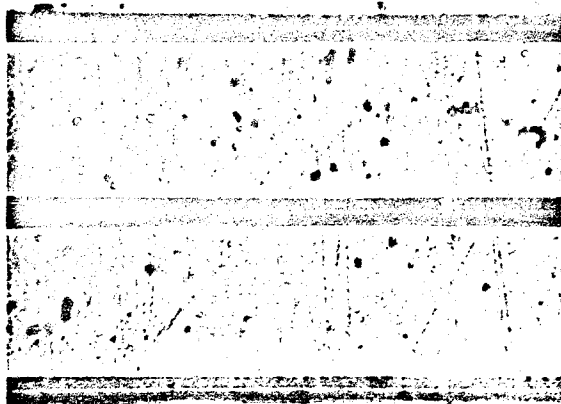
Figure 2.1 Photomicrograph of a 25 micron (1016 lines/inch)
reflective diffraction grating on polycarbonate

A collimated monochromatic light beam incident on such a grating is diffracted into a number of separate rays, as shown in Figure 2.2. The angular positions of these rays depend on the wave length of the incident light, the separation of the grating grooves, and the angle at which the incident light beam strikes the grating surface. Under proper conditions - to be discussed later - the surface strain perpendicular to

the grating grooves and the surface rotation at the grating site can be
determined by observation of the angular shifts of any two diffracted
beams, hence the grating's utility as a strain transducer.
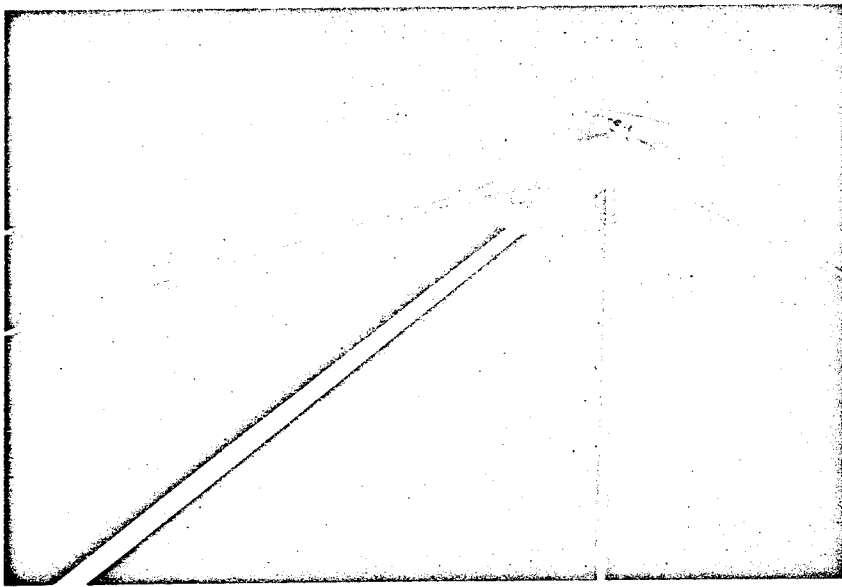
Figure 2.2   Diffracted beams from a reflective diffraction grating

The diffraction grating strain transducer possesses a number of
desirable characteristics in applications involving severe dynamic
environments. Some of these characteristics are:

1. The diffraction grating is formed directly into the surface to be
   studied, eliminating any question about a "bond" at the gage-material
   interface. Thus, it should faithfully follow the surface deformation.

2. There is no inherent upper limit on the magnitude of strain which
   can be reported by the transducer; to a large extent the limit

depends upon the characteristics of the material into which it is formed.

3. As long as the grating survives as an ordered diffraction source, it will report both elastic and plastic behavior.

4. It has no inherent high-temperature or low-temperature limitations; the temperature extremes within which it can be used depend to a large extent on the characteristics of the material into which it is formed. (Bell (7) has used gratings on 1100F aluminum at temperatures of 1100°F, 120°F below the melting point of the metal).

5. No mechanical or electrical contact – only optical – is made with the material being studied. Thus, the transducer neither impedes the material deformation nor is it subject to stray electrical signals generated during material deformation.

6. The transducer can be as small as a few thousandths of an inch on a side, facilitating studies in regions of high strain gradients. Since the transducer has no inertia and its reporting element is a diffracted light beam, its response time to changing dynamic conditions is determined primarily by the time required for wave propagation across the grating.

Despite the advantages of the diffraction grating strain transducer, little use has been made of it, primarily due to the difficulties of making gratings of sufficient quality. Bell (3, 4) formed gratings on cylindrical rods by ruling into the surface of the cylinder, by means of an exactingly modified lathe, "threads" of densities up to 30,000 "threads" per inch. Douglas *et al.* (24, 25) first produced usable diffraction gratings here using a modified rotary microtome. This microtome, ordinarily used for pathological studies, provides a

reciprocating vertical motion coupled with a stepwise horizontal advance; with a wedge-shaped diamond indenter properly attached to the microtome, diffraction gratings can be produced. A third-generation machine developed by Douglas is employed currently; it uses a similar indentation process to form gratings. This machine has produced gratings of up to 50,000 grooves per inch, and can form gratings into virtually any surface at any desired orientation.

In this investigation, the diffraction grating strain transducer is used in conjunction with pulsed ruby laser illumination and high-speed streak recording cameras to determine the axial surface strain-time and surface rotation-time histories along Lexan rods during the propagation of large-amplitude strain waves caused by longitudinal impact on the rods. The readout technique used here differs from the technique used by Bell, in that the time variation of the diffraction pattern from a grating subjected to strain and surface rotation is recorded by direct photographic means using high-speed streak recording cameras rather than by indirect photoelectric means. Data recording by direct photographic means removes any ambiguities that may exist where indirect means are used to identify the position of a diffracted beam, as well as allowing several gratings to be read simultaneously by the same recording system (26).

2.2 Diffraction-Strain Relationships for Measurement of Axial Surface Strain and Surface Rotation

Under well-chosen conditions, the observation of the angular shifts of any two beams of light diffracted from a diffraction grating provides information sufficient to determine the surface strain perpendicular to

the grating grooves and the surface rotation at the grating site. These

relationships are developed in the following paragraph.

Assume that collimated, monochromatic light is incident on the

grating such that it is perpendicular to the grooves, although it may

be inclined to the plane of the grating, and that, during deformation,

the only component of surface rotation at the grating is about a line

parallel to the grooves. Under these conditions, the incident beam and

the diffracted beams (orders) - both before and during deformation · lie

in a plane which is perpendicular to both the grating grooves and the

plane of the grating, as in Figure 2.2. Under the stated conditions,

the theory of optical diffraction from gratings (36) provides the

relationship

$$\sin \theta_n - \sin i = n\lambda m \quad , \qquad (2.1)$$

where the terms are defined below and illustrated in Figure 2.3:

  n = order of interference associated with a particular
    diffracted beam (n may take on positive, negative, or
    zero integral values).

  θ_n = angle between the grating surface normal and the nth order
    diffracted beam (shown positive in Figure 2.3).

  i = angle between the grating surface normal and the incident
    beam (shown positive in Figure 2.3).

  λ = wavelength of the incident collimated monochromatic light.

  m = number of grooves per unit length of grating.

Although the observation of any two diffracted orders furnishes

information sufficient to determine the surface strain perpendicular

to the grating grooves and the surface rotation, attention is directed

here to the $+k^{th}$ and $-k^{th}$ diffracted orders, where k is a positive

integer. The following quantities are defined in Figure 2.3:

θ_{no}, θ_n = initial and current n^{th} order diffraction angles.

i_o, i = initial and current angles of incidence.

ω = rotation of grating surface (shown positive in Figure 2.3).

ψ_n = angular displacement of nth diffracted order (shown positive in Figure 2.3).
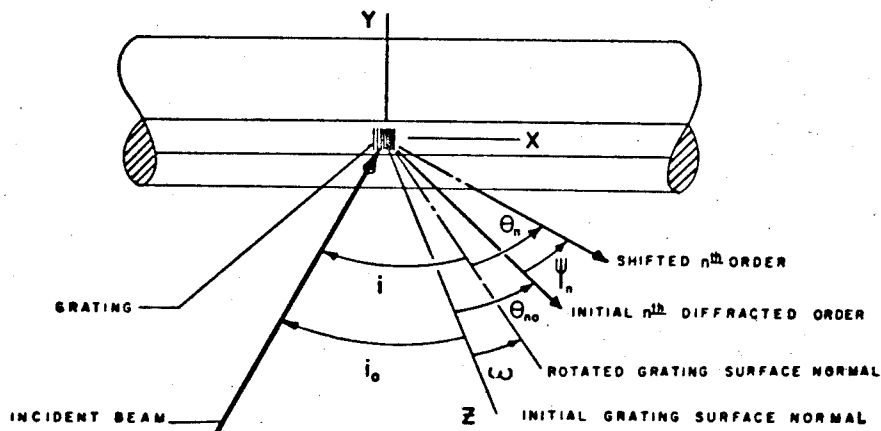
Figure 2.3 Diffracted beams before and after normal strain and grating surface rotation (for clarity, only incident beam and n^{th} order diffracted beam shown)

In the initial state, Equation (2.1) gives, for the $+k^{th}$ and $-k^{th}$ orders, respectively, the relations

$$\sin \theta_{ko} - \sin i_o = k\lambda m_o \qquad (2.2)$$

and

$$\sin \theta_{-ko} - \sin i_o = -k\lambda m_o \;, \qquad (2.3)$$

where

m_o = initial number of grooves per unit length of grating.

After a surface rotation ω and an axial strain which produces an m different from m_o, Equation (2.1) again applied to the $+k^{th}$ and $-k^{th}$ orders gives

$$\sin \theta_k - \sin i = k\lambda m \qquad (2.4)$$

and

$$\sin \theta_{-k} - \sin i = -k\lambda m \quad , \qquad (2.5)$$

where

$$i = i_o + \omega \quad . \qquad (2.6)$$

From Figure 2.3, it is seen that

$$\omega + \theta_k = \theta_{ko} + \psi_k \qquad (2.7)$$

and, similarly,

$$\omega + \theta_{-k} = \theta_{-ko} + \psi_{-k} \quad . \qquad (2.8)$$

Define the positions of the observed $+k^{th}$ and $-k^{th}$ orders, respectively, by

$$\alpha = \theta_{ko} + \psi_k \qquad (2.9)$$

and

$$\beta = \theta_{-ko} + \psi_{-k} \quad . \qquad (2.10)$$

Introduce the Eulerian and Lagrangian extensional strains, defined, respectively, as

$$e_E = \frac{d - d_o}{d} = \frac{m_o - m}{m_o} \qquad (2.11)$$

and

$$e_L = \frac{d - d_o}{d_o} = \frac{m_o - m}{m} , \qquad (2.12)$$

where $d = \frac{1}{m}$. Then, Equations (2.2) through (2.12) may be combined to yield

$$\omega = \arctan \left[\frac{\sin \alpha + \sin \beta - 2 \sin i_o}{\cos \alpha + \cos \beta + 2 \cos i_o} \right] , \qquad (2.13)$$

$$e_E = \frac{2 k\lambda m_o - \sin (\alpha - \omega) + \sin (\beta - \omega)}{2 k\lambda m_o} , \qquad (2.14)$$

and

$$e_L = \frac{2 k\lambda m_o - \sin (\alpha - \omega) + \sin (\beta - \omega)}{\sin (\alpha - \omega) - \sin (\beta - \omega)} . \qquad (2.15)$$

Equations (2.13) through (2.15), along with Equations (2.9) and (2.10), determine the surface strain perpendicular to the grating grooves and the surface rotation at the grating site. These equations do not embody any small rotation or small strain assumptions. To compute the surface strain and surface rotation as a function of time during deformation, it is necessary only to determine the angular shifts ψ_k and ψ_{-k} as functions

of time; all other quantities are known or can be determined prior to deformation.

The diffraction-strain relationships developed here are useful and valid only under rather special conditions; other diffraction-strain relationships which are valid under more general conditions have been developed by Blake (14) and Blake *et al.* (15).

3 EXPERIMENTAL EQUIPMENT AND PROCEDURES

3.1 Introduction

This chapter describes the experimental system and the experimental procedures used to determine the axial surface strains and the surface rotations in circular cylindrical rods during the propagation of large-amplitude strain waves caused by high-velocity axial impact on the rods. The topics dealt with in the various sections of this chapter are as follows: Sections 3.2 through 3.6 discuss the experimental system, its components, and the various procedures associated with their use. Section 3.7 discusses the preparation of the Lexan strikers and specimens used in testing. Section 3.8 discusses the reduction of surface strain-time data and surface rotation-time data from test photographs. Section 3.9 gives some general comments about the performance of the system. These various topics will now be discussed in more detail.

3.2 Experimental System Configuration

To determine the axial surface strains and surface rotations in circular cylindrical rods during axial impact, a system is employed which consists essentially of four subsystems:

1. The striker accelerator and target chamber with provision for supporting the target specimen and aligning it with the striker.

2. The diffraction grating illuminator.

3. The diffracted beam observer and recorder.

4. The system control and monitor.

A schematic diagram and a photograph of the entire system are shown in Figures 3.1 and 3.2, respectively. The various components of the experimental system are discussed in subsequent sections of this chapter.
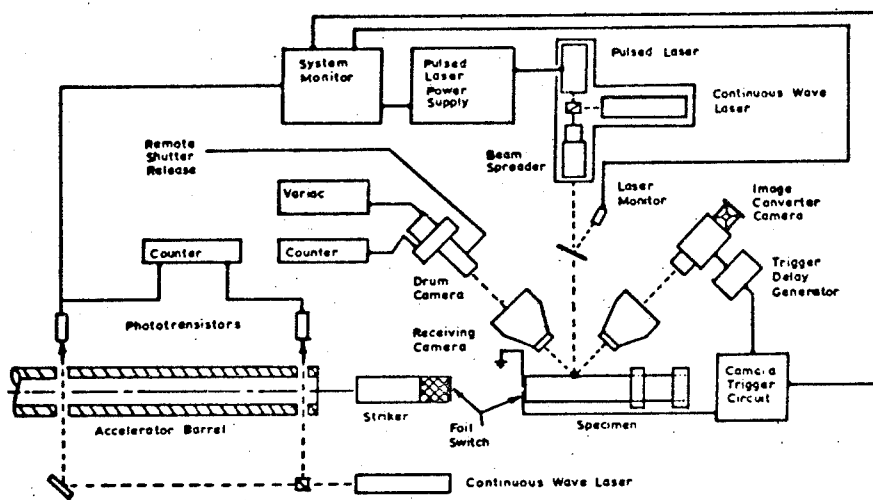
Figure 3.1   Schematic of the experimental system
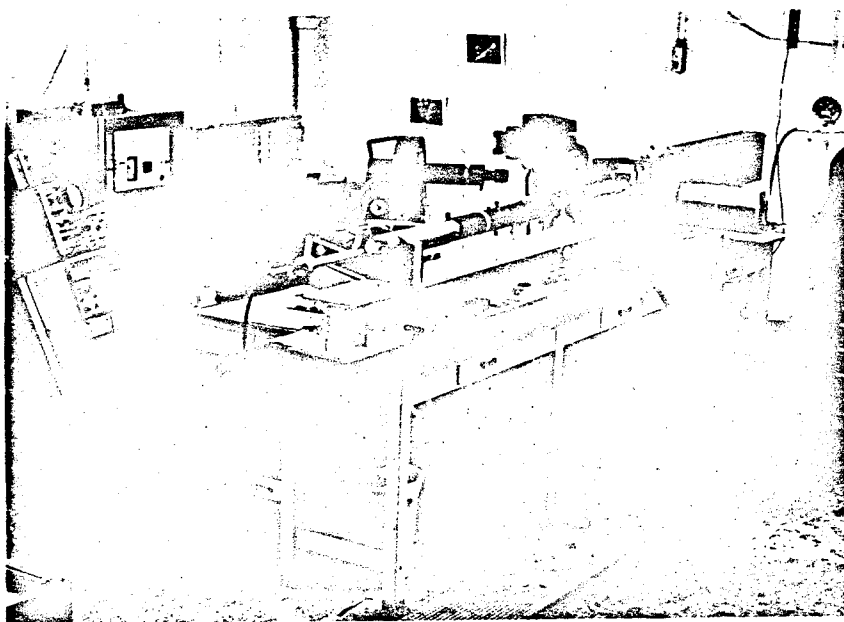
Figure 3.2   The experimental system

3.3   Striker Accelerator; Specimen Support and Alignment

The accelerator used has a smoothbore barrel of 19 mm bore and propels a striker of the same rod-like configuration as the specimen, with the axial impact of the striker and specimen taking place in an evacuated target chamber. The accelerator may be operated either as a powder accelerator or as a compressed-gas accelerator. The design of this accelerator is discussed in (35, 67).

As a powder accelerator, the energy for the acceleration is furnished by the expanding powder gas from a standard 12 gauge shotgun load with the shot removed. By selecting different standard loads and varying the striker weight, striker velocities from 500 fps to 1800 fps are readily achievable and quite reproducible, usually within 2 percent.

For use as a compressed-gas accelerator, the 19 mm accelerator is converted from powder operation to compressed-gas (in this case, nitrogen) operation by a simple conversion unit consisting of a 14 inch long thick-wall compressed-gas reservoir, a chamber bushing to take the place in the accelerator breech of the shotgun shell case (to provide a constant diameter bore), and a connecter which attaches the gas reservoir to the accelerator breech and houses the striker release mechanism. The conversion unit attached to the accelerator breech is shown in Figures 3.2 and 3.3; Figure 3.4 shows the internal detail of the connecter and striker release mechanism. In use, the bore-diameter striker is inserted into the connecter through an O-ring which seals around the striker, and is held fast by a pin which is inserted into a shallow hole drilled in the rear side of the striker. The chamber bushing is inserted in the breech, and the connecter with striker is screwed onto the breech.
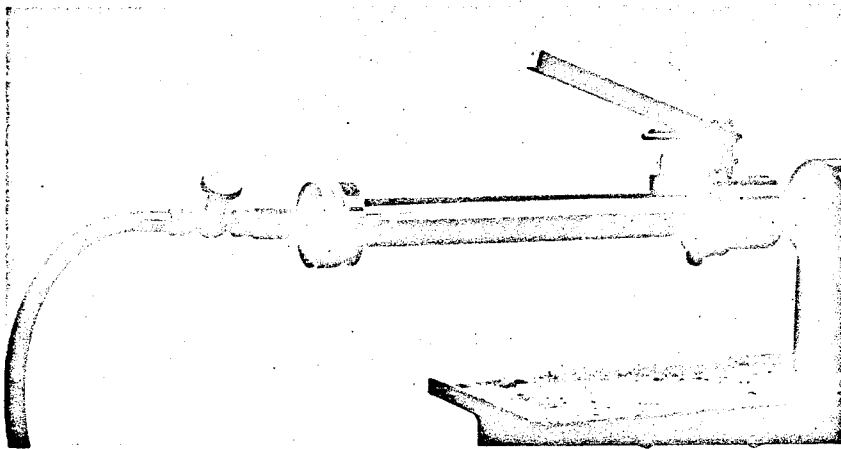
Figure 3.3   Compressed-gas converter assembly
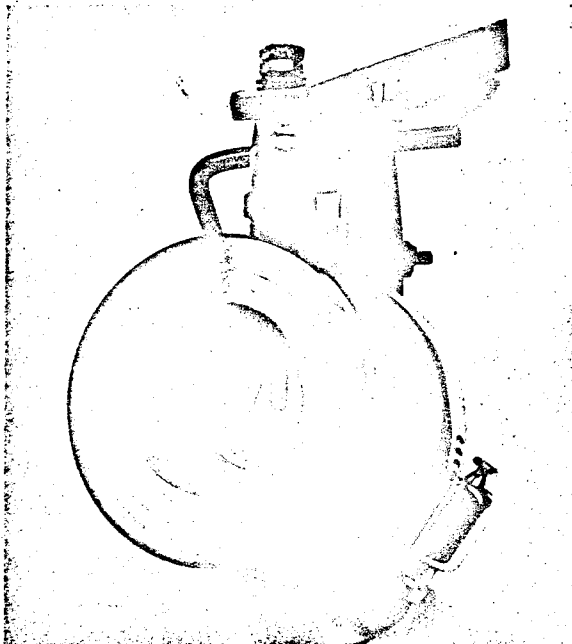
Figure 3.4   Detail of converter connecter and striker release mechanism

The gas reservoir then is attached to the other end of the connecter and pressurized, using bottled compressed nitrogen, with the rear of the striker sealing the reservoir. For pressures up to about 250 psi, a two-stage regulator is used to obtain the desired reservoir pressure, while for pressures from 250 psi upward to the nitrogen cylinder pressure (about 2600 psi), a large-diameter pressure gage (on which 5 psi can be estimated) and a valving arrangement are used. The latter can be seen in Figure 3.2. To release the striker, a safety is removed, and the firing lever depressed to pull the pin from the rear of the striker.

Due to the relatively light weight of the strikers used in these tests (approximately 33.5 grams for the four-inch strikers and 8.3 grams for the one-inch strikers), apparently identical strikers often behave quite differently when fired, particularly the lighter ones. Therefore, before the actual test is conducted, the striker to be used is test-fired several times to determine the reservoir pressure necessary to obtain the desired velocity. In these test-firings, the strikers are soft-caught undamaged in a large mass of nylon parachute cloth. By means of these test-firings, velocities usually can be reproduced within plus or minus 1 percent (see Appendix Table 6.28).

The reservoir pressure necessary to attain a desired velocity with a given projectile is estimated before test-firing by assuming that the work done by an adiabatic expansion of the compressed nitrogen gas is entirely converted into kinetic energy of the striker. For the experimental configuration used, this yields the following expression for the required reservoir pressure (47):

$$P_o = \left[\frac{V_s}{141.6}\right]^2 W_s \; , \qquad\qquad (3.1)$$

where

P_o = initial reservoir pressure (psia),

V_s = desired striker velocity at impact (ft/sec), and

W_s = striker mass (grams).

Using reservoir pressures estimated by Equation (3.1), the actual striker velocity is approximately 7.5 percent low when using one-inch and four-inch Lexan strikers. Equation (3.1) becomes more accurate as the striker weight increases (47).

The specimen is positioned in the evacuated target chamber by means of a specimen holder of seamless mechanical tubing, which is aligned concentric with the accelerator bore using a mandrel. The specimen is aligned inside the specimen holder by 1.118 inch diameter Lexan guide rings which are machined concentric with the specimen, and which fit snugly inside the specimen holder. The specimen holder is slotted to provide a light path for the laser beam incident on the diffraction grating and for the diffracted rays. High-quality plate-glass ports provide optical access to the evacuated target chamber.

The high degree of reproducibility of the strain-time and surface rotation-time data indicates that axial impact is realized using this alignment procedure, which is essentially the same as that discussed in (26).

3.4 Diffraction Grating Illuminator

A grating illuminator must satisfy the following criteria:

1. Collimation is required so that a given order is diffracted by a unique angle regardless of the translational position of the

grating in the field of illumination, *i.e.*, among other things, the angular position of a given diffracted order is dependent on the angle at which the incident light strikes the grating.

2. A monochromatic light source is necessary to simplify the problem of data reduction, since a polychromatic incident light would produce a spectrum of rays that would be difficult to identify individually and difficult to follow.

3. Since the diffracted orders are to be photographically recorded, the light intensity must be adequate to give high intensities in the diffracted orders, even from small gratings. The requirement of high writing rates magnifies the need for high intensities.

4. The size of the block of collimated light must be large enough to continue to cover the grating as it translates after impact.

An essential ingredient in the solution found here to the above-specified problem is a Korad Model K-1C Jr. conventional mode ruby pulsed laser with rated full power output of 8 joules at 6943 Å, fitted with a beam spreader constructed of cylindrical lenses (Figure 3.5). The beam spreader was adjusted so that a horizontally-collimated light block 1-1/2 inches wide is obtained. Measurements indicate that the resulting beam diverges less than 0.15 milliradian in the horizontal plane. A narrow band pass filter is used to block the flash from the xenon flash tube in the pulsed laser. A Spectra-Physics Model 124 helium-neon continuous-wave laser with rated output of 15 milliwatts at 6328 Å is used to align the recording cameras with the diffracted orders. This is done by placing a dowel-located removable beam diverter in the pulsed laser cavity to direct the cw laser beam through the beam spreader parallel to the pulsed laser beam. The cw laser beam then is used for

alignment of the pulsed laser. Allowance is made for the slight angular

shift in diffracted orders due to the difference in wavelengths between

the cw laser and the pulsed laser. Measurements indicate that the cw

laser and the pulsed laser beams are parallel within 0.44 milliradian.

The entire illumination unit is mounted on a base which adjusts for

elevation and tilt and which can be translated on a leveled surface

plate.
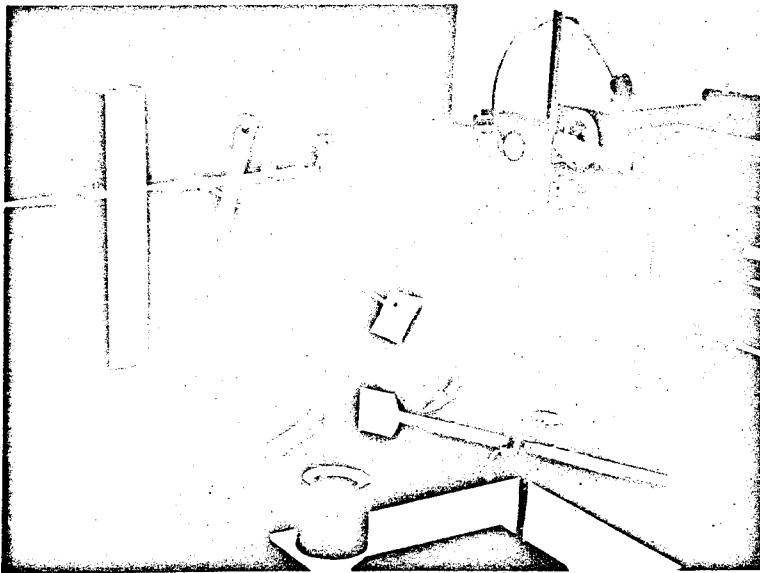
Figure 3.5   Diffraction grating illuminator

Approximately 600 µsec are required to initiate the pulsed lasing

action, so the laser trigger circuit is activated before impact by the

passage of the striker down the accelerator barrel, where it interrupts

a light beam incident on a phototransitor, shown in Figure 3.1.

To reduce the background illumination reaching the recording cameras, slits and non-reflective materials are used at various points along the incident and diffracted light paths.

3.5 Diffracted Beam Tracking and Recording

In the particular experimental configuration employed, the incident light beam from the grating illuminator is adjusted so that it is initially normal to the grating surface ($i_o = 0$). Two camera systems observe the symmetrically-located $+k^{th}$ and $-k^{th}$ diffracted orders, as seen in Figures 3.1 and 3.2.

In order to track and record the movements of the observed diffracted orders over as large an angular displacement as possible, two "filmless" receiving cameras are placed quite near the observation port in the target chamber. These are simple devices, constructed of a Kodak Aero-Ektar, f/2.5, 7 inch focal length lens and a strip of ground glass placed in the focal plane of the lens. This placement ensures that translation of the grating in the incident collimated light bundle causes no shift in the position of the diffracted order on the ground glass strip. These cameras are shown in Figure 3.6. The receiving cameras are calibrated so that the relationship between the angular shift of the diffracted order and its displacement on the ground glass strip is known. The cameras were calibrated by reflecting an attenuated cw laser beam off a sextant-mounted front-surface mirror and through the camera lens, then measuring the displacement of the focused beam on the ground glass as the mirror's angular orientation was changed by known amounts. The maximum angle of acceptance of the receiving cameras' lenses is about 34°, with the angular shift-displacement relationship

constant within about 0.4 percent within about 28° centered on the

optical axes of the lenses.
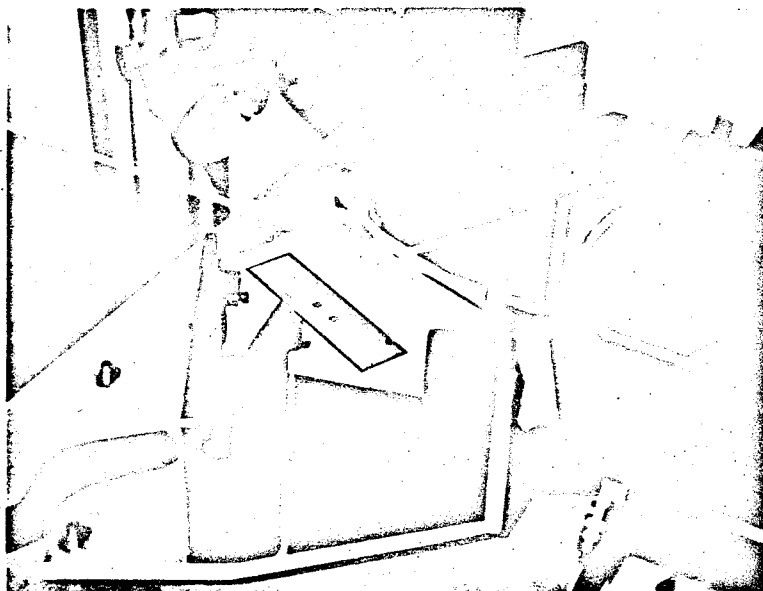
Figure 3.6   Receiving cameras, showing diffracted rays
and calibration plate

The high-speed streak recording cameras are focused on the ground
glass strips in the receiving cameras' focal planes. Two different
types of cameras are used (not by design, but by reason of availability).
One is a TRW Model 1D image converter camera with a Model 8B 200 µsec
streak unit (which was adjusted to give a 250 µsec streak duration),
operating at a writing rate of 0.22 mm/µsec, using Polaroid Type 51
high-contrast film. The other camera is a Beckman and Whitley Model 318
drum camera, operated at its maximum writing rate of about 0.26 mm/µsec
(providing several thousand microseconds of recording time), using Kodak

2485 high-speed recording film. Exposure control for the cameras is effected either by neutral density filters placed in front of the receiving camera lens or by using the proper f/stop on the recording camera lens. The proper exposure to use for a particular grating is found by making trial exposures prior to the actual test. The drum camera is continuous-writing and thus needs no synchronization (the shutter is simply opened during the moment of impact), whereas the image converter camera is triggered at impact by a contact of striker and specimen, as described later. During impact, the recording cameras mechanically or electronically streak the film perpendicular to the motion of the diffracted orders on the screens of the receivers described above. (In this configuration, the movement of the diffracted orders is in a horizontal plane). Typical film records are shown in Figure 3.7.

3.6   System Control and Monitoring

The proper coordination of the various functions which the experimental system must perform is accomplished by the pulsed laser trigger circuit and the image converter camera trigger circuit. The velocity of the striker is determined by the velocity measurement circuit. The pulsed laser output and the impact time are monitored on a dual-beam oscilloscope as a check on proper functioning of the control circuits.
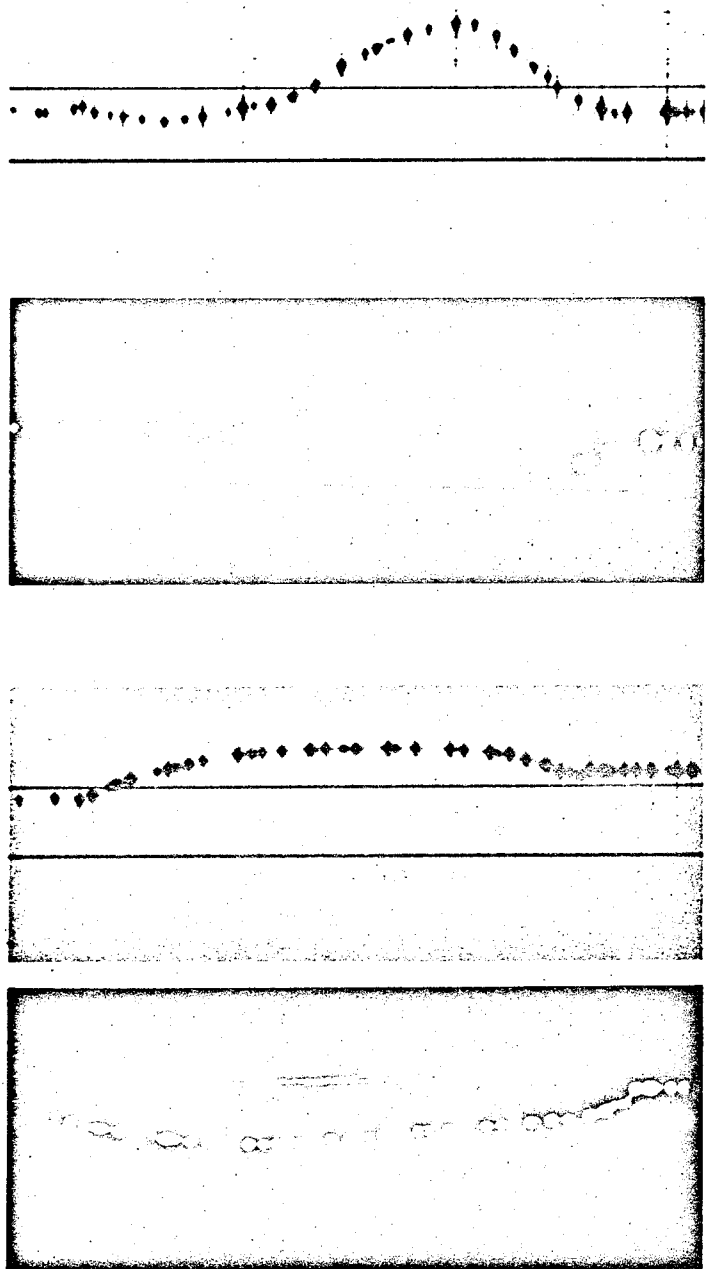
Figure 3.7 Typical pairs of streak photographs of diffracted orders

The pulsed laser trigger circuit is activated by the striker's
passage down the accelerator bore, where it interrupts a light beam
incident on a Texas Instruments LS-400 N-P-N phototransistor, which has
a fall time of approximately 10 μsec. This provides a signal to a
Tektronix Type 556 dual-beam oscilloscope, which, after an experimentally-
determined delay, provides a pulse to the pulsed laser power supply and
fires the laser. The delay is so chosen that impact takes place from
25 to 50 μsec after lasing action commences.

The image converter camera trigger circuit is activated at impact
by a contact switch to be described later. The circuit consists of the
contact switch, a 22.5v battery, and a 47 kilohm resistor in series.
The rising emf at impact provides a signal to a trigger delay generator
which then triggers the image converter camera. Delay times of 0 to
99.99 μsec can be set on the delay generator. (Zero delay is used in
these tests). The total minimum inherent delay from impact to start of
streak on the image converter camera is about 125 nsec.

The velocity of the striker is measured by recording the striker
travel time over a known distance. Two LS-400 phototransistors are
placed in ports 10.88 inches apart in the accelerator barrel, with the
second port at the muzzle. The passing striker interrupts light incident
on the phototransistors, providing signals which successively start and
stop a Beckman Instruments Model 6380 counter. The elapsed time (measured
to 0.1 μsec) is then converted to striker velocity. The accelerator was
not vented in these tests, so that the striker had a slight acceleration
during the time its average velocity was measured; a calculation using
the accelerator characteristics indicates that the striker velocity at
impact was higher than the average velocities reported in Appendix Table

6.28 by about 1.5 and 1.7 percent for one-inch and four-inch strikers, respectively.

The outputs of the pulsed laser and the image converter camera trigger circuit are monitored on the dual-beam oscilloscope. All the inputs are displayed on a 2000 μsec sweep. The upper beam displays the character of the laser pulse as read from the incident laser beam by an EG&G SGD-100 photodiode, which has a rise time of 4 nsec and a fall time of 15 nsec. A small percentage of the incident laser beam is diverted for this purpose by placing an inclined clear glass plate in the path of the beam, seen in Figure 3.5. The lower beam displays impact time and duration of contact between striker and specimen. Figure 3.8 shows a typical oscilloscope record.
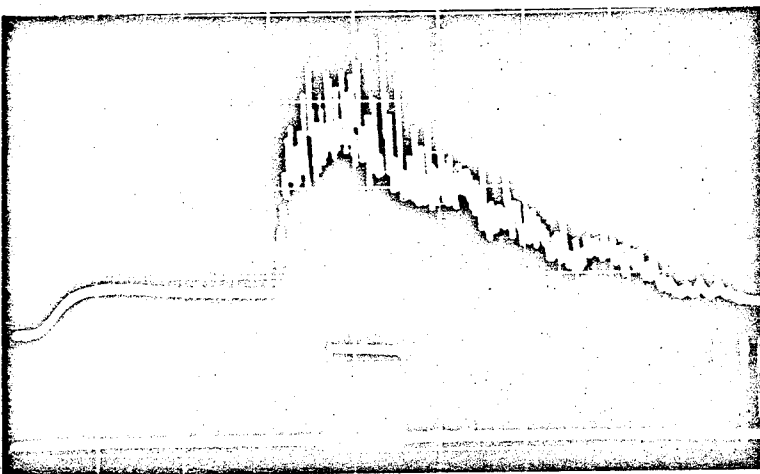
Figure 3.8   Typical system monitor record

3.7 Striker and Specimen Preparation

Typical specimens and strikers are shown in Figure 3.9; these are prepared from as-received 3/4 inch diameter Lexan rods supplied by the Cadillac Plastic Company.
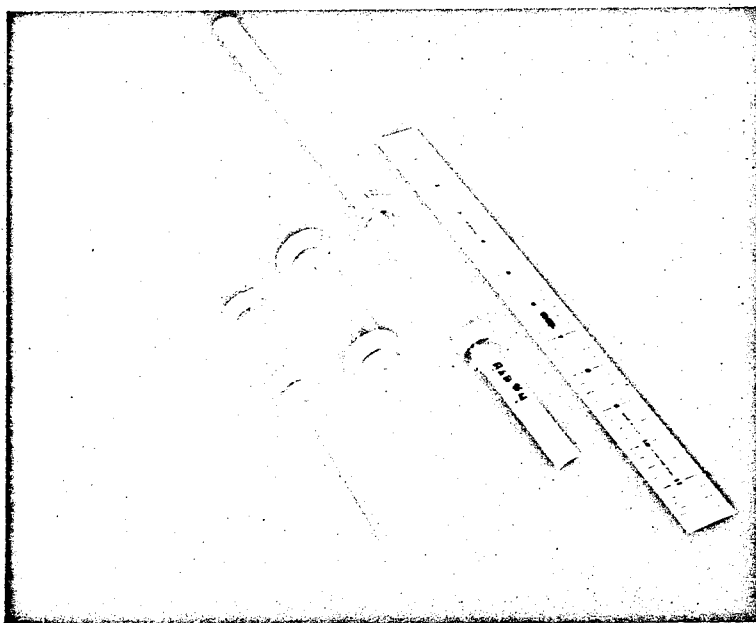
Figure 3.9 Typical Lexan specimens and strikers

The specimens are prepared as follows:

1. The specimen is turned to bore diameter (approximately 0.741 inch) and cut to desired length in a lathe. (The lengths of the various specimens are tabulated in Appendix Table 6.28).

2. A flat approximately 3/16 inch wide is formed along the length of the specimen and polished, using procedures common in metallographic practice.

3. A diffraction grating is formed on the flat at the desired location by impressing parallel grooves one at a time with a wedge-shaped diamond indenter, using a previously-mentioned machine developed by Douglas. The grooves are formed perpendicular to the direction of the strain component to be measured, $i.e.$, the axial strain component. The tests reported here generally utilized gratings having 18,000 to 19,500 grooves per inch (although several gratings reached 23,600 grooves per inch), with groove depths on the order of 3×10^{-4} mm. (Sharpe (60) has found that in aluminum, groove depths up to approximately 38×10^{-4} mm have no appreciable effect on the dynamic strain distribution in the vicinity of the groove).

4. Information sufficient to determine the initial line density m_o of the grating is obtained by measuring to within about ±2 minutes the angle between, say, the +1 and −1 diffracted orders, with the grating illuminated by a cw laser in normal incidence ($i = 0$). The angle between the two orders is measured by traversing a sextant-mounted front-surface mirror in a straight line so that it intersects both orders, and at its intersection with each order, orienting the mirror so that the diffracted ray is reflected back along itself. The change in angular orientation of the mirror then gives the angle between the two diffracted orders, and Equation (2.1) may be employed to compute m_o.

5. Lexan guide rings are pressed onto the specimen using approximately 0.007 inch diametrical interference, and are turned concentric with the specimen to a 1.118 inch outside diameter. In the test results, no evidence is seen of any appreciable wave reflection from these guide rings (as discussed in Section 4.9).

6. A very thin aluminum film is vacuum evaporated onto the grating
   site. This increases the intensity of the diffracted orders and
   allows the grating to be masked off to a small size (approximately
   1/32 to 1/64 inch long). The aluminum film must be very thin, or
   it sometimes flakes off during impact, causing the intensities of
   the diffracted orders to fall below the exposure threshold of the
   recording film.

7. A 0.00075-inch-thick split-foil contact switch is attached to the
   specimen's nose by spraying a thin film of Scotch Spra-ment adhesive
   onto the foil, and then pressing the nose of the specimen onto the
   cement-coated foil with the foil resting on a surface plate. (The
   nose of the striker is foil-covered in the same fashion, and closes
   the switch on impact). Camera trigger circuit lead wires are
   attached to the two halves of the foil switch on the specimen's nose,
   and led back through slots in the guide rings. The presence of the
   foil switch between striker and specimen is of concern only in the
   analysis presented in Section 4.9, which deals with approximate
   predictions of surface strain-time histories. In that approximate
   analysis, which involves wave propagation across the striker-specimen
   interface, the presence of the foil switch is neglected.

8. The area surrounding the grating is blackened and the grating masked
   off by painting with a permanent-type felt-tip marking pen. This
   helps reduce the background illumination reaching the recording
   cameras; it also improves the quality of the diffracted orders,
   since the highest quality portion of the grating can be selected as
   the sensing element. The felt-tip marker has the advantage that its
   ink does not flake off during impact; in some previous tests, the

diffracted orders being observed apparently were obscured during portions of the recording time by flaking paint, leaving gaps in the photographic record.

The strikers are prepared as follows:

1. The striker is turned to bore diameter in a lathe, with 3/8 inch of its nose turned 0.005 inch undersize. (The lengths of the various strikers are tabulated in Appendix Table 6.28).

2. A hole 5/32 inch in diameter and 1/8 to 3/16 inch deep is drilled in the side of the striker 3/16 inch from the rear for insertion of the pin which holds the striker prior to firing. (This pin can be seen in Figure 3.4).

3. The undersize portion of the striker is spray-painted flat black to provide the opaque section necessary for the striker to reliably interrupt the photosensors used in the various timing and monitoring circuits.

4. The nose of the striker is covered with foil, using the same procedure as used for the specimen.

3.8   Data Reduction

The two streak photographs taken by the high-speed recording cameras determine the diffracted order angular shifts ψ_k and ψ_{-k} as functions of time. Typical pairs of photographs are shown in Figure 3.7. These photographs do not exhibit a continuous record due to the rapidly fluctuating nature of the pulsed laser light (see Figure 3.8). The streak photograph, consequently, consists of a series of dots at 2 to 5 μsec intervals. The vertical reference lines are placed on the film before the test by streaking the images of two 0.35 mm diameter

illuminated holes which are a known distance apart in a calibration
plate placed in the focal plane of the receiving camera. This plate can
be seen between the receiving cameras in Figure 3.6. These lines serve
the purposes of (1) establishing the streak direction ($i.e.$, the time
axis) on the film record, (2) determining the magnification from the
receiving camera to the recording camera, and (3) establishing a reference
which determines the location of any diffraction spot on the receiving
camera screen.

Measurements are made on each film record using an x-y vernier
microscope reading to 0.01 mm. The image converter camera record begins
with a point which is recorded in a framing mode of the camera before
the test, and which defines the initial point of the streak (time $t = 0$
or impact), as well as the initial spatial location of that diffracted
order. The drum camera is continuous-writing, and thus its record will
contain a number of diffraction dots recorded before impact, which serve
to define the initial spatial location of that order. The image converter
camera and drum camera film records are matched, using the timewise
spacing and intensities of the orders, and thus impact time is fixed on
the drum camera. Displacements of the diffracted orders in the time and
spatial directions are measured from these initial points on each film
record. These data, with other known quantities and system
characteristics, are employed in a computer program to compute surface
rotation, strain, and other desired quantities at each data point after
impact. The time after impact at each data point is computed from the
drum camera film record.

The time during which the striker and specimen are in contact can
be determined to some degree of approximation from the duration of the

impact signal on the lower trace on the system monitor record (Figure 3.8).

An uncertainty analysis (34) of the data reduction technique and the experimental configuration indicates that the uncertainty in the strain measurements is about 0.002 in/in, so that a strain of 0.1 in/in could be measured with an uncertainty of 2 percent. However, the reproducibility of the experimental results indicates that under good conditions the uncertainty in the strain measurements is probably under 0.001 in/in. In a check to ascertain observer bias in reduction of the data, a set of test data was reduced from test photographs by two independent observers - one inexperienced; the results generally agreed with 0.1 µsec and 0.001 in/in for time and strain, respectively.

3.9   Summary

The experimental system has proven to be an excellent one for measuring surface strain-time and surface rotation-time detail during the propagation of large-amplitude strain waves in Lexan rods; it should perform equally well for any material whose surface - like Lexan's - remains smooth during deformation.

When testing materials like Lexan - whose surfaces remain smooth during deformation - one of the primary factors limiting the maximum strain which can be recorded by the system is the amount of surface rotation present at the grating site. Large surface rotations cause large angular shifts in the diffracted beams; when these are coupled with large angular shifts due to strain, the diffracted beam for which these two effects are additive is likely to move out of the angle of acceptance of the receiving camera, and hence terminate the experimental

record. In the absence of large surface rotations, quite large strains can be recorded (to 20 percent in test LS2-21; also see (48)). (The primary factor which limits the maximum strain which can be reported by a grating formed into a crystalline material is the disordering of the surface during deformation, which impairs the regularity of the grating and thus destroys the coherence of the diffracted beams (47)).

The test procedure, once the experimental system is set up and functioning properly, is not particularly difficult or time-consuming. Starting with a prepared specimen, the test itself and the reduction of data from the test photographs entails approximately 6 to 8 man-hours; one person can set up and perform a test without a great deal of difficulty, although two persons are desirable from the standpoint of safety and efficiency.

4   EXPERIMENTAL RESULTS AND CONCLUSIONS

4.1   Introduction

In this chapter, the surface strain-time and the surface rotation-
time data obtained from the tests involving Lexan rods subjected to
longitudinal impact are analyzed to examine some aspects of the dynamic
behavior of Lexan and to determine some of its dynamic elastic properties.
The topics dealt with in the various sections of this chapter are
discussed in the following paragraphs.

Section 4.2 discusses briefly the surface strain-time and surface
rotation-time data. It gives the ranges of grating location, strain,
and strain rate for the tests, as well as some pertinent experimental
conditions.

In Section 4.3, strain wave speeds along Lexan rods are determined
as functions of strain level and distance from the impact site. These
wave speeds are computed from the strain-time histories at various
positions along the rods, and show the transformation of the initial
dilatational wave (uniaxial strain) into a rod wave (uniaxial stress) as
the wave travels along the rod. They give the dilatational wave speed
for small strain in Lexan, and are used in subsequent calculations to
determine some of the dynamic elastic properties of Lexan.

In Section 4.4, the strain wave speeds under approximate uniaxial
stress conditions in Lexan rod are found, and are seen to be essentially
constant for a given strain level. Young's modulus, Poisson's ratio,
and the shearing modulus for Lexan are computed using the wave speed
data and the equations of linear elasticity, and are compared to
published quasi-static and dynamic values.

In Section 4.5, a dynamic stress-strain relation for Lexan is developed using some of the results of the von Karman rate-independent theory of one-dimensional longitudinal stress wave propagation in rods (42, 65) and the strain wave speeds for approximate one-dimensional stress conditions. This dynamic stress-strain relation is compared to published quasi-static data.

In Section 4.6, the variation of Poisson's ratio with strain under dynamic conditions in Lexan is investigated using the strain-time history, the surface rotation-time history, and the strain wave speeds at a position along a rod. The procedure is one employed by Bell (5, 6) to investigate the variation of Poisson's ratio with strain in annealed 1100F aluminum. The results are compared to published quasi-static data.

In Section 4.7, the yield point strain in Lexan rods subjected to short-duration loading-unloading pulses is investigated. This is done by impacting Lexan specimens, recording the strain-time histories at chosen grating sites, and then making post-test measurements of the grating groove spacing to determine the amount (if any) of permanent plastic deformation.

In Section 4.8, the effect of a previous elastic impact on the strain-time history obtained during a subsequent impact is investigated by subjecting Lexan specimens to two separate impacts under essentially identical conditions.

In Section 4.9, attempts are made to predict some of the experimentally-observed strain-time histories in impacted Lexan rods. These predictions are attempted as a check on the accuracy of the experimentally determined strain wave speeds and to test the feasibility of predicting - in a simple fashion - the strain-time history at a point

along a Lexan rod given the strain-time history at some other point.
The predictions are made assuming that strain level superposition is
valid and that each strain level propagates at a constant speed as
found in Section 4.4.

Section 4.10 gives a summary of the experimental results and some
recommendations for future investigations.

These various topics will now be discussed in more detail.

4.2   Strain-Time and Surface Rotation-Time Data

Presented in Appendix 6.1 (Appendix Tables 6.1 through 6.27) are
the strain-time and surface rotation-time data from 27 tests utilizing
0.741 inch diameter Lexan rods subjected to longitudinal impact.   In
these tests, recording times are generally on the order of 250 μsec
after impact.   In one group of tests, strain-time and surface rotation-
time histories are obtained at locations ranging from two to four
diameters from the impact site; these histories show the propagation of
elastic strain pulses having amplitudes to 8.65 percent and strain rates
in excess of 2200 sec^{-1}, produced by the impact of one inch and four
inch Lexan strikers at striker velocities of approximately 540 ft/sec.
In another group of tests, strain-time and surface rotation-time histories
are obtained at one-third diameter from the impact site, with striker
velocities ranging up to 700 ft/sec; strains to 13.3 percent and strain
rates to 15,700 sec^{-1} are recorded in these tests.   Other tests give
strain-time and surface rotation-time histories from impacted short
specimens which are epoxied to steel back-up bars; strains to 20 percent
are recorded in these tests.   The pertinent experimental conditions for

these tests are given in Appendix Table 6.28; the strain-time data for
the tests of interest are plotted in Appendix Figures 6.1 through 6.13.

The striker velocities reported in Appendix Table 6.28 are the
average velocities measured over the last 11 inches of striker travel
before impact. In this series of tests, the compressed-gas accelerator
which propels the striker was not vented, so that the striker had a
slight acceleration at impact; hence the striker velocity at impact was
slightly higher than the measured average. A calculation using the air
gun characteristics indicates that the actual striker velocity at impact
is higher than the measured average velocity by about 1.5 and 1.7 percent
for one-inch and four-inch strikers, respectively.

**4.3   Strain Wave Speeds as a Function of Strain Level and Distance
from the Impact Site; Dilatational Wave Speed**

In this section, strain wave speeds along the Lexan rods are
determined as functions of strain level and distance from the impact
site. These wave speeds show the transformation of the initial
dilatational wave (uniaxial strain) into a rod wave (uniaxial stress)
as the wave travels along the rod. They give the dilatational wave
speed for small strain, and are used in subsequent calculations to
determine some of the dynamic elastic properties of Lexan.

The average strain wave speeds along the Lexan rods as a function
of strain level and distance from the impact site are computed from the
strain-time histories at various locations along the rod. These average
wave speeds are calculated by dividing the distance between adjacent
grating locations by the time required for a given strain level to
propagate from one grating location to the other. Toward this end, 15
tests are placed in nine groups of one or two tests each, with tests

grouped by similarity in grating location, striker length, and striker velocity. The nine groups are made up from the tests listed in Appendix Table 6.28 as follows: test 5, tests 6 and 26, tests 11 and 12, tests 28 and 29, test 3, tests 13 and 27, tests 15 and 16, tests 17 and 19, and test 18. The maximum variation in striker velocity between any two tests in the same group is 1.7 percent; the maximum variation in grating position for any two tests in the same group is 2 percent for tests 28 and 29, with less than 1 percent variation for all other groups.

To determine the time required for various levels of strain to propagate from one grating location to another, portions of the strain-time histories in each of the nine test groups are fitted with least-square polynomial equations. In the initial loading portions of the strain-time histories, only data that are free from the effect of unloading waves reflected from either the rear of the striker or the rear of the specimen are used; in the tensile reloading portions of the strain-time histories of the four latter groups, only data that are free of the effect of compressive unloading waves reflected from the specimen rear are used. (This necessitated refitting of some curves after preliminary wave speed values were found). The order of polynomial to be fitted is determined using a single-precision polynomial regression curve-fitting program (IBM Scientific Subroutine) which terminates when there is no reduction in the residual sum of squares between two successive degrees of polynomials. The polynomial used to determine wave transit times is fitted using a double-precision polynomial regression curve-fitting program (UCLA Biomedical Program BMD05R). This program also provides a plot of the experimental data and the data as computed from the fitted curve, thereby giving a visual check on the

fitted curve. In all test groups, the initial steeply-rising portions of the strain-time histories are fitted by third-order polynomials; the slowly-rising latter portions of the strain-time histories in the first four test groups are fitted by second-order polynomials. The polynomials fitted to the two regions of the strain-time histories overlap at the knee of the curve to provide a smooth transition between the two fitted polynomials. The tensile reloading portions of the strain-time histories in the latter four test groups are fitted with second-, third-, or fourth-order polynomial equations.

The average wave speeds for various levels of strain are calculated at various average distances from the impact site by dividing the distance between two different grating locations by the wave transit time between the two locations, with the wave transit time determined from the polynomials fitted to the strain-time histories at the two locations. The average distance from the impact site for this average wave speed is taken as midway between the two locations. The nine test groups previously mentioned are paired by similarity in striker velocity in the 18 combinations given in Table 4.1 to compute the average wave speeds at various average locations along the rods. The maximum variation in striker velocity between paired groups is 4.7 percent for tests 3 and 18, and is less than 3 percent for all other groups. The results of these wave speed calculations are given in Table 4.2, with some representative results plotted in Figure 4.1.

Table 4.1 Pairings of test groups for computation of average wave speeds

Tests	Approximate X range (in)	Average X (in)	Range of strain for approximate 1-D stress (percent)	Strain rates in approximate 1-D stress range (sec^{-1})		
				0-2 percent	2-5 percent	5-7 percent
3-13,27	1/4-1 1/2	0.888	3.8-5.0	-	7100-1800	-
3-6,26			3.8-7.0	-	7100-1900	3500-400
3-5			3.8-7.0	-	7100-1900	3500-400
3-15,16	1/4-2 1/4	1.262	2.3-4.0	-	7100-1400	-
3-11,12			2.3-7.0	-	7100-1500	3500-450
3-17,19	1/4-3	1.632	2.3-3.8	-	7100-1300	-
3-18			2.3-3.8	-	7100-1300	-
3-28,29			2.3-7.0	-	7100-1100	3500-300
13,27-17,19	1 1/2-3	2.266	2.0-3.8	-	1800-1300	-
6,26-18			2.0-3.8	-	1900-1300	-
5-28,29			2.0-7.0	-	1900-1100	450-350
15,16	2 1/4-9 3/4	5.991	0.0-2.0	1400-700	-	-
13,27	1 1/2-10 1/2		0.0-1.5	1800-600	-	-
17,19-15,16	3-9 3/4	6.365	0.0-2.0	1300-700	-	-
18	3-13	8.004	0.0-1.5	1300-500	-	-
17,19			0.0-1.5	1300-500	-	-
15,16-18	9 3/4-13	11.361	0.0-1.5	700-500	-	-
15,16-17,19			0.0-1.5	700-500	-	-

50

Table 4.2 Wave speeds in 0.741 inch diameter Lexan rods at 72°F as a function of strain level and distance from impact

Strain (per-cent)	Average wave speeds (in/μsec $\times$ 10^3)								
	0.888 in	1.262 in	1.632 in	2.266 in	5.991 in	6.365 in	8.004 in	11.361 in	Average of values to right of dots
0.1	87.45	85.63	75.64	67.84	55.79	55.68	56.32	57.32	56.36
0.2	83.05	81.11	72.84	65.96	55.74	55.22	55.89	56.99	56.07
0.3	79.28	77.27	70.40	64.31	55.52	54.81	55.49	56.65	55.73
0.5	73.17	71.08	66.34	61.55	54.76	54.15	54.79	55.92	55.01
0.8	66.47	64.40	61.78	58.42	53.47	53.41	53.91	54.84	53.98
1.0	63.11	61.10	59.45	56.80	52.80	53.01	53.43	54.21	53.41
1.3	59.19	57.32	56.69	54.87	52.10	52.45	52.82	53.54	52.77
1.5	57.11	55.35	55.20	53.81	51.69	52.03	52.47	53.35	52.44
1.8	54.56	52.99	53.33	52.44	51.43	51.26	-	-	51.35
2.0	53.14	51.70	52.25	51.61	50.78	50.59	-	-	50.97
2.3	51.30	50.06	50.78	50.41	-	-	-	-	50.46
2.5	50.20	49.11	49.84	49.58	-	-	-	-	49.56
2.8	48.38	47.78	48.44	48.25	-	-	-	-	48.20
3.0	47.70	46.94	47.46	46.61	-	-	-	-	47.01
3.3	46.24	45.66	45.90	45.63	-	-	-	-	45.74
3.5	45.24	44.77	44.78	44.40	-	-	-	-	44.64
3.8	43.66	43.35	42.95	42.38	-	-	-	-	43.06
4.0	42.54	42.33	42.80	42.90	-	-	-	-	42.57
4.3	40.76	41.42	40.94	41.04	-	-	-	-	40.95
4.5	39.49	40.18	39.64	39.72	-	-	-	-	39.67
4.8	37.47	38.38	37.60	37.64	-	-	-	-	37.67
5.0	36.07	37.27	36.41	36.60	-	-	-	-	36.42
5.3	33.95	35.28	34.05	34.00	-	-	-	-	34.25
5.5	32.39	33.79	32.42	32.18	-	-	-	-	32.63
5.8	30.02	31.43	29.96	29.44	-	-	-	-	30.17
6.0	28.68	29.82	28.35	27.63	-	-	-	-	28.63
6.3	26.82	27.42	26.03	24.73	-	-	-	-	26.36
6.5	24.35	25.86	24.55	24.20	-	-	-	-	24.66
6.8	22.14	23.64	22.47	21.92	-	-	-	-	22.46
7.0	20.13	22.24	21.17	21.26	-	-	-	-	20.99
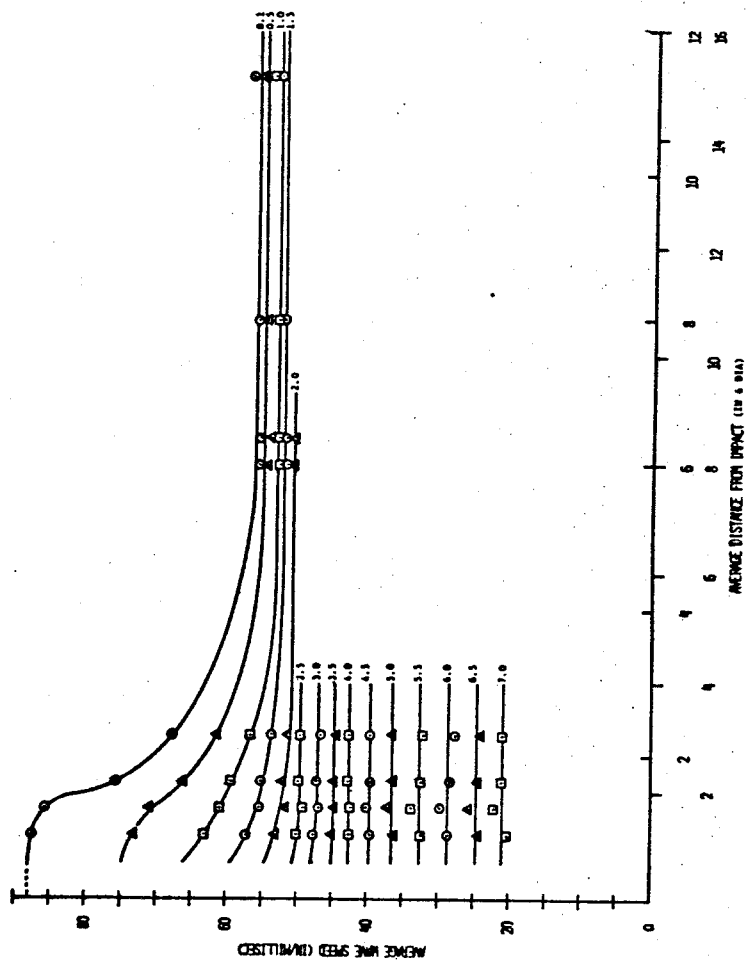
Figure 4.1   Average wave speeds along 0.741 inch diameter Lexan rods at 72°F
as a function of strain level and average distance from impact

The results for locations from 0.888 inches to 2.266 inches from
the impact site are computed using transit times of incident compressive
waves between different grating locations; the results for locations
from 5.991 inches to 8.004 inches are computed using transit times
between initial compressive loading and tensile reloading at the same
grating; the results at 11.361 inches are computed using transit times
of reflected tensile waves between different grating locations. In
reporting the strain wave speeds, no distinction is made between tensile
and compressive wave speeds, as there does not seem to be a significant
difference between the two for a given strain level, at least not for
small strains (see Figure 4.1).

According to Rinehart (57), the observed decrease in wave speeds
with increasing distance from the impact site for the lower strain
levels is due to the transformation of the initial dilatational wave
(uniaxial strain), which travels at a speed

$$c_d^2 = \frac{(1 - \nu)}{(1 - 2\nu)\,(1 + \nu)}\,\frac{E}{\rho} \quad , \tag{4.1}$$

into a rod wave (uniaxial stress), which travels at a speed

$$c_r^2 = \frac{E}{\rho} \quad , \tag{4.2}$$

where E, ν, and ρ are Young's modulus, Poisson's ratio, and the material
density, respectively. According to Rinehart, this transformation is
fairly well accomplished in a wave travel of two to three diameters down
the rod; however, from Figure 4.1, it seems that approximately eight
diameters of wave travel are required for this transformation, at least
for the lower strain levels. The more or less constant wave speeds for

the higher strain levels can probably be accounted for by a non-zero

rise time for the strain at the striker-specimen interface, so that the

higher strain levels originate at the impact face at later times than

the lower strain levels, and hence propagate through material which is

approaching an approximate state of uniaxial stress. Support for this

conjecture is provided by a plot of the times after impact - as a

function of striker velocity - at which various strain levels reach a

grating location at one-third diameter from the impact site. This plot -

made for tests 3, 36, 30, and 31 but not included here - shows that

these times decrease markedly with increasing striker velocity.

The highest average wave speed, 87.5 in/millisec, occurs between

one-third and two diameters from the impact site for 0.1 percent strain,

the smallest strain level considered. This value differs by 0.3 percent

from the value of 87.8 in/millisec for the dilatational wave speed in

Lexan at 72°F as given by Asay and Guenther (2).

Further use is made of these wave speed data in subsequent

sections.

4.4 Strain Wave Speeds for Approximate One-Dimensional Stress Conditions; Young's Modulus and Poisson's Ratio

In this section, the strain wave speeds under approximate uniaxial

stress conditions are found, and are used along with previous results

and the equations of linear elasticity to compute Young's modulus,

Poisson's ratio, and the shearing modulus for Lexan under dynamic

conditions. These values are then compared to published quasi-static

and dynamic values.

The wave speeds in Lexan at 72°F under approximate one-dimensional

stress conditions are given in the last column of Table 4.2, and are

plotted in Figure 4.2. These values are obtained by averaging the wave speed values to the right of the dotted line in Table 4.2. The wave speeds are found to be essentially constant for a given strain level in a range of strain rates of approximately 300 sec^{-1} to 2000 sec^{-1}. A fourth-order least-square polynomial fitted to this data gives an equation for wave speeds c as a function of strain e_L in Lexan for approximate one-dimensional stress conditions at 72°F, which is

$$c = 56.66508 - 3.54930e_L + 0.78076e_L^2 - 0.26414e_L^3 + 0.01724e_L^4 \quad , \quad (4.3)$$

where

c = wave speed at 72°F (in/millisec), and

e_L = absolute value of Lagrangian strain (percent).

This equation is shown as a solid line in Figure 4.2.

From Equation (4.3), the approximate one-dimensional stress wave speed in Lexan at 72°F is 56.7 in/millisec for very small strain; the dilatational wave speed for small strain from Table 4.2 is 87.5 in/millisec. By use of Equations (4.1) and (4.2), with the density ρ of Lexan taken as the manufacturer's published value of 1.20 grams/cm^3, values for Young's modulus E, Poisson's ratio ν, and the shearing modulus G for small strain in Lexan under dynamic conditions at 72°F are found to be

$$E = 3.61 \times 10^5 \text{ psi} \quad ,$$

$$\nu = 0.41 \quad ,$$

and

$$G = 1.28 \times 10^5 \text{ psi} \quad .$$
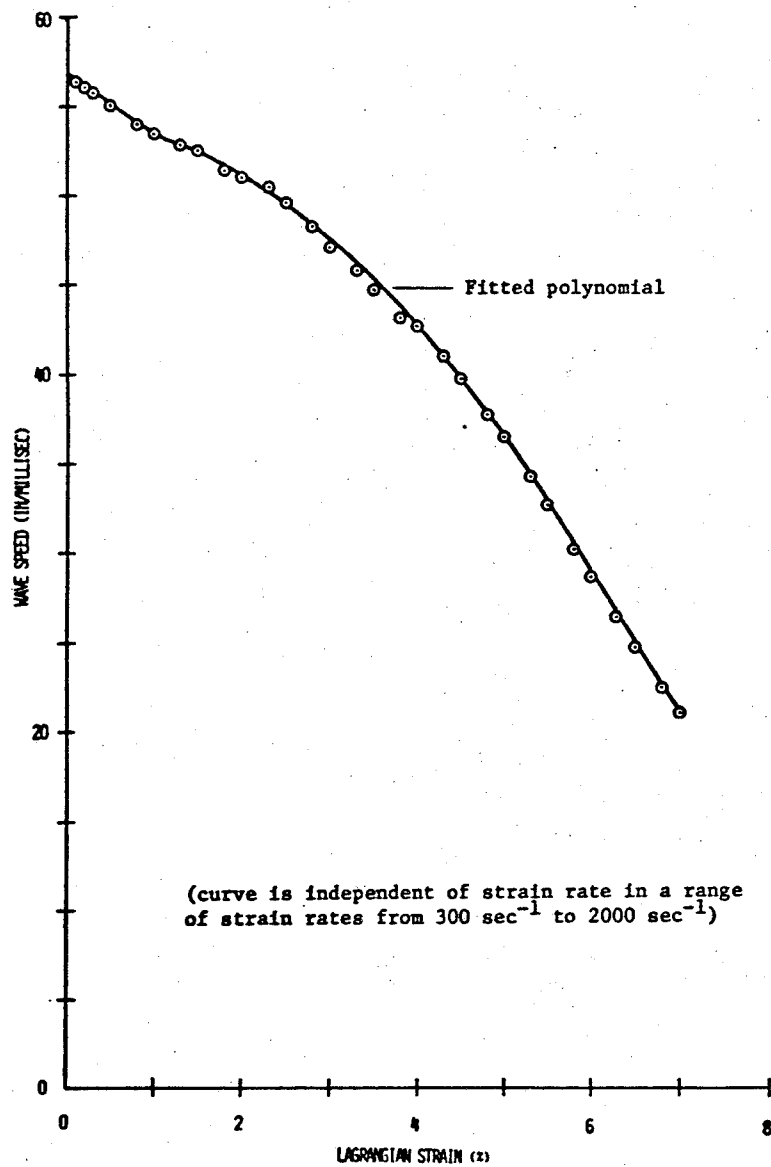
Figure 4.2　Strain wave speeds versus Lagrangian strain under approximate one-dimensional stress conditions in Lexan at 72°F

The value of G is computed from E and ν using the relation

$$G = \frac{E}{2(1 + \nu)} \ . \tag{4.4}$$

Quasi-static values of these elastic constants as reported by other investigators are discussed in the following paragraphs.

Approximate values found here in quasi-static tensile tests on round Lexan specimens machined from the rod used in these tests, at strain rates from 10^{-4} to 10^{-3} sec^{-1} and room temperature, are

$$E = 3.30 \times 10^5 \text{ psi}$$

and

$$\nu = 0.37 \ ,$$

which give

$$G = 1.20 \times 10^5 \text{ psi} \ .$$

Gurtman *et al.* (30) performed tensile tests on Lexan flat sheet at 74° ± 3°F, with maximum strain rates of 0.2 min^{-1}. They obtained the values

$$E = 3.1 \times 10^5 \text{ psi}$$

and

$$\nu = 0.38 \ ,$$

which give

$$G = 1.12 \times 10^5 \text{ psi} \ .$$

Whitfield and Smith (68), repeating some of the tests described by Gurtman, obtained for Young's modulus the value

$$E = 3.45 \times 10^5 \text{ psi} \quad .$$

They attributed the difference to the fact that Gurtman apparently did not account for strain outside the gage length when deducing strain from the head motion of the testing machine.

Data from the General Electric Company, obtained from standard ASTM tests at room temperature, give Young's modulus in both tension and compression as

$$E = 3.45 \times 10^5 \text{ psi} \quad .$$

(The General Electric Company provides a wide range of electrical, thermal, chemical, and elastic properties of Lexan).

Brill (16) performed tensile tests on flat specimens at strain rates on the order of 10^{-4} sec^{-1}, with the strains computed by using a grid placed on the specimens. He obtained the values

$$E = 3.3 \times 10^5 \text{ psi}$$

and

$$\nu = 0.32$$

which give

$$G = 1.25 \times 10^5 \text{ psi} \quad .$$

Stormont et al. (62) have found that the cold rolling of Lexan sheet to a 50 percent reduction in thickness leads to orthotropic behavior of the sheet, with large variations in elastic properties as measured in different directions. They report variations in Young's modulus from 3.96×10^5 psi to 2.44×10^5 psi and variations in Poisson's

ratio from 0.43 to 0.26, using tensile specimens cut parallel to or
perpendicular to the rolling direction, respectively.

Some published dynamic values of the elastic constants are
discussed in the following paragraph.

Asay and Guenther (2) measured the longitudinal (dilatational) and
shear wave speeds through 1-10 mm thick large Lexan sheets as a function
of temperature, and computed the elastic constants "by use of the
appropriate equations of elasticity." (The dilatational wave speed is
given in terms of the Lamé constants λ and G and the material density ρ
by the equation

$$c_d^2 = \frac{\lambda + 2G}{\rho} ,$$ (4.5)

the shear wave speed is given by

$$c_s^2 = \frac{G}{\rho} ,$$ (4.6)

and Young's modulus E is related to the Lamé constants by

$$E = \frac{G(3\lambda + 2G)}{\lambda + G}).$$ (4.7)

The values reported by Asay for the elastic constants at 77°F are

$$E = 3.73 \times 10^5 \text{ psi}$$

and

$$G = 1.45 \times 10^5 \text{ psi} ,$$

which give

$$\nu = 0.286 .$$

However, Asay's reported values for the shear and dilatational wave
speeds at 77°F, 0.908 mm/μsec and 2.22 mm/μsec, respectively, when used
in Equations (4.5) and (4.6) with the density of Lexan taken as 1.20
grams/cm^3, give the values

$$E = 4.02 \times 10^5 \text{ psi}$$

and

$$G = 1.44 \times 10^5 \text{ psi} \quad ,$$

which give

$$\nu = 0.40 \quad .$$

These values differ quite a bit from the previous set of values,
perhaps indicating some error in Asay's computation or a typographical
error in the publication of (2). From polynomials fitted by Asay to his
wave speed data (down to 77°F), an extrapolation to 72°F gives the shear
and dilatational wave speeds as 0.0359 in/μsec and 0.0878 in/μsec,
respectively. Use of these in Equations (4.5) and (4.6), with the
density of Lexan taken as 1.20 grams/cm^3, gives the values

$$E = 4.06 \times 10^5 \text{ psi}$$

and

$$G = 1.45 \times 10^5 \text{ psi} \quad ,$$

which give

$$\nu = 0.40 \quad .$$

The values of E, G, and ν computed from the experimental wave speed data
presented in this thesis differ from these last values by 11.1, 11.7,

and 2.5 percent, respectively. However, a comparison here is difficult,
as there does seem to be some inconsistency in (2).

4.5 A Dynamic Stress-Strain Relation for Lexan

In this section, a dynamic stress-strain relation for Lexan is
developed using some of the results of the von Karman rate-independent
theory of one-dimensional longitudinal stress wave propagation in rods
(42, 65) and the strain wave speeds found in Section 4.4 for approximate
one-dimensional stress conditions.

Von Karman's theory is based on the assumptions that:

1. Plane cross sections of the rod remain plane, with stress uniform
    across the cross section.

2. The lateral inertia effects are negligible.

3. The stress-strain relation during loading of the material is
    single-valued, concave toward the strain axis, and rate-independent,
    with the form $\sigma = \sigma(e)$, where σ and e are the "engineering" stress
    and strain, respectively.

Under these assumptions, one of the results of the theory is that
every strain increase from e to e + de (or every strain level e) travels
at a constant speed c given by the equation

$$c^2 = \frac{1}{\rho_o} \frac{d\sigma}{de} \quad , \tag{4.8}$$

where ρ_o is the initial material density and $d\sigma/de$ is evaluated at
strain e.

If it is assumed that the strain levels which exhibit the constant
wave speeds given in Table 4.2 are propagating under conditions which
satisfy the first two assumptions above to an acceptable degree of

approximation, then Equation (4.8) can be used to develop a dynamic stress-strain relation for Lexan, *i.e.*, from Equation (4.8), we have

$$\sigma = \rho_o \int_o^e c^2 \, de \quad .$$

(4.9)

Equation (4.3) for the strain wave speeds as a function of strain could be used in Equation (4.9) to give a dynamic stress-strain relation, but this would produce a rather unwieldly expression. Rather than do this, stress-strain data are calculated using the wave speeds as given by Equation (4.3) and an incremental relation developed from Equation (4.8), which is

$$\sigma(e + \Delta e) = \sigma(e) + \rho_o \left[\frac{c(e) + c(e + \Delta e)}{2} \right]^2 \Delta e \quad .$$

(4.10)

The density ρ_o is taken as the manufacturer's published value of 1.20 gram/cm^3 and Δe is taken as 0.001. The resulting dynamic stress-strain data for Lexan are plotted in Figure 4.3. A third-order least-squares polynomial fitted to this computed stress-strain data gives the equation

$$\sigma = 3560.64375e - 138.55185e^2 - 8.93634e^3 \quad ,$$

(4.11)

where

σ = absolute value of engineering stress (psi), and

e = absolute value of engineering strain (percent).

Equation (4.11) is shown plotted through the computed data in Figure 4.3, along with a quasi-static stress-strain curve for Lexan obtained from tensile tests made at a strain rate of 0.2 min^{-1}.
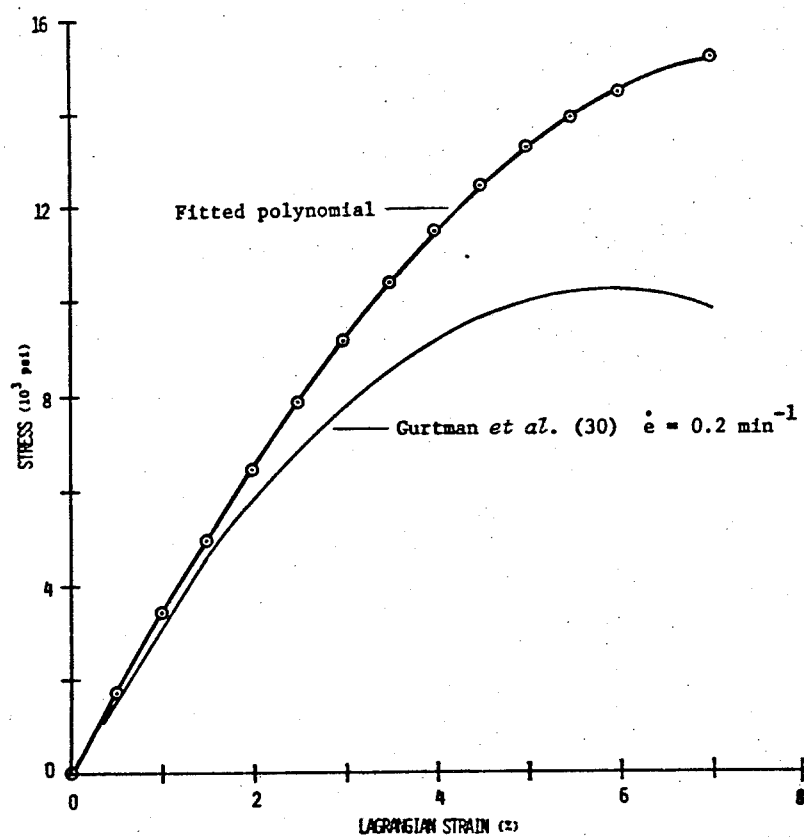
Figure 4.3 Dynamic stress-strain curve for Lexan at 72°F
(curve is independent of strain rate in a range
of strain rates from 300 sec^{-1} to 2000 sec^{-1})

This curve is one of a family of stress-strain curves obtained by Gurtman *et al.* (30) in tensile tests run at strain rates ranging up to 0.2 min^{-1}, which show higher stresses at given strains on curves run at higher strain rates. They found that the difference in stress between a "static" curve and a finite strain rate curve is closely proportional to $e^{2.6}ln(10^{7}\dot{e})$ for the strain rates used in the tests. Thus, it seems that the stress-strain curve found here may be a not inconsistent consequence of strain rates approximately 10^{6} times higher than those considered by Gurtman.

4.6   Poisson's Ratio as a Function of Strain Under Dynamic Conditions

In this section, the variation of Poisson's ratio with strain in Lexan under dynamic conditions is investigated using the strain-time history, the surface rotation-time history, and the strain wave speeds at a position along a rod. The procedure used is one employed by Bell (5, 6) to investigate the variation of Poisson's ratio with strain in fully-annealed 1100F aluminum under dynamic conditions. The necessary relationships are developed in the following paragraph.

If it is assumed that the rod under consideration is in a state of uniaxial stress which is uniform over the cross section of the rod, then the strains in the plane of the cross section are equal in all directions and uniform over the cross section; consequently, the radial displacement u_r of the outer surface of the rod can be expressed as

$$u_r = R\nu e \quad , \tag{4.12}$$

where axial compressive strain e is taken positive and R is the initial radius of the rod. With the coordinate x measured along the rod in the

direction of wave propagation, the surface rotation ω is given by

$$\omega = \frac{\partial u_r}{\partial x} \quad , \qquad (4.13)$$

where Equation (4.13) has the proper sign for ω corresponding to the surface rotation-time data in Appendix 6.1. From Equations (4.12) and (4.13), with $\nu = \nu(e)$ and $e = e(x,t)$,

$$\omega = R \frac{\partial}{\partial x} (\nu e) = R \left[e \frac{\partial \nu}{\partial x} + \nu \frac{\partial e}{\partial x} \right] = R \left[e \frac{d\nu}{de} + \nu \right] \frac{\partial e}{\partial x} \quad . \qquad (4.14)$$

To express Equation (4.14) in a more useful form, a substitution is made for the term $\partial e / \partial x$. Consider the propagation of a given strain level

$$e(x,t) = \text{constant}$$

along the rod. The total derivative gives

$$de = \frac{\partial e}{\partial x} dx + \frac{\partial e}{\partial t} dt = 0 \quad ,$$

from which the wave speed of that constant strain level is

$$c = \frac{dx}{dt} = - \frac{\partial e / \partial t}{\partial e / \partial x} \quad , \qquad (4.15)$$

giving

$$\frac{\partial e}{\partial x} = - \frac{1}{c} \frac{\partial e}{\partial t} \quad . \qquad (4.16)$$

Thus, the term $\partial e / \partial x$ can be expressed by Equation (4.16), which involves quantities readily determined from the strain wave speed data and the axial strain-time histories. Substitute Equation (4.16) into Equation

(4.14) and rearrange to obtain a first-order, linear, ordinary
differential equation for ν as a function of e, which is

$$\frac{d\nu}{de} + \frac{1}{e}\nu = -\frac{\omega c}{R(\partial e/\partial t)} = g(e) \quad , \tag{4.17}$$

where the function

$$g(e) = -\frac{\omega c}{R(\partial e/\partial t)} \tag{4.18}$$

must be determined from the experimental data. Solution of Equation
(4.17) by standard methods gives

$$\nu(e) = \frac{1}{e}\left[\int g(e)de + c_1\right] \quad , \tag{4.19}$$

where c_1 is a constant of integration to be determined.

The variation of Poisson's ratio with strain is investigated by
developing a $\nu(e)$ relationship from each of two sets of tests. Test sets
LS2-17, 19 and LS2-28, 29 are selected because of the reproducibility of
their strain-time and surface rotation-time data, and because their
grating locations are furthest of all tests from the impact face, so
that stress conditions there are most nearly one-dimensional.

The functions g(e) for the two sets of tests are determined as
follows. Fifth-order least-squares polynomials are fitted to the initial
sharply-rising portions of the strain-time data, with a second-order
polynomial fitted to the slowly-rising latter portion of the e-t data
in tests LS2-28, 29. Data points affected by unloading waves are not
included. The polynomials fitted to the e-t data have the functional
form t = t(e); at the particular grating location, these polynomials

determine the arrival time t of a given strain level e, and the slope $\partial e/\partial t$ of the e-t curve at that strain level. The surface rotation-time data for tests LS2-17, 19 are fitted by a fifth-order polynomial; data and polynomial are shown in Figure 4.4. The ω-t data for tests LS2-28, 29 are fitted by a third-order polynomial to t = 55 μsec, and by a fifth-order polynomial from t = 52 μsec to 152 μsec; data and polynomials are shown in Figure 4.5. The polynomials fitted to the ω-t data have the functional form $\omega = \omega(t)$. The wave speeds c(e) at the grating location are determined from Figure 4.1 and/or the data in Table 4.2. These polynomials and wave speed data are combined in a computer program using Equation (4.18) to calculate the functions g(e) for tests LS2-17, 19 and tests LS2-28, 29. The results of these calculations are shown in Figures 4.6 and 4.7.

To evaluate $\nu(e)$, the g(e) data for tests LS2-17, 19 and tests LS2-28, 29 are fitted with sixth- and seventh-order polynomials, respectively - shown in Figures 4.6 and 4.7 - which are then used in Equation (4.19). The constant c_1 in Equation (4.19) is evaluated by setting ν = 0.41 at e = 1.5 percent strain; it is necessary to use e = 1.5 percent since the nature of Equation (4.19), the difficulty of obtaining $\partial e/\partial t$ at low strains, and the high order of polynomials used to fit the experimental data cause the $\nu(e)$ data to be erratic for low strains. The results of these calculations are shown in Figure 4.8, which indicates that Poisson's ratio remains between approximately 0.41 and 0.43 up to a strain of approximately 4 percent, where it begins to increase in an almost linear fashion until it reaches 0.5 at 7 percent strain, the largest strain considered in this calculation.
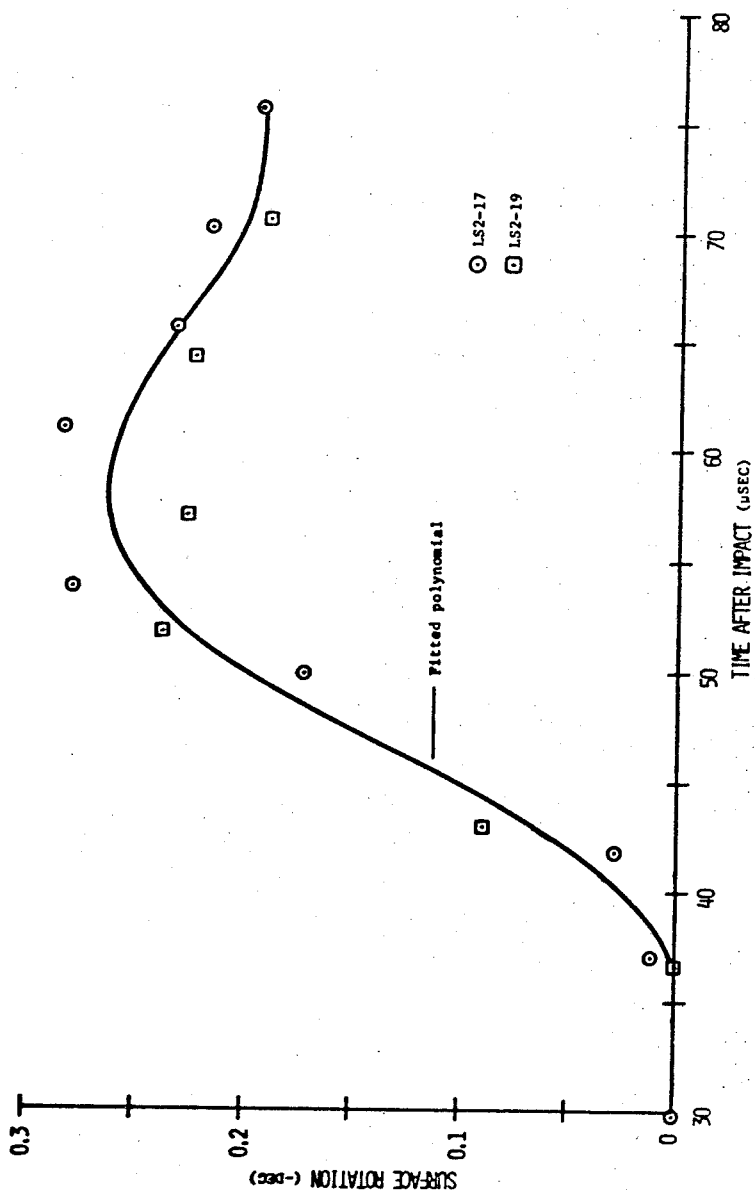
Figure 4.4   Surface rotation ω versus time after impact for tests LS2-17 and LS2-19

68
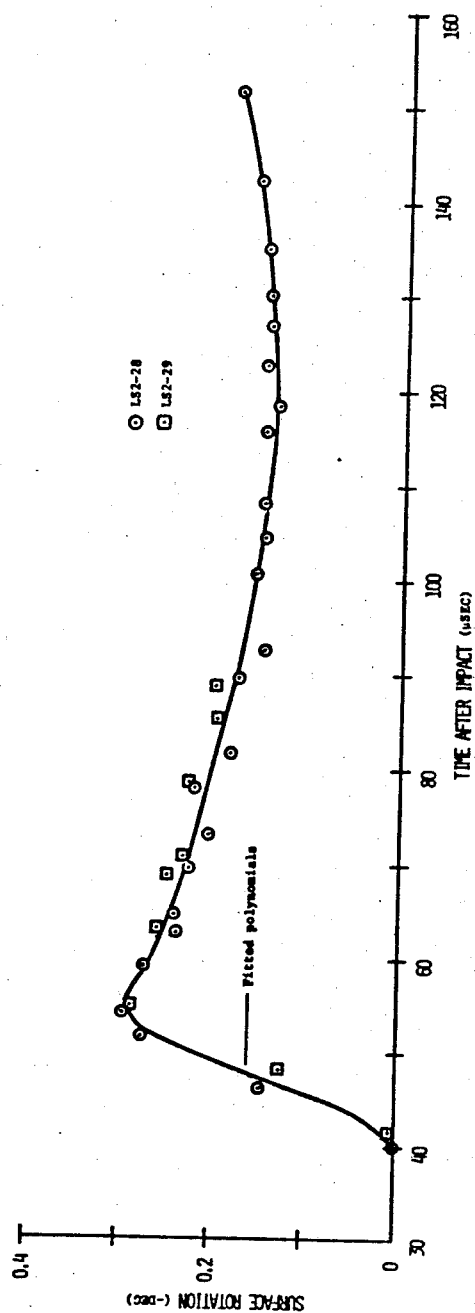
Figure 4.5 Surface rotation ω versus time after impact for tests LS2-28 and LS2-29
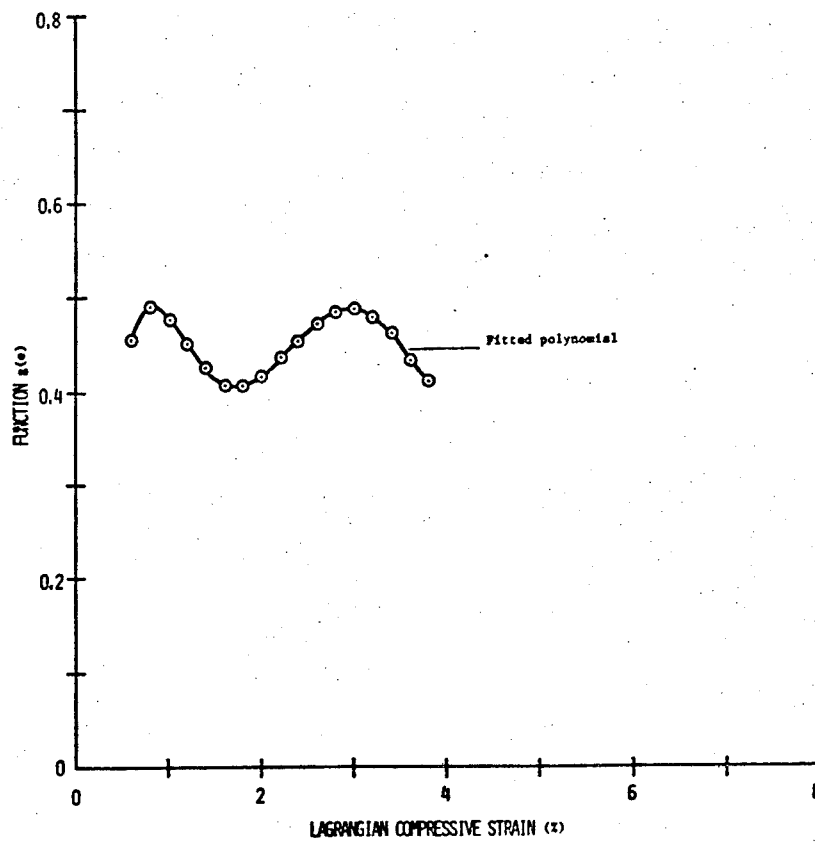
Figure 4.6   Function g(e) for tests LS2-17 and LS2-19
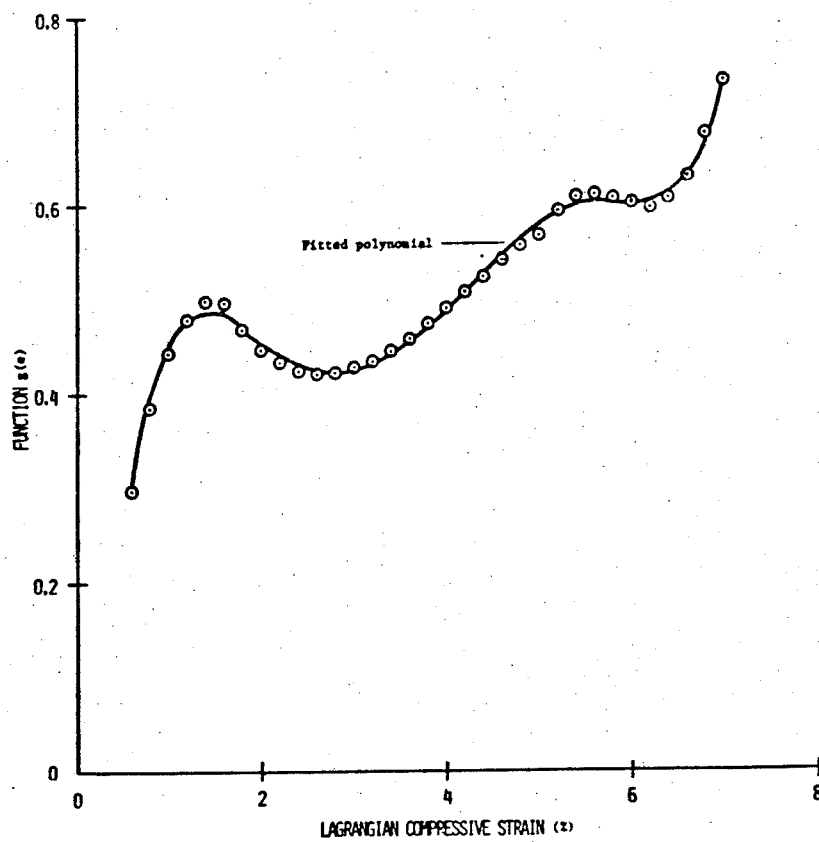
Figure 4.7   Function g(e) for tests LS2-28 and LS2-29
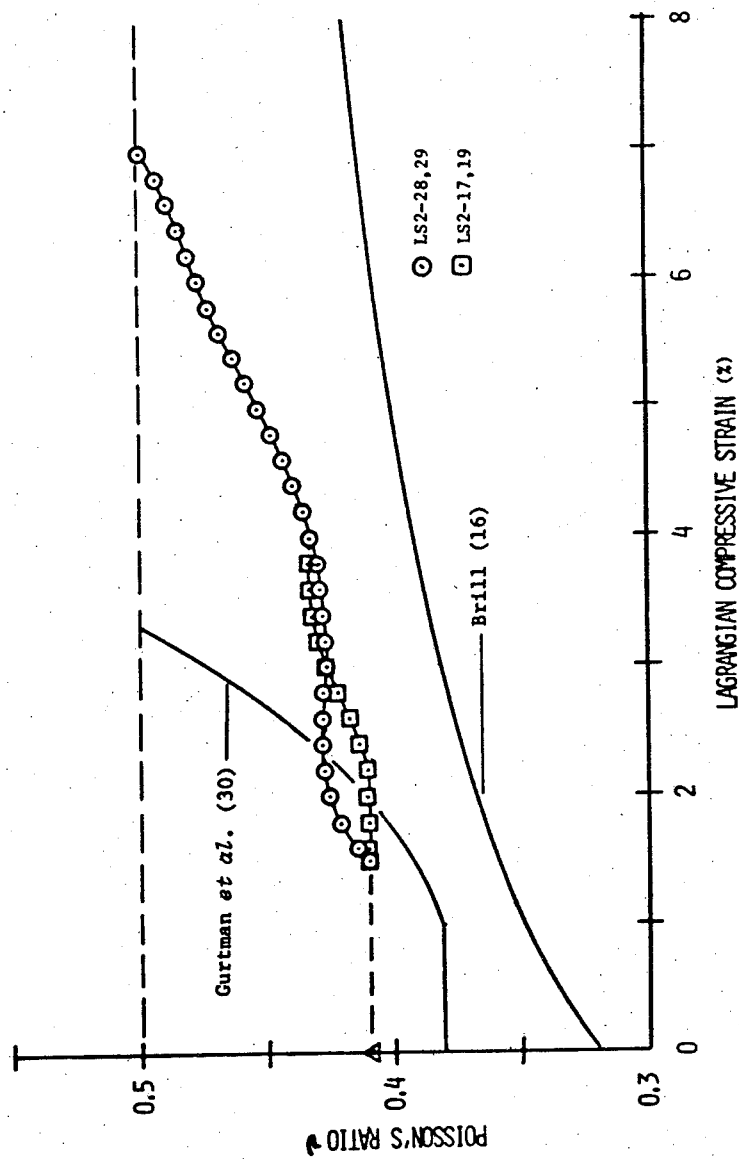
Figure 4.8 Poisson's ratio as a function of strain under dynamic conditions at 72°F and strain rates of 300 sec^{-1} to 2000 sec^{-1}.

The discrepancy between the two sets of $\nu(e)$ data probably is due to scatter in the ω-t data in tests LS2-17, 19; from Figure 4.4 and Appendix Figure 6.8, this scatter is seen to persist to t = 65 μsec, corresponding to e = 3 percent, at which time the two sets of $\nu(e)$ data in Figure 4.8 converge.

Several investigators report variations in Poisson's ratio with strain as found from quasi-static tensile tests. Gurtman *et al.* (30) report that Poisson's ratio is 0.38 up to a strain of approximately 1 percent, where it begins to increase until it reaches a limiting value of 0.5 at approximately 3.3 percent longitudinal strain. Brill (16) reports that Poisson's ratio increases gradually from 0.32 to approximately 0.42 at 8 percent longitudinal strain. Thus, there seems to be little agreement on this point, as seen from Figure 4.8.

4.7   Yield Point Strain in Lexan Under Compressive Pulse-Type Loading

In this section, the yield point strain in Lexan rods subjected to compressive short-duration (approximately 120 μsec) loading-unloading pulses is investigated by recording the strain-time histories at selected grating sites on impacted rods, then making post-test measurements of the grating groove spacing to determine the amount (if any) of permanent plastic deformation.

The yield point strain in Lexan for pulse-type loadings is investigated using tests LS2-3, 30, 31, and 36. In these tests, strain-time histories are recorded at locations approximately 1/4 inch from the impact site, using one-inch strikers traveling at velocities up to 700 ft/sec. The strain-time data for these tests are shown in Appendix Figures 6.10 and 6.11; these e-t histories, along with post-test

measurements of the grating groove spacing made approximately 5 minutes after impact, show that the yield point strain for this type of loading is approximately 11.5 percent. The 11.5 percent yield point strain in compression for this type of loading is almost double the approximately 6 percent at which tensile specimens in quasi-static tests exhibit large-scale yielding (16, 30). The e-t histories in these tests also show a marked change in the character of the unloading as the yield point strain is exceeded (compare tests LS2-3 and LS2-36 with tests LS2-30 and LS2-31).

4.8 Effect of a Previous Impact on the Strain-Time History During a Second Impact

In this section, the effect of a previous elastic impact on the strain-time history obtained during a subsequent impact is investigated by subjecting Lexan specimens to two separate impacts under essentially identical conditions.

To study the effect of a previous elastic impact on a subsequent strain-time history, two specimens which had previously been impacted (tests LS2-5 and LS2-8) were impacted a second time under the same conditions (tests LS2-25 and LS2-24); the previous and subsequent strain-time histories for the specimens are compared in Figure 4.9. Test LS2-8 has not been included in Figure 4.9 since its surface rotation behavior was aberrant, indicating that the impact in test LS2-8 was somewhat non-axial. Figure 4.9 indicates that a previous impact which produces an elastic strain-time history has no significant effect on the strain-time history produced by a second impact.
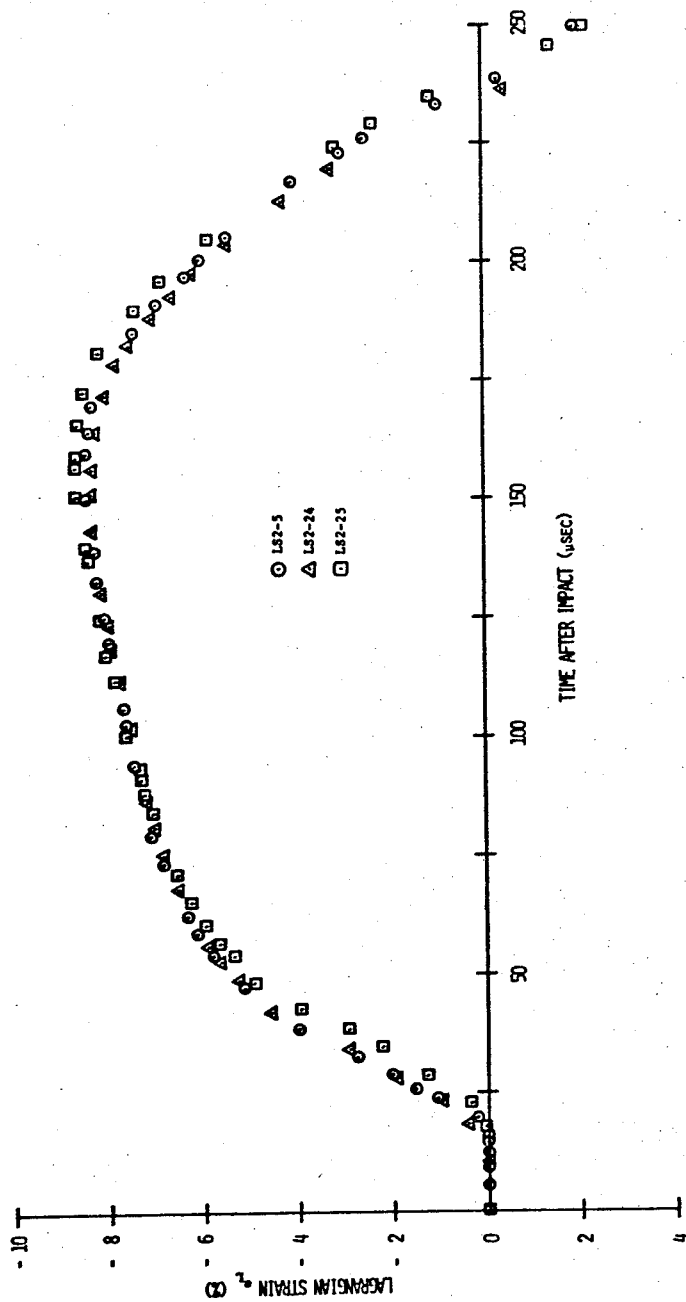
Figure 4.9 Lagrangian strain e_L versus time after impact for tests LS2-5, LS2-24, and LS2-25

75

4.9   Prediction of Strain-Time Histories

In this section, predictions are made of some of the experimentally observed strain-time histories in impacted Lexan rods. These predictions are undertaken as a check on the accuracy of the experimentally-determined constant strain wave speeds under approximate one-dimensional stress conditions and to test the feasibility of predicting - in a simple fashion - the strain-time history at a point along a Lexan rod given the strain-time history at some other point. The predictions are made assuming that strain level superposition is valid, and that each strain level propagates at a constant speed as found in Section 4.4 and given in Table 4.2 and Figure 4.1.

Predictions are first made for the tensile reloading portions of the strain-time histories of tests 13 and 27, tests 15 and 16, and tests 17 and 19. The strain-time histories for these tests are shown in Appendix Figures 6.6, 6.7, and 6.8, respectively, and represent wave travel between approximately three and 14 diameters from the impact site. Thus, since the waves are propagating under conditions which should approximate one-dimensional stress, the results of the predictions should afford some check on the accuracy of the experimentally-determined strain wave speeds, as well as give some indication of the utility of the prediction procedure. The predictions are made according to the following procedure, which disregards the presence of the Lexan guide rings on the specimen. The initial compressive loading-unloading portions of the e-t histories are assumed to be the result of the superposition of two different effects: a compressive strain wave which rises to the maximum compressive strain, $-e_m$, and thereafter remains constant, and a following tensile strain wave which rises to a tensile

strain, e_m, and thereafter remains constant. These two waves are assumed to propagate along the rod uninfluenced by each other, with each strain level propagating at its constant wave speed as given by Equation 4.3. The striker and specimen are assumed to separate when the first tensile strain wave - from the initial compressive strain wave which reflects from the free rear of the specimen as a tensile strain wave - reaches the already-unloaded striker-specimen interface. Thus, both ends of the specimen are treated as free as regards wave reflection at these boundaries. Then, at a given time, the strain at a given position is predicted by superposing the various tensile and compressive strain levels in the various direct and reflected strain waves which have reached that position by that time, using 0.1 percent strain increments. The results of this procedure are shown in Figures 4.10, 4.11, and 4.12.

Examination of the experimental and predicted strain-time histories in Figures 4.10, 4.11, and 4.12 shows that:

1. The tensile loading portions of the strain-time histories are predicted fairly well, indicating that the experimentally determined strain wave speeds are fairly accurate and that the prediction procedure is of some utility. The recorded parts of the unloading portions of the tensile e-t histories of tests 13, 27 and tests 15, 16 are not predicted as well, although this may be due in part to the scatter which has started to occur in the experimental data; unfortunately, the 250 µsec recording time was not long enough to allow the entire tensile unloading process to be observed, so that the ultimate success or failure of the prediction in this region remains somewhat in doubt.
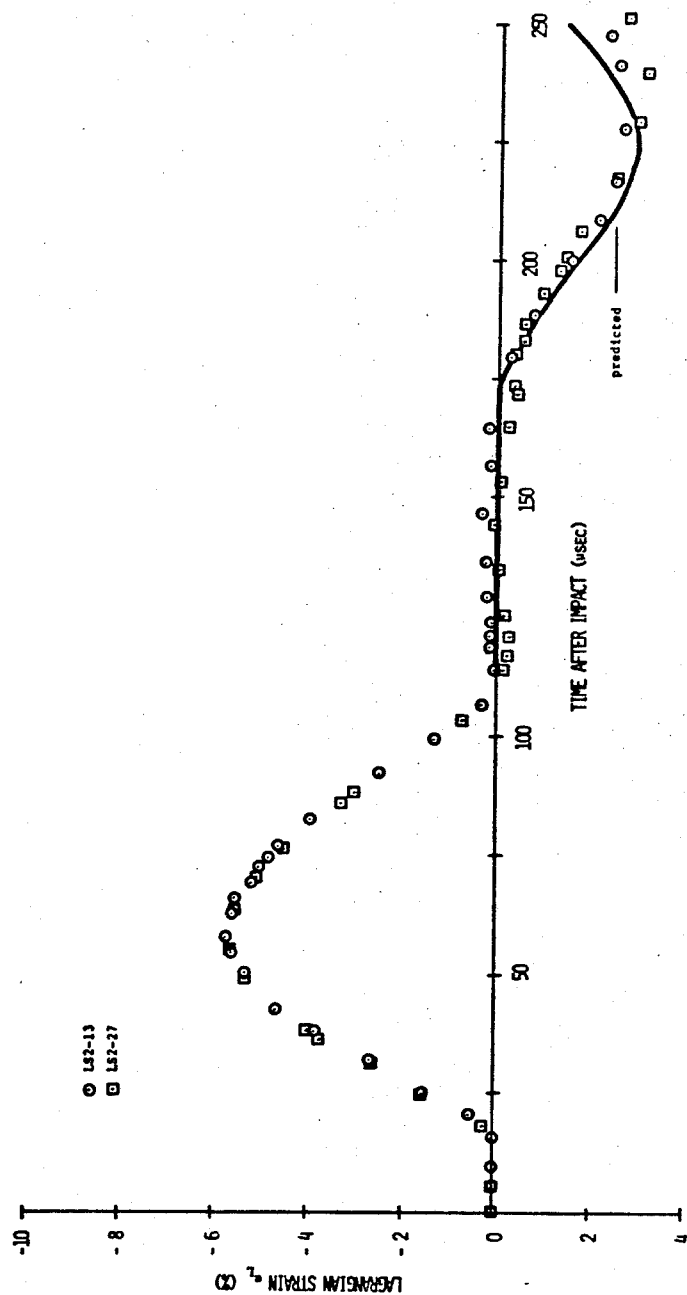
Figure 4.10 Experimental and predicted tensile reloading strain-time histories for tests LS2-13, 27

78
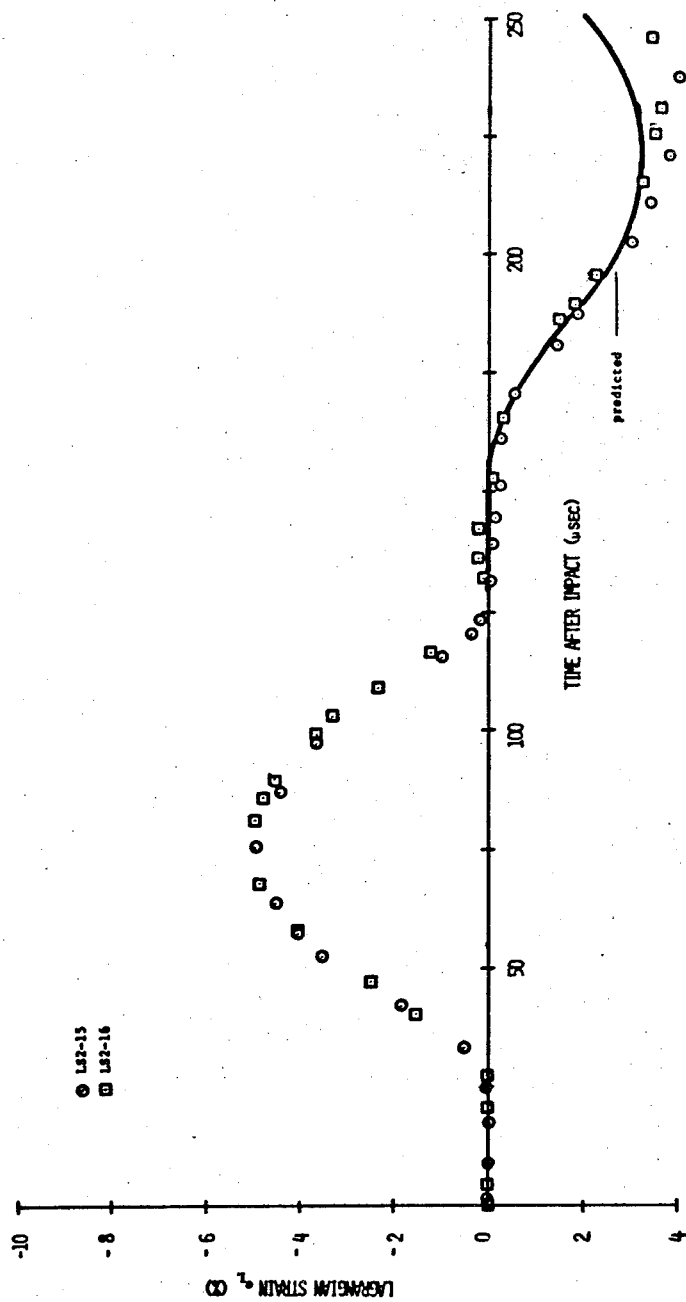
Figure 4.11   Experimental and predicted tensile reloading strain-time histories for tests LS2-15, 16
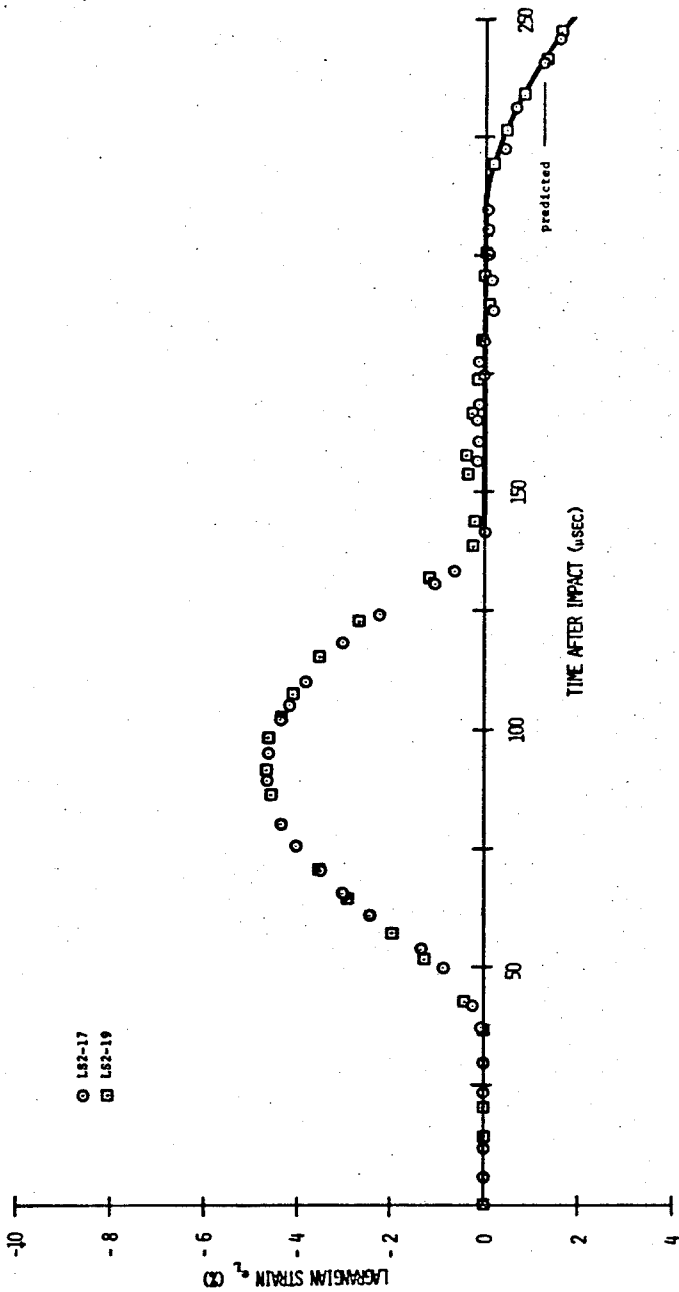
Figure 4.12   Experimental and predicted tensile reloading strain-time histories for tests LS2-17, 19

2. The Lexan guide rings fitted to the specimens do not affect

   significantly the strain wave propagation in the rod: the

   experimental strain-time histories follow closely the predicted

   strain-time histories which neglect the presence of the guide

   rings, indicating that there is no appreciable wave reflection

   from the guide rings.

   As a more rigorous test of the prediction procedure, a prediction

is made - using basically the same procedure as just described - of the

entire strain-time history of test LS2-22. Test LS2-22 involves the

impact of a 0.996 inch long striker on a 2.898 inch long Lexan specimen

which is epoxied to a 15 inch long mild steel back-up bar, with the

grating location 2.135 inches from the impact site (0.763 inch from the

Lexan-steel interface). The input data are taken from the initial

compressive loading-unloading e-t history of tests LS2-13, 27 - which is

taken at 1.517 inches from the impact face - and is treated as the sum

of a compressive strain wave and a tensile strain wave as described

previously. The prediction of the strain-time history for test LS2-22

involves a much more complicated situation than before, so some additional

assumptions and preliminary predictions are necessary before the e-t

history for LS2-22 can be predicted:

1. The presence of the foil switch on the noses of striker and

   specimen is disregarded in considering wave propagation across

   the striker-specimen interface.

2. The contact or separation of the striker-specimen interface and

   the Lexan-steel interface will greatly influence the e-t history,

   so separate predictions are made of the e-t histories at these

   two interfaces. At the Lexan-steel interface, a compressive

strain pulse lasting from 40 µsec to 157 µsec after impact is predicted, with a maximum strain of 10.3 percent at 90 µsec after impact; a tensile strain pulse is predicted to begin at the interface at 178 µsec after impact. Since the epoxy bond at the interface is most likely broken by the initial compressive strain pulse, separation of the Lexan-steel interface is assumed to occur at t = 178 µsec, after which the specimen rear is treated as a free end as regards wave reflection. Until t = 178 µsec, the Lexan interface is assumed completely fixed, *i.e.*, total wave reflection at the interface is assumed. At the striker-specimen interface, the initial three-dimensional strain effects render an e-t prediction of the nature attempted here a bit dubious; nevertheless, striker-specimen separation is assumed to occur with the first predicted tensile strain at the interface - which occurs at 168 µsec after impact - after which the specimen nose is assumed to be free. However, the oscilloscope record which monitors the contact switch on the nose of the specimen and striker during the test indicates continuous contact from t = 0 to t = 70 µsec, rapid making and breaking of contact - with predominately contact - from t = 70 µsec to 150 µsec, then breakage of contact except for one brief contact at approximately 167 µsec. On this basis, a prediction of the e-t history for LS2-22 is also made assuming striker-specimen separation at t = 150 µsec. As will be seen from the predicted e-t curves, the condition of the striker-specimen interface considerably influences the e-t prediction.

3. At the time that striker-specimen separation is assumed to occur, various levels of direct and reflected tensile and compressive strain waves are present at the interface, some about to cross

the interface from specimen to striker, and others just entering
the specimen from the striker. Separation of the striker and
specimen introduces discontinuities in these various waves, since
portions of the waves are captured in the separated striker. These
discontinuities are assumed to disperse in the specimen in accordance
with the constant wave speeds used in this analysis; strain levels
reaching the interface after separation are treated by simple
reflection from the free end. (This discontinuity condition does
not arise at the Lexan-steel interface, which is unloaded for a
time before separation).

With these additional assumptions and supplementary predictions, the
strain-time history for test LS2-22 can be predicted; the results of
this prediction are shown in Figure 4.13.

Examination of the experimental and predicted strain-time histories
in Figure 4.13 shows that:

1. The compressive loading portion of the experimental strain-time
    history - which exhibits the effects of strain intensification due
    to strain wave reflection from the steel interface - is predicted
    remarkably well except for its maximum amplitude.

2. The shape of the compressive unloading portion of the strain-time
    history is predicted very well, with an approximately uniform
    difference in amplitude between experimental and predicted
    histories.

3. The latter portion of the predicted strain-time history is markedly
    affected by the assumed time of separation of striker and specimen;
    the approximate time of separation as determined from the
    experimental record provides the best prediction.
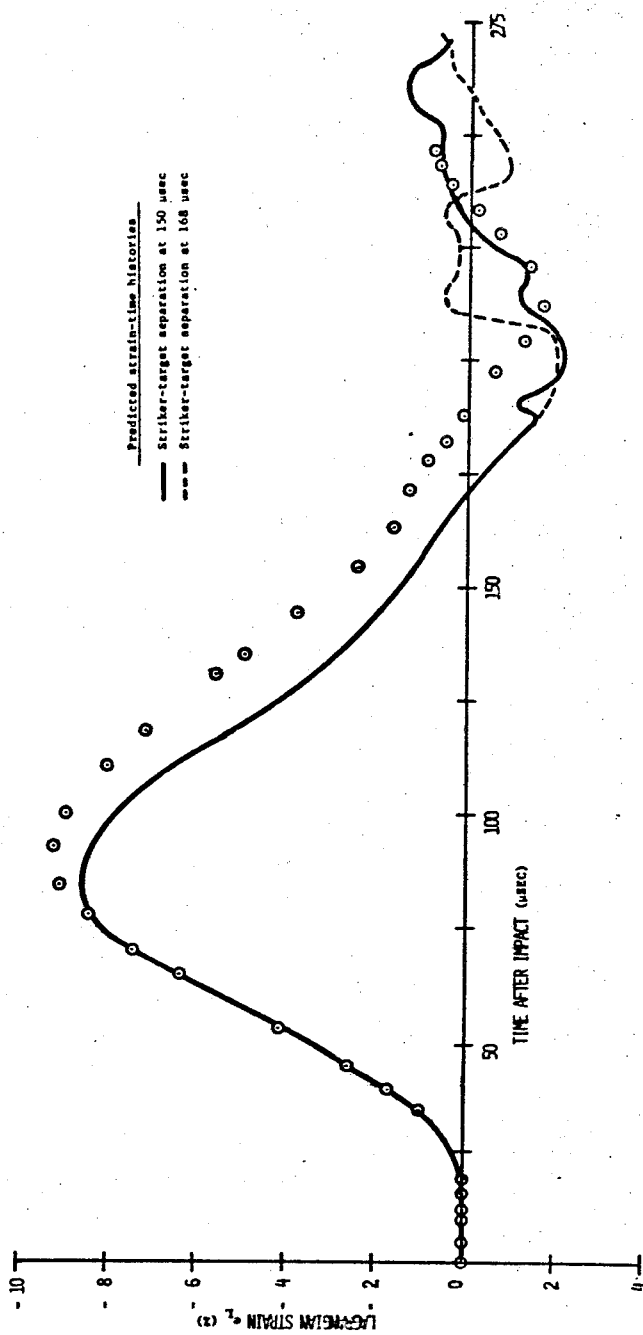
Figure 4.13 Experimental and predicted strain-time histories for test LS2-22

84

Over-all, the predicted strain-time history agrees fairly well with the experimental history – this in spite of the elementary procedure used to make the prediction, and the fact that the test conditions hardly approximate one-dimensional stress.

The results of this section indicate that the experimentally-determined strain wave speeds under approximate one-dimensional stress conditions are fairly accurate, and that the approximate procedure presented for determining strain-time histories is of some utility.

4.10 Summary of Experimental Results and Recommendations for Future Investigations

The experimental system described in this thesis has been applied with some success to the investigation of the propagation of large-amplitude strain waves in Lexan rods subjected to high-speed axial impact. The quality of the surface strain-time and surface rotation-time data indicates that the experimental system is an excellent one for studies of this type of phenomenon, at least in certain materials. Strains to 20 percent and strain rates to 15,700 sec^{-1} – which do not represent the upper limits of the system's capability – are recorded in the investigation. The strain-time data are estimated to be accurate within approximately 0.002 in/in and 0.1 μsec for strain and time, respectively.

Analysis of the experimental data leads to the following observations and conclusions. The results of major importance are:

1. A dynamic stress-strain relation for Lexan at 72°F at strain rates of approximately 300 sec^{-1} to 2000 sec^{-1} is described by a third-order least-squares polynomial fitted to computed stress-strain data:

$$\sigma = 3560.64375e - 138.55185e^2 - 8.93634e^3 \, ,$$

where

      σ = absolute value of engineering stress (psi), and

      e = absolute value of engineering strain (percent).

The stress-strain data are computed from the strain wave speed data for approximate one-dimensional stress conditions using von Karman's rate-independent theory of one-dimensional longitudinal stress wave propagation in rods. This dynamic stress-strain curve is not inconsistent with the published results of quasi-static tests on Lexan at strain rates up to 0.2 $\min^{-1}$, which show higher stresses at given strains on curves run at higher strain rates (30).

2. Reasonably successful predictions of the strain-time histories at points along an impacted Lexan rod can be made using the strain-time history at some other point along the rod and an approximate procedure which assumes strain level superposition and constant strain wave speeds.

3. At 72°F and strain rates of approximately 300 sec^{-1} to 2000 sec^{-1}, Poisson's ratio is found to remain between approximately 0.41 and 0.43 up to about 4 percent strain, where it begins to increase in an almost linear fashion to 0.5 at 7 percent strain. This behavior differs markedly from two sets of reported quasi-static data (16, 30), which differ even more markedly from each other; thus there seems to be little agreement on this point. Poisson's ratio as a function of strain is determined here using a procedure employed by Bell (5,6) which utilizes the strain-time history, the surface

rotation-time history, and the strain wave speeds at a point along
a rod.

The results of lesser importance are:

4. The dilatational wave speed and the rod wave speed are found to be
   c_d = 87.5 in/millisec and c_r = 56.7 in/millisec, respectively, for
   a strain level of approximately 0.1 percent. This value of the
   dilatational wave speed differs by 0.3 percent from a published
   value (2).

5. Dynamic values for Young's modulus, Poisson's ratio, and the
   shearing modulus are found to be E = 3.61×10^5 psi, ν = 0.41,
   and G = 1.28×10^5 psi. These values are calculated using the
   dilatational and rod wave speeds for approximately 0.1 percent
   strain and the equations of linear elasticity. The dynamic value
   found for E is approximately 10 percent higher than published
   quasi-static values, and approximately 3 percent lower than a
   published dynamic value (2).

6. An impact which produces only elastic strains in a Lexan rod seems
   to have no significant effect on the strain-time behavior during
   a second impact under the same conditions.

7. The yield point strain is approximately 11.5 percent in Lexan
   subjected to compressive short-duration (approximately 120 μsec)
   loading-unloading pulses. This is almost double the 6 percent
   strain at which specimens exhibit large-scale yielding under
   quasi-static conditions (16, 30).

8. The strain wave speeds in Lexan under approximate one-dimensional
   stress conditions are found to be essentially constant for a given
   strain level. A fourth-order least-squares polynomial fitted to

the wave speed data gives the wave speeds as a function of strain at strain rates of 300 sec^{-1} to 2000 sec^{-1}:

$$c = 56.66508 - 3.54930e_L + 0.78076e_L^2 - 0.26414e_L^3 + 0.01724e_L^4 \quad ,$$

where

        c = wave speed at 72°F (in/millisec), and

        e_L = absolute value of Lagrangian strain (percent).

9. The wave speeds for the lower strain levels - less than 4 percent - are found to decrease with increasing distance from the impact site, becoming essentially constant by the time they have propagated approximately eight diameters from the impact site. The higher strain levels - above 4 percent - do not exhibit decreases in wave speeds, but travel at essentially constant speeds from the impact site. The decrease in wave speeds for the lower strain levels is attributed to the transformation of the initial dilatational wave (uniaxial strain) into a rod wave (uniaxial stress) as the waves travel along the rod. The constant wave speeds for the higher strain levels are attributed to a non-zero rise time for the strains at the impact site, so that higher strain levels propagate through material in an approximate state of uniaxial stress.

It is hoped that these results will afford a better understanding of some of the aspects of the dynamic behavior of Lexan, and will be useful in design applications which utilize this material to fabricate objects subjected to severe dynamic environments.

In the course of this study, several topics have suggested themselves as possibilities for further investigation in this area:

1. As an extension of the investigation reported here, a similar series of tests could be conducted to refine the results presented here and to extend these results to higher strain levels. This would require longer specimens and strikers to afford more recording time before unloading begins at a grating site, higher striker velocities to produce higher strain levels, and grating locations numerous enough and far enough from the impact site to afford a more accurate determination of the strain wave speeds. None of these requirements are outside the capabilities of the present system.

2. It might be possible to predict the strain-time behavior of an impacted Lexan rod - at least in regions where conditions approximate uniaxial stress - by using one-dimensional viscoelastic wave theory. Watson (66) has used this approach - with success - to predict strain-time histories for the case of a strain pulse of 0.1 percent amplitude propagating along a slender Lexan rod.

3. A study could be made of the influence of maximum strain and pulse duration on the permanent deformation suffered by Lexan rods subjected to pulse-type loading, thereby defining different strain-time histories which produce the same permanent deformation. The maximum strain amplitude and pulse duration can be varied by changing the striker velocity and striker length, respectively.

4. The influence of strain rate on the dynamic stress-strain relation for Lexan could be studied by performing tests similar to those reported here; by judiciously varying striker velocity and grating location so that strain wave velocity data - and hence the dynamic stress-strain relations derived therefrom - are within a desired range of strain rates, it might be possible to develop a

stress-strain-strain rate relation for Lexan which would encompass
a wide range of conditions.

5. A numerical study of two-dimensional wave propagation in Lexan rods
   using the material properties found here might be made and compared
   to experimental results in order to verify or to disprove the
   accuracy of these material properties.

It should be noted that these suggestions for further work are tentative;
close examination may show some or all not to be feasible.

5 LIST OF REFERENCES

1. Abramson, H. N., H. J. Plass, and E. A. Ripperberger. 1958.
     Stress wave propagation in rods and beams. Advances in
     Applied Mechanics 5:111-194.

2. Asay, J. R., and A. H. Guenther. 1967. Experimental determination
     of ultrasonic wave velocities in plastics as functions of
     temperature. IV. Shear velocities in common plastics.
     Journal of Applied Polymer Science 11:1087-1100.

3. Bell, J. F. 1956. Determination of dynamic plastic strain through
     the use of diffraction gratings. Journal of Applied Physics
     27(10):1109-1113.

4. Bell, J. F. 1956. 10,000 threads to the inch! American Machinist,
     July, pp. 112-113.

5. Bell, J. F. 1959. Propagation of plastic waves in solids. Journal
     of Applied Physics 30(2):196-201.

6. Bell, J. F. 1960. Propagation of large amplitude waves in annealed
     aluminum. Journal of Applied Physics 31(2):277-282.

7. Bell, J. F. 1962. Experimental study of dynamic plasticity at
     elevated temperatures. Experimental Mechanics 2(6):181-186.

8. Bell, J. F. 1964. The initiation of finite amplitude waves in
     annealed metals, pp. 166-182. In H. Kolsky and W. Prager
     (eds.), Stress Waves in Anelastic Solids. Springer-Verlag,
     Berlin, Germany.

9. Bell, J. F. 1965. The dynamic plasticity of metals at high strain
     rates - an experimental generalization, pp. 19-41. In N. J.
     Huffington (ed.), Behavior of Materials Under Dynamic Loading.
     American Society of Mechanical Engineers, New York.

10. Bertholf, L. D. 1966. Longitudinal elastic wave propagation in
     finite cylindrical bars. Unpublished PhD thesis, Department
     of Engineering Science, Washington State University, Pullman,
     Washington. University Microfilms, Inc., Ann Arbor, Michigan.

11. Bertholf, L. D. 1967. Numerical solution for two-dimensional
     elastic wave propagation in finite bars. Journal of Applied
     Mechanics 34(9):725-734.

12. Bertholf, L. D., and C. H. Karnes. 1969. Axisymmetric elastic-
     plastic wave propagation in 6061-T6 aluminum bars of finite
     length. Journal of Applied Mechanics 36(9):533-541.

13. Bingham, W. L., R. A. Douglas, and W. L. Liddell. 1970. Plastic
    wave detection and measurement by diffraction, pp. 87-95. In
    B. Washburn (ed.), Proceedings of the Sixteenth International
    ISA Aerospace Instrumentation Symposium, May 11-13, 1970,
    Seattle, Washington, Instrumentation in the Aerospace Industry,
    vol. 16. Instrument Society of America, Pittsburgh,
    Pennsylvania.

14. Blake, H. W. 1970. General optical diffraction-strain relationships.
    Unpublished PhD thesis, Department of Engineering Mechanics,
    North Carolina State University at Raleigh, Raleigh, North
    Carolina. University Microfilms, Inc., Ann Arbor, Michigan.

15. Blake, H. W., H. H. Stadelmaier, and R. A. Douglas. 1969.
    Diffraction of light by a grating subjected to homogeneous
    strains and rigid body rotations. Contract N00014-68-A-0187,
    Technical Report 69-8. Office of Naval Research, Department
    of the Navy, Washington, D. C.

16. Brill, W. A. 1965. Basic studies in photoplasticity. Unpublished
    PhD thesis, Division of Engineering Mechanics, Stanford
    University, Stanford, California. University Microfilms, Inc.,
    Ann Arbor, Michigan.

17. Brinson, H. F. 1970. The ductile fracture of polycarbonate.
    Experimental Mechanics 10(2):72-77.

18. Butcher, B. M., and C. H. Karnes. 1966. Strain-rate effects in
    metals. Journal of Applied Physics 37(1):402-411.

19. Campbell, W. R. 1952. Determination of dynamic stress-strain
    curves from strain waves in long bars. Proceedings of the
    Society for Experimental Stress Analysis 10(1):113-124.

20. Chang, H. L., and Y. Horie. 1973. Two-dimensional stress waves
    resulting from axisymmetric impact of finite-length rods.
    Contract N00014-78-A-0187, Technical Report 73-1. Office of
    Naval Research, Department of the Navy, Washington, D. C.

21. Christopher, W. F., and D. W. Fox. 1962. Polycarbonates. Reinhold
    Publishing Company, New York.

22. Cristescu, N. 1967. Dynamic Plasticity. John Wiley and Sons, Inc.,
    New York.

23. Donnell, L. H. 1930. Longitudinal wave transmission and impact.
    Transactions American Society of Mechanical Engineers 52(1):
    153-167.

24. Douglas, R. A., C. Akkoc, and C. E. Pugh. 1964. A diffraction
    grating method for measuring elastic-plastic surface strains
    in metal sheets. N.R.L. Technical Memo No. 252. U. S. Naval
    Research Laboratory, Washington, D. C.

25. Douglas, R. A., C. Akkoc, and C. E. Pugh. 1965. Strain field investigations with plane diffraction gratings. Experimental Mechanics 5(7):233-238.

26. Douglas, R. A., W. L. Bingham, H. W. Blake, and W. L. Liddell. 1969. Experimental method for diffraction studies during impact. Contract N00014-68-A-0187, Technical Report 69-1. Office of Naval Research, Department of the Navy, Washington, D. C.

27. Duffy, J., J. D. Campbell, and R. H. Hawley. 1971. On the use of a torsional split Hopkinson bar to study rate effects in 1100-0 aluminum. Journal of Applied Mechanics 38(3):83-91.

28. Gerard, G., R. Papirno, and H. Becker. 1962. On experimental solid dynamics. Symposium on Dynamic Behavior of Materials, ASTM Special Publication No. 336, pp. 82-103. American Society for Testing and Materials, Philadelphia, Pennsylvania.

29. Goldsmith, W. 1960. Impact. Edward Arnold, London, England.

30. Gurtman, G. A., W. C. Jenkins, and T. K. Tung. 1965. Characterization of a birefringent material for use in photoplasticity. Douglas Report SM-47796. Douglas Aircraft Company, Inc., Santa Monica, California.

31. Habberstad, J. L. 1971. A two-dimensional numerical solution for elastic waves in variously configured rods. Journal of Applied Mechanics 38(3):62-70.

32. Hauser, F. E., J. A. Simmons, and J. E. Dorn. 1961. Strain rate effects in plastic wave propagation, pp. 93-114. In P. G. Shewmon and V. F. Zackay (eds.), Response of Metals to High Velocity Deformation. Interscience Publishers, New York.

33. Hoggatt, C. R., and R. F. Recht. 1969. Dynamic stress-strain relationships obtained from an expanding ring experiment. Experimental Mechanics 9(10):441-448.

34. Holman, J. P. 1966. Experimental Methods for Engineers. McGraw-Hill Book Company, Inc., New York.

35. Jeelani, S., J. K. Whitfield, and R. A. Douglas. 1971. Design and performance of powder accelerator systems for impact studies. Contract N00014-68-A-0187, Technical Report 71-2. Office of Naval Research, Department of the Navy, Washington, D. C.

36. Jenkins, F. A., and H. E. White. 1957. Fundamentals of Optics. McGraw-Hill Book Company, Inc., New York.

37. Johnson, P. C., B. A. Stein, and R. S. Davis. 1962. Measurement of dynamic plastic flow properties under uniform stress. Symposium on Dynamic Behavior of Materials, ASTM Special Publication No. 366, pp. 195-207. American Society for Testing and Materials, Philadelphia, Pennsylvania.

38. Jones, E. O., and R. A. Graham. 1968. Shear strength effects on phase transition "pressures" determined from shock-compression experiments. Symposium on Accurate Characterization of the High-Pressure Environment, National Bureau of Standards Special Publication No. 326, pp. 229-242. National Bureau of Standards, Gaithersburg, Maryland.

39. Karnes, C. H. 1967. The plate impact configuration for determining properties of materials at high strain rates, pp. 270-393. *In* U. S. Lindholm (ed.), Mechanical Behavior of Materials under Dynamic Loads. Springer-Verlag New York, Inc., New York.

40. Karnes, C. H., and L. D. Bertholf. 1969. Numerical investigation of two-dimensional axisymmetric elastic-plastic wave propagation near the impact end of identical 1100-0 aluminum bars, pp. 501-519. *In* M. F. Kanninen (ed.), Inelastic Behavior of Solids. McGraw-Hill Book Company, Inc., New York.

41. Kolsky, H. 1949. An investigation of the mechanical properties of materials at very high rates of loading. Proceedings of the Physical Society 62:676-700.

42. Kolsky, H. 1963. Stress Waves in Solids. Dover Publications, Inc., New York.

43. Kolsky, H. 1965. The propagation of mechanical pulses in anelastic solids, pp. 1-18. *In* N. J. Huffington (ed.), Behavior of Materials Under Dynamic Loading. American Society of Mechanical Engineers, New York.

44. Krafft, J. M. 1960. Instrumentation for high-speed strain measurement, pp. 9-49. *In* P. G. Shewmon and V. F. Zackay (eds.), Response of Metals to High Velocity Deformation. Interscience Publishers, New York.

45. Lee, E. H., and H. Wolf. 1951. Plastic-wave propagation effects in high-speed testing. Journal of Applied Mechanics 18: 379-386.

46. Liddell, W. L., Y. Horie, and R. A. Douglas. 1972. An experimental investigation of the behavior of polycarbonate (Lexan) subjected to impact loading: large-amplitude elastic wave propagation and dynamic material properties. Contract N00014-68-A-0187, Technical Report 72-2. Office of Naval Research, Department of the Navy, Washington, D. C.

47. Liddell, W. L., R. S. Steele, W. L. Bingham, and R. A. Douglas. 1970. Experimentally-determined plastic wave velocities in fully-annealed 1100F aluminum (striker velocity 89 ft/sec to 788 ft/sec). Contract N00014-68-A-0187, Technical Report 70-11. Office of Naval Research, Department of the Navy, Washington, D. C.

48. Liddell, W. L., R. S. Steele, W. L. Bingham, and R. A. Douglas. 1970. Experimentally-determined plastic wave velocities in polycarbonate (Lexan). Contract N00014-68-A-0187, Technical Report 70-10. Office of Naval Research, Department of the Navy, Washington, D. C.

49. Liddell, W. L., R. S. Steele, W. L. Bingham, and R. A. Douglas. 1971. Experimental investigation of large-amplitude elastic wave propagation and the elastic-plastic transition of polycarbonate (Lexan). Contract N00014-68-A-0187, Technical Report 71-6. Office of Naval Research, Department of the Navy, Washington, D. C.

50. Lindholm, U. S. 1965. Dynamic deformation of metals, pp. 42-61. In N. J. Huffington (ed.), Behavior of Materials Under Dynamic Loading. American Society of Mechanical Engineers, New York.

51. Lindholm, U. S., and L. M. Yeakley. 1968. High strain-rate testing: tension and compression. Experimental Mechanics 8(1):1-9.

52. Maiden, C. J., and S. J. Green. 1966. Compressive strain-rate tests on six selected materials at strain rates from 10^{-3} to 10^4 in/in/sec. Journal of Applied Mechanics 33(9):496-504.

53. Malvern, L. E. 1965. Experimental studies of strain-rate effects and plastic wave propagation in annealed aluminum, pp. 81-92. In N. J. Huffington (ed.), Behavior of Materials Under Dynamic Loading. American Society of Mechanical Engineers, New York.

54. Mok, C. H., and J. Duffy. 1964. The dynamic stress-strain relation of metals as determined from impact tests with a hard ball. Brown University Report Nonr-562(20)137. Brown University, Providence, Rhode Island.

55. Perrone, N. 1968. On the use of the ring test for determining rate-sensitive material constants. Experimental Mechanics 8(5):232-236.

56. Rakhmatulin, K. A. 1948. Propagation of a wave of unloading. Translation A11-T2/15. Brown University, Providence, Rhode Island.

57. Rinehart, J. S. 1970. Mechanics of Wave Behavior in Explosively Loaded Rod. Naval Weapons Center, China Lake, California.

58. Ripperberger, E. A. 1965. Dynamic plastic behavior of aluminum, copper, and iron, pp. 62-80. *In* N. J. Huffington (ed.), Behavior of Materials Under Dynamic Loading. American Society of Mechanical Engineers, New York.

59. Ripperberger, E. A., and H. Watson. 1968. The relationship between the constitutive equation and one-dimensional wave propagation, pp. 294-313. *In* U. S. Lindholm (ed.), Mechanical Behavior of Materials Under Dynamic Loads. Springer-Verlag New York, Inc., New York.

60. Sharpe, W. N. 1970. Dynamic strain measurement with the interferometric strain gage. Experimental Mechanics 10(2): 89-92.

61. Sharpe, W. N., and K. G. Hoge. 1972. Specimen strain measurement in the split-Hopkinson-pressure-bar experiment. Experimental Mechanics 12(12):570-574.

62. Stormont, C. W., H. Gonzales, Jr., and H. F. Brinson. 1972. The ductile fracture of anisotropic materials. Experimental Mechanics 12(12):557-563.

63. Taylor, G. I. 1958. The plastic wave in a wire extended by an impact load. The Scientific Papers of Sir Geoffrey Ingram Taylor 1:467-479. Cambridge University Press, London, England.

64. von Karman, T. 1942. On the propagation of plastic deformations in solids. National Defense Research Committee Report No. A-29 (OSRD No. 365). United States Department of Defense, Washington, D. C.

65. von Karman, T., and P. Duwez. 1950. The propagation of plastic deformation in solids. Journal of Applied Physics 21:987-994.

66. Watson, H. 1972. Gage-length errors in the resolution of dispersive stress waves. Experimental Mechanics 12(8):352-359.

67. Whitfield, J. K., R. A. Douglas, and S. Jeelani. 1969. Powder accelerator systems for axial impact studies. Contract N00014-68-A-0187, Technical Report 69-3. Office of Naval Research, Department of the Navy, Washington, D. C.

68. Whitfield, J. K., and C. W. Smith. 1972. Characterization studies of a potential photoelastoplastic material. Experimental Mechanics 12(2):67-74.

6   APPENDICES

6.1   Computer Printouts of Strain, Surface Rotation, and
Approximate Strain Rate Versus Time After Impact for
Lexan Series 2 (LS2) Tests

Appendix Table 6.1   Results of test LS2-1

LEXAN SERIES 2 - TEST NUMBER 1 (LS2- 1), 3/23/71
●●

STRIKER VELOCITY (FT/SEC) = 535.5
STRIKER LENGTH (IN) = 3,000
TARGET LENGTH (IN) = 6,000
GRATING DISTANCE FROM IMPACT (IN) = 1,536
GRATING LENGTH (IN) = 0,0146
AMBIENT TEMPERATURE (DEG F) = 80,0
RESIDUAL STRAIN APPROX, FIVE MIN, AFTER TEST (%) = 0,0

DATA POINT	TIME (MICSEC)	SURF, ROT, (DEGREES)	EUL, STRAIN (PERCENT)	LAG, STRAIN (PERCENT)	AVG, STRAIN RATE(SEC-1)
1	0,0	0,0	0,0	0,0	0,
2	1,68	0,0	0,0	0,0	0,
3	6,87	-0,0058	-0,04	-0,04	-73,
4	10,15	-0,0056	-0,04	-0,04	0,
5	16,71	-0,0018	0,01	0,01	75,
6	21,44	-0,0303	-0,08	-0,08	-194,
7	30,71	-0,3235	-1,91	-1,88	-1939,
8	36,13	-0,4275	-2,96	-2,87	-1837,
9	41,01	-0,3666	-3,97	-3,82	-1935,
10	43,03	-0,3103	-4,46	-4,27	-2213,
11	44,41	-0,3159	-4,79	-4,57	-2223,
12	46,08	-0,3045	-5,06	-4,82	-1462,
13	52,91	-0,2695	-5,70	-5,40	-848,
14	59,59	-0,1887	-6,34	-5,97	-855,
15	63,10	-0,1958	-6,30	-5,93	115,
16	68,75	-0,1505	-6,42	-6,03	-185,

COMMENTS-

Appendix Table 6.2   Results of test LS2-2

LEXAN SERIES 2 - TEST NUMBER 2 (LS2- 2), 3/30/71
••

STRIKER VELOCITY (FT/SEC) = 544.8
STRIKER LENGTH (IN) = 1.000
TARGET LENGTH (IN) = 6.000
GRATING DISTANCE FROM IMPACT (IN) = 1.504
GRATING LENGTH (IN) = 0.0197
AMBIENT TEMPERATURE (DEG F) = 75.0
RESIDUAL STRAIN APPROX. FIVE MIN. AFTER TEST (%) = 0.0

DATA POINT	TIME (MICSEC)	SURF. ROT. (DEGREES)	EUL. STRAIN (PERCENT)	LAG. STRAIN (PERCENT)	AVG. STRAIN RATE(SEC-1)
1	0.0	0.0	0.0	0.0	0.
2	5.53	0.0	0.0	0.0	0.
3	12.97	0.0	0.0	0.0	0.
4	20.98	-0.0754	-0.33	-0.33	-415.
5	28.96	-0.3720	-1.85	-1.82	-1861.
6	32.92	-0.3653	-2.53	-2.47	-1650.
7	38.42	-0.3339	-3.78	-3.64	-2133.
8	43.72	-0.2973	-4.97	-4.74	-2064.
9	47.34	-0.2490	-5.34	-5.07	-916.
10	51.12	-0.2579	-5.56	-5.26	-512.
11	53.41	-0.1845	-5.75	-5.44	-779.
12	57.41	-0.0691	-5.93	-5.60	-394.
13	60.73	-0.0384	-6.04	-5.69	-282.
14	65.62	0.1309	-5.88	-5.55	291.
15	70.39	0.2300	-5.44	-5.16	824.
16	74.24	0.2481	-5.19	-4.94	573.
17	77.98	0.3280	-4.71	-4.49	1185.
18	79.88	0.3509	-4.48	-4.29	1059.
19	82.56	0.3563	-4.05	-3.90	1479.
20	87.21	0.4088	-3.49	-3.37	1123.
21	88.74	0.4437	-3.27	-3.17	1335.
22	90.19	0.4819	-3.06	-2.96	1421.
23	137.03	-0.0341	-0.46	-0.46	536.
24	144.93	0.0481	-0.43	-0.43	33.
25	152.18	0.0400	-0.39	-0.39	59.
26	155.65	0.0693	-0.22	-0.21	497.
27	159.16	0.1515	-0.19	-0.19	75.
28	165.61	0.2475	-0.00	-0.00	289.
29	168.89	0.2436	0.10	0.10	302.
30	170.83	0.2243	0.20	0.20	532.
31	172.44	0.2222	0.31	0.31	684.

COMMENTS-

Appendix Table 6.3   Results of test LS2-3

LEXAN SERIES 2 - TEST NUMBER 3 (LS2- 3), 4/ 8/71
●●

STRIKER VELOCITY (FT/SEC) = 548.0
STRIKER LENGTH (IN) = 1.250
TARGET LENGTH (IN) = 6.000
GRATING DISTANCE FROM IMPACT (IN) = 0.254
GRATING LENGTH (IN) = 0.0244
AMBIENT TEMPERATURE (DEG F) = 82.0
RESIDUAL STRAIN APPROX. FIVE MIN. AFTER TEST (%) = 0.0

DATA POINT	TIME (MICSEC)	SURF. ROT. (DEGREES)	EUL. STRAIN (PERCENT)	LAG. STRAIN (PERCENT)	AVG. STRAIN RATE(SEC-1)
1	0.0	0.0	0.0	0.0	0.
2	2.21	0.0	0.0	0.0	0.
3	7.59	-1.8974	-3.66	-3.53	-6567.
4	9.15	-2.1678	-4.30	-4.12	-3802.
5	9.76	-1.9663	-4.85	-4.62	-8202.
6	16.43	-1.5828	-7.28	-6.79	-3244.
7	18.95	-1.6085	-8.57	-7.73	-3731.
8	25.50	-1.4371	-10.32	-9.35	-2480.
9	32.10	-1.4909	-11.21	-10.08	-1097.
10	40.14	-1.6690	-12.02	-10.73	-809.
11	50.97	-1.6502	-12.19	-10.87	-130.
12	66.49	-1.6617	-9.88	-8.99	1211.
13	72.63	-1.6798	-8.49	-7.83	1897.
14	75.60	-1.5000	-7.44	-6.92	3035.
15	77.47	-1.4323	-6.89	-6.44	2565.
16	81.01	-1.3568	-5.81	-5.49	2691.
17	87.99	-1.4267	-4.28	-4.11	1981.
18	97.60	-1.4094	-3.05	-2.96	1200.
19	101.37	-1.2171	-2.60	-2.54	1107.
20	107.74	-0.7955	-1.93	-1.89	1010.
21	112.20	-0.6072	-1.21	-1.20	1559.
22	116.09	-0.4556	-0.86	-0.85	892.
23	122.38	-0.1604	-0.52	-0.52	528.
24	128.44	0.0028	-0.30	-0.30	358.
25	133.28	0.0891	-0.24	-0.23	142.
26	136.94	0.1865	-0.28	-0.28	-125.
27	140.22	0.2362	-0.30	-0.30	-51.
28	144.49	0.2209	-0.30	-0.30	-5.
29	151.12	0.2650	-0.28	-0.28	26.
30	155.32	0.2630	-0.29	-0.29	-28.
31	161.30	0.2610	-0.31	-0.31	-20.
32	165.65	0.2592	-0.30	-0.29	26.
33	170.76	0.2499	-0.21	-0.21	157.
34	175.07	0.2557	-0.20	-0.20	29.

COMMENTS-

Appendix Table 6.4   Results of test LS2-4

LEXAN SERIES 2 - TEST NUMBER 4 (LS2- 4), 5/ 2/71
●●●

STRIKER VELOCITY (FT/SEC) = 561.2
STRIKER LENGTH (IN) = 1,000
TARGET LENGTH (IN) = 6,000
GRATING DISTANCE FROM IMPACT, (IN) = 2,007
GRATING LENGTH (IN) = 0,0138
AMBIENT TEMPERATURE (DEG F) = 75,0
RESIDUAL STRAIN APPROX, FIVE MIN, AFTER TEST (%) = 0,0

DATA POINT	TIME (MICSEC)	SURF. ROT. (DEGREES)	EUL. STRAIN (PERCENT)	LAG. STRAIN (PERCENT)	AVG. STRAIN RATE(SEC-1)
1	0,0	0,0	0,0	0,0	0.
2	7,37	0,0	0,0	0,0	0,
3	11,22	0,0	0,0	0,0	0,
4	16,37	0,0	0,0	0,0	0,
5	20,49	-0,0059	-0,03	-0,03	-75,
6	22,06	-0,0118	-0,06	-0,06	-197,
7	26,14	-0,0900	-0,29	-0,29	-555,
8	27,51	-0,0006	-0,06	-0,06	1673,
9	30,11	-0,2073	-0,72	-0,72	-2533,
10	34,84	-0,1736	-1,20	-1,19	-1001,
11	45,91	-0,3970	-3,12	-3,02	-1659,
12	51,10	-0,2655	-4,22	-4,05	-1978,
13	54,88	-0,3090	-4,56	-4,36	-812,
14	56,75	-0,2605	-4,81	-4,59	-1223,
15	62,78	-0,2341	-5,24	-4,98	-655,
16	68,42	-0,1182	-5,62	-5,32	-605,
17	71,02	-0,0822	-5,81	-5,49	-643,
18	73,31	-0,0314	-5,65	-5,35	609,
19	77,16	0,0155	-5,68	-5,37	-55,
20	81,32	0,1537	-5,49	-5,21	395,
21	86,13	0,2038	-5,25	-4,99	452,
22	89,26	0,2299	-5,05	-4,80	595,
23	107,45	0,4377	-2,85	-2,77	1121,
24	129,18	0,0249	-0,09	-0,09	1232,
25	167,80	-0,0507	0,10	0,10	49,
26	172,72	0,0675	0,57	0,58	969,
27	178,52	0,0983	0,52	0,52	-102,

COMMENTS-

Appendix Table 6.5   Results of test LS2-5

LEXAN SERIES 2 - TEST NUMBER 5 (LS2- 5), 7/13/71
●●●

STRIKER VELOCITY (FT/SEC) = 545.3
STRIKER LENGTH (IN) = 3.997
TARGET LENGTH (IN) = 5.994
GRATING DISTANCE FROM IMPACT (IN) = 1.525
GRATING LENGTH (IN) = 0.0224
AMBIENT TEMPERATURE (DEG F) = 72.0
RESIDUAL STRAIN APPROX. FIVE MIN. AFTER TEST (%) = 0.0

DATA POINT	TIME (MICSEC)	SURF. ROT. (DEGREES)	EUL. STRAIN (PERCENT)	LAG. STRAIN (PERCENT)	AVG. STRAIN RATE(SEC-1)
1	0.0	0.0	0.0	0.0	0.
2	5.37	0.0	0.0	0.0	0.
3	9.03	0.0	0.0	0.0	0.
4	12.12	0.0	0.0	0.0	0.
5	14.56	0.0	0.0	0.0	0.
6	19.74	-0.0115	-0.22	-0.22	-419.
7	23.65	-0.3866	-1.10	-1.09	-2243.
8	25.80	-0.4030	-1.57	-1.55	-2104.
9	28.62	-0.3467	-2.07	-2.03	-1699.
10	32.36	-0.4647	-2.84	-2.76	-1962.
11	38.64	-0.4047	-4.18	-4.01	-1990.
12	47.14	-0.3705	-5.41	-5.13	-1318.
13	54.16	-0.2601	-6.15	-5.80	-951.
14	58.88	-0.2856	-6.53	-6.13	-702.
15	62.50	-0.2598	-6.77	-6.34	-598.
16	73.75	-0.2730	-7.31	-6.81	-415.
17	79.65	-0.2732	-7.64	-7.10	-490.
18	94.52	-0.3072	-8.05	-7.45	-233.
19	102.98	-0.3306	-8.26	-7.63	-219.
20	106.41	-0.3478	-8.32	-7.68	-149.
21	120.24	-0.4037	-8.67	-7.98	-214.
22	125.42	-0.4422	-8.79	-8.08	-199.
23	133.20	-0.4693	-8.99	-8.24	-209.
24	139.83	-0.5151	-9.03	-8.29	-62.
25	151.95	-0.5918	-9.25	-8.47	-150.
26	160.52	-0.6226	-9.25	-8.47	-2.
27	164.98	-0.6604	-9.16	-8.39	181.
28	170.85	-0.6741	-9.10	-8.34	82.
29	185.91	-0.7768	-8.05	-7.45	592.
30	191.89	-0.8173	-7.47	-6.95	841.
31	197.45	-0.8481	-6.75	-6.32	1127.
32	201.04	-0.8527	-6.44	-6.05	756.
33	205.76	-0.8589	-5.73	-5.42	1332.
34	217.23	-0.9183	-4.24	-4.07	1179.
35	225.41	-0.9616	-3.17	-3.03	1680.
36	226.34	-1.0055	-2.60	-2.53	1703.
37	233.59	-1.0598	-0.95	-0.94	2251.
38	238.77	-1.0411	0.35	0.33	2364.
39	249.44	-0.7222	1.93	1.97	1542.

COMMENTS-

Appendix Table 6.6 · Results of test LS2-6

LEXAN SERIES 2 - TEST NUMBER 6 (LS2- 6), 7/13/71
••

STRIKER VELOCITY (FT/SEC) = 526.5
STRIKER LENGTH (IN) = 4,000
TARGET LENGTH (IN) = 5,994
GRATING DISTANCE FROM IMPACT (IN) = 1,518
GRATING LENGTH (IN) = 0,0224
AMBIENT TEMPERATURE (DEG F) = 72,0
RESIDUAL STRAIN APPROX, FIVE MIN, AFTER TEST (%) = 0,0

DATA POINT	TIME (MICSEC)	SURF, ROT, (DEGREES)	EUL, STRAIN (PERCENT)	LAG, STRAIN (PERCENT)	AVG, STRAIN RATE(SEC-1)
1	0,0	0,0	0,0	0,0	0,
2	3,78	0,0	0,0	0,0	0,
3	11,49	0,0	0,0	0,0	0,
4	15,68	0,0	0,0	0,0	0,
5	19,20	-0,0539	-0,32	-0,32	-911,
6	24,81	-0,4169	-1,52	-1,49	-2091,
7	35,11	-0,4491	-3,51	-3,39	-1842,
8	44,73	-0,3515	-5,23	-4,97	-1644,
9	56,44	-0,2903	-6,37	-5,99	-868,
10	64,23	-0,2555	-6,81	-6,37	-495,
11	70,98	-0,3085	-7,14	-6,67	-433,
12	78,92	-0,2971	-7,44	-6,93	-327,
13	82,54	-0,3293	-7,56	-7,03	-288,
14	89,76	-0,3359	-7,81	-7,24	-292,
15	95,18	-0,3579	-7,93	-7,55	-204,
16	105,90	-0,4105	-8,24	-7,62	-246,
17	111,62	-0,4345	-8,38	-7,74	-210,
18	118,99	-0,4708	-8,51	-7,84	-140,
19	125,90	-0,5133	-8,64	-7,95	-164,
20	132,19	-0,5521	-8,82	-8,11	-245,
21	146,58	-0,6777	-9,04	-8,29	-124,
22	153,53	-0,7151	-9,07	-8,32	-48,
23	159,98	-0,7501	-9,07	-8,32	0,
24	163,37	-0,7768	-9,07	-8,31	8,
25	180,89	-0,8758	-8,14	-7,53	451,
26	186,04	-0,9061	-7,58	-7,05	932,
27	193,83	-0,9904	-6,78	-6,35	892,
28	204,05	-1,0535	-5,59	-5,11	1211,
29	209,13	-1,0710	-4,74	-4,53	1149,
30	212,07	-1,0867	-4,37	-4,19	1169,
31	215,31	-1,1087	-3,75	-3,61	1767,
32	217,07	-1,1278	-3,53	-3,41	1144,
33	225,84	-1,1961	-1,88	-1,85	1781,
34	231,49	-1,2402	-0,58	-0,57	2257,
35	246,41	-0,9934	2,22	2,27	1906,

COMMENTS-

Appendix Table 6.7   Results of test LS2-8

STRIKER VELOCITY (FT/SEC) = 540.5
STRIKER LENGTH (IN) = 4.000
TARGET LENGTH (IN) = 6.000
GRATING DISTANCE FROM IMPACT (IN) = 1.518
GRATING LENGTH (IN) = 0.0264
AMBIENT TEMPERATURE (DEG F.) = 72.0
RESIDUAL STRAIN APPROX. FIVE MIN. AFTER TEST (%) = 0.0

DATA POINT	TIME (MICSEC)	SURF. ROT. (DEGREES)	EUL. STRAIN (PERCENT)	LAG. STRAIN (PERCENT)	AVG. STRAIN RATE(SEC-1)
1	0.0	0.0	0.0	0.0	0.
2	1.98	0.0	0.0	0.0	0.
3	7.39	0.0	0.0	0.0	0.
4	11.35	0.0	0.0	0.0	0.
5	16.53	0.0	0.0	0.0	0.
6	20.45	-0.0168	-0.16	-0.16	-410.
7	24.38	-0.4294	-1.37	-1.35	-3030.
8	25.59	-0.4202	-1.49	-1.47	-953.
9	26.96	-0.3884	-1.66	-1.64	-1250.
10	33.55	-0.4551	-2.87	-2.79	-1745.
11	41.40	-0.3764	-4.62	-4.41	-2075.
12	46.88	-0.3447	-5.32	-5.06	-1168.
13	49.28	-0.3274	-5.47	-5.18	-529.
14	58.58	-0.2157	-6.30	-5.93	-805.
15	65.20	-0.1272	-6.61	-6.20	-409.
16	67.11	-0.1110	-6.66	-6.24	-212.
17	70.31	-0.1376	-6.78	-6.35	-334.
18	85.39	-0.0622	-7.29	-6.80	-298.
19	96.62	0.0020	-7.68	-7.13	-297.
20	101.04	0.0320	-7.79	-7.22	-206.
21	108.77	0.0679	-7.93	-7.35	-159.
22	119.29	0.1347	-8.10	-7.49	-136.
23	127.28	0.1648	-8.35	-7.71	-270.
24	143.47	0.2645	-8.55	-7.88	-107.
25	151.92	0.3215	-8.66	-7.97	-104.
26	159.01	0.3968	-8.64	-7.96	16.
27	172.49	0.5117	-8.47	-7.81	106.
28	196.94	0.5703	-6.61	-6.20	659.
29	201.09	0.5742	-6.01	-5.67	1274.
30	220.40	0.6025	-3.30	-3.19	1283.
31	232.25	0.6310	-0.86	-0.86	1973.
32	242.61	0.7272	1.24	1.25	2037.
33	244.59	0.7173	1.45	1.48	1126.
34	251.37	0.6881	2.29	2.34	1276.

COMMENTS-BAD IMPACT,ABERRANT SURFACE ROTATION.

Appendix Table 6.8   Results of test LS2-11

LEXAN SERIES 2 - TEST NUMBER 11 (LS2-11), 7/21/71
•••

STRIKER VELOCITY (FT/SEC) = 549.5
STRIKER LENGTH (IN) = 3.971
TARGET LENGTH (IN) = 5.994
GRATING DISTANCE FROM IMPACT (IN) = 2.290
GRATING LENGTH (IN) = 0.0134
AMBIENT TEMPERATURE (DEG F) = 72.0
RESIDUAL STRAIN APPROX. FIVE MIN. AFTER TEST (%) = 0.0

DATA POINT	TIME (MICSEC)	SURF. ROT. (DEGREES)	EUL. STRAIN (PERCENT)	LAG. STRAIN (PERCENT)	AVG. STRAIN RATE(SEC-1)
1	0.0	0.0	0.0	0.0	0.
2	2.98	0.0	0.0	0.0	0.
3	7.83	0.0	0.0	0.0	0.
4	14.93	0.0	0.0	0.0	0.
5	24.25	0.0	0.0	0.0	0.
6	30.32	-0.1503	-0.42	-0.42	-691.
7	35.44	-0.1317	-0.77	-0.77	-677.
8	41.36	-0.2933	-1.70	-1.67	-1531.
9	45.29	-0.3090	-2.39	-2.34	-1694.
10	51.17	-0.2967	-3.51	-3.40	-1798.
11	58.16	-0.2557	-4.41	-4.23	-1188.
12	63.66	-0.2822	-4.98	-4.74	-944.
13	67.17	-0.2219	-5.39	-5.12	-1060.
14	73.78	-0.2292	-5.87	-5.54	-644.
15	78.93	-0.1720	-6.18	-5.82	-543.
16	83.29	-0.1707	-6.42	-6.04	-489.
17	87.14	-0.1734	-6.66	-6.25	-553.
18	92.03	-0.1334	-6.88	-6.43	-381.
19	97.11	-0.1637	-7.06	-6.59	-311.
20	104.56	-0.1394	-7.41	-6.90	-409.
21	109.75	-0.1513	-7.57	-7.04	-268.
22	115.27	-0.1349	-7.90	-7.32	-335.
23	129.04	-0.1373	-8.29	-7.66	-314.
24	140.61	-0.1051	-8.64	-7.95	-253.
25	156.95	-0.0559	-8.90	-8.18	-138.
26	167.68	-0.0537	-8.71	-8.01	151.
27	186.89	-0.0886	-7.02	-6.56	760.
28	207.86	-0.1450	-3.95	-3.80	1313.
29	218.59	-0.1696	-1.97	-1.93	1744.
30	225.23	-0.0256	-0.80	-0.80	1710.
31	237.26	0.1606	0.58	0.58	1143.

COMMENTS-

Appendix Table 6.9   Results of test LS2-12

LEXAN SERIES 2 = TEST NUMBER 12 (LS2-12), 7/21/71
●●

STRIKER VELOCITY (FT/SEC) = 551.6
STRIKER LENGTH (IN) = 3.977
TARGET LENGTH (IN) = 6.023
GRATING DISTANCE FROM IMPACT (IN) = 2.279
GRATING LENGTH (IN) = 0.0233
AMBIENT TEMPERATURE (DEG F) = 73.0
RESIDUAL STRAIN APPROX. FIVE MIN. AFTER TEST (X) = 0.0

DATA POINT	TIME (MICSEC)	SURF. ROT. (DEGREES)	EUL. STRAIN (PERCENT)	LAG. STRAIN (PERCENT)	AVG. STRAIN RATE(SEC-1)
1	0.0	0.0	0.0	0.0	0.
2	2.18	0.0	0.0	0.0	0.
3	13.74	0.0	0.0	0.0	0.
4	22.90	0.0	0.0	0.0	0.
5	26.68	-0.0541	-0.16	-0.16	-414.
6	31.71	-0.1783	-0.45	-0.45	-582.
7	37.36	-0.2140	-0.99	-0.98	-930.
8	45.41	-0.3002	-2.34	-2.29	-1634.
9	50.83	-0.3197	-3.48	-3.37	-1986.
10	53.73	-0.3100	-3.72	-3.58	-745.
11	59.30	-0.2541	-4.53	-4.33	-1347.
12	67.66	-0.2128	-5.39	-5.11	-931.
13	75.94	-0.2069	-5.98	-5.65	-645.
14	86.17	-0.1538	-6.64	-6.22	-564.
15	93.50	-0.1229	-6.92	-6.47	-341.
16	106.78	-0.1310	-7.51	-6.98	-384.
17	116.05	-0.1204	-7.83	-7.26	-296.
18	129.79	-0.1649	-8.28	-7.65	-286.
19	133.22	-0.1761	-8.41	-7.75	-300.
20	141.28	-0.1988	-8.67	-7.98	-282.
21	151.62	-0.2198	-8.98	-8.24	-249.
22	156.18	-0.2347	-9.08	-8.32	-124.
23	165.01	-0.2751	-9.15	-8.38	-85.
24	180.47	-0.3950	-8.23	-7.60	501.
25	187.34	-0.4533	-7.69	-7.14	679.
26	199.17	-0.5782	-5.96	-5.63	1277.
27	201.73	-0.6068	-5.61	-5.31	1232.
28	210.39	-0.7467	-4.09	-3.93	1598.
29	218.40	-0.7942	-2.49	-2.43	1867.
30	222.33	-0.7133	-1.79	-1.75	1725.
31	232.64	-0.3402	-0.30	-0.50	1413.
32	242.41	-0.5184	0.47	0.48	792.
33	247.63	-0.5283	0.91	0.92	847.

COMMENTS-

Appendix Table 6.10   Results of test LS2-13

```
   LEXAN  SERIES  2 - TEST  NUMBER 13 (LS2-13),  7/22/71
   ---------------------------------------------------------

STRIKER VELOCITY (FT/SEC) =  533.0
STRIKER LENGTH (IN) = 1.001
TARGET LENGTH (IN) = 5.994
GRATING  DISTANCE FROM IMPACT (IN) = 1.517
GRATING LENGTH (IN) = 0.0114
AMBIENT TEMPERATURE (DEG F) = 73.0
RESIDUAL STRAIN APPROX. FIVE MIN. AFTER TEST (%) =  0.0
```

DATA POINT	TIME (MICSEC)	SURF. ROT. (DEGREES)	EUL. STRAIN (PERCENT)	LAG. STRAIN (PERCENT)	AVG. STRAIN RATE(SEC-1)
1	0.0	0.0	0.0	0.0	0.
2	5.69	0.0	0.0	0.0	0.
3	9.81	0.0	0.0	0.0	0.
4	15.73	0.0	0.0	0.0	0.
5	20.58	-0.0540	-0.52	-0.52	-1069.
6	25.05	-0.3682	-1.55	-1.52	-2248.
7	32.08	-0.4193	-2.74	-2.67	-1630.
8	38.15	-0.3673	-4.00	-3.84	-1936.
9	42.81	-0.2825	-4.89	-4.66	-1758.
10	50.41	-0.2471	-5.60	-5.31	-849.
11	54.80	-0.1823	-5.94	-5.61	-679.
12	58.12	-0.1467	-6.08	-5.73	-389.
13	63.94	-0.0331	-5.93	-5.60	227.
14	66.06	0.0196	-5.87	-5.55	251.
15	69.54	0.0375	-5.48	-5.19	1027.
16	72.79	0.0502	-5.30	-5.03	488.
17	74.85	0.0829	-5.11	-4.86	828.
18	77.10	0.0785	-4.88	-4.65	926.
19	82.91	0.0622	-4.11	-3.95	1210.
20	92.30	0.2121	-2.55	-2.49	1561.
21	99.40	0.1488	-1.32	-1.30	1642.
22	106.66	-0.1172	-0.31	-0.31	1370.
23	113.72	-0.3310	-0.08	-0.08	529.
24	118.65	-0.1049	-0.16	-0.16	-164.
25	121.02	-0.0584	-0.14	-0.14	69.
26	123.73	-0.0522	-0.13	-0.13	63.
27	129.07	-0.1459	-0.21	-0.21	-160.
28	136.29	-0.1364	-0.24	-0.24	-46.
29	146.79	-0.0510	-0.32	-0.32	-73.
30	156.76	-0.2260	-0.18	-0.18	139.
31	164.36	-0.1478	-0.20	-0.20	-21.
32	179.71	-0.2135	0.26	0.26	299.
33	188.68	-0.2224	0.75	0.74	558.
34	200.14	-0.2659	1.51	1.53	671.
35	208.85	-0.3040	2.08	2.12	681.
36	216.98	-0.3275	2.41	2.47	424.
37	227.98	-0.3148	2.59	2.66	173.
38	241.31	-0.3572	2.46	2.52	-105.
39	247.68	-0.3721	2.26	2.31	-321.

COMMENTS-

Appendix Table 6.11 Results of test LS2-15

LEXAN SERIES 2 - TEST NUMBER 15 (LS2-15), 7/26/71
••

STRIKER VELOCITY (FT/SEC) = 529.9
STRIKER LENGTH (IN) = 1.004
TARGET LENGTH (IN) = 5.985
GRATING DISTANCE FROM IMPACT (IN) = 2.265
GRATING LENGTH (IN) = 0.0272
AMBIENT TEMPERATURE (DEG F) = 72.0
RESIDUAL STRAIN APPROX. FIVE MIN. AFTER TEST (%) = 0.0

DATA POINT	TIME (MICSEC)	SURF. ROT. (DEGREES)	EUL. STRAIN (PERCENT)	LAG. STRAIN (PERCENT)	AVG. STRAIN RATE(SEC-1)
1	0.0	0.0	0.0	0.0	0.
2	1.49	0.0	0.0	0.0	0.
3	8.74	0.0	0.0	0.0	0.
4	17.33	0.0	0.0	0.0	0.
5	24.62	-0.0569	-0.08	-0.08	-108.
6	33.10	-0.1028	-0.53	-0.53	-530.
7	42.15	-0.2584	-1.90	-1.87	-1481.
8	52.87	-0.2824	-3.68	-3.54	-1564.
9	57.54	-0.2368	-4.22	-4.05	-1138.
10	63.75	-0.1969	-4.73	-4.52	-727.
11	75.85	-0.0133	-5.21	-4.95	-359.
12	87.42	0.1786	-4.69	-4.48	807.
13	97.42	0.1881	-3.82	-3.68	808.
14	115.59	0.3630	-1.01	-1.00	1474.
15	120.10	0.1378	-0.39	-0.39	1356.
16	123.19	-0.1162	-0.20	-0.20	616.
17	131.44	-0.2953	0.04	0.04	287.
18	139.11	0.0527	0.05	0.05	16.
19	144.64	-0.1076	0.12	0.13	137.
20	151.29	-0.2173	0.24	0.24	167.
21	161.52	0.0161	0.24	0.25	9.
22	170.76	-0.1396	0.64	0.65	437.
23	180.99	-0.0647	1.43	1.45	786.
24	187.25	-0.1176	1.86	1.90	708.
25	202.21	-0.0684	2.95	3.04	765.
26	210.42	-0.0189	3.32	3.44	484.
27	220.46	-0.0903	3.73	3.88	438.
28	237.41	-0.1495	3.91	4.07	111.

COMMENTS-

Appendix Table 6.12   Results of test LS2-16

STRIKER VELOCITY (FT/SEC) = 533.9
STRIKER LENGTH (IN) = 0.994
TARGET LENGTH (IN) = 5.990
GRATING DISTANCE FROM IMPACT (IN) = 2.243
GRATING LENGTH (IN) = 0.0134
AMBIENT TEMPERATURE (DEG F) = 73.0
RESIDUAL STRAIN APPROX. FIVE MIN. AFTER TEST (%) = 0.0

DATA POINT	TIME (MICSEC)	SURF. ROT. (DEGREES)	EUL. STRAIN (PERCENT)	LAG. STRAIN (PERCENT)	AVG. STRAIN RATE(SEC-1)
1	0.0	0.0	0.0	0.0	0.
2	4.84	0.0	0.0	0.0	0.
3	20.93	0.0	0.0	0.0	0.
4	27.79	0.0	0.0	0.0	0.
5	40.72	-0.3177	-1.55	-1.52	-1178.
6	47.58	-0.3429	-2.55	-2.49	-1406.
7	58.48	-0.2293	-4.23	-4.05	-1438.
8	68.13	-0.1670	-5.10	-4.85	-824.
9	81.81	0.0745	-5.22	-4.96	-82.
10	86.35	0.1066	-5.01	-4.77	413.
11	90.20	0.1616	-4.73	-4.52	665.
12	99.58	0.1733	-3.75	-3.62	960.
13	103.32	0.2028	-3.42	-3.30	842.
14	109.19	0.2995	-2.42	-2.37	1596.
15	116.58	0.3477	-1.25	-1.24	1528.
16	132.10	-0.2789	-0.15	-0.15	699.
17	136.18	-0.2210	-0.25	-0.25	-254.
18	142.09	-0.0123	-0.23	-0.23	30.
19	153.03	-0.1511	0.08	0.08	286.
20	165.76	0.0413	0.29	0.29	165.
21	186.12	-0.0508	1.49	1.51	596.
22	189.48	-0.1008	1.76	1.82	918.
23	195.65	-0.1600	2.20	2.25	698.
24	214.98	-0.0876	3.20	3.30	546.
25	225.47	-0.1159	3.44	3.56	247.
26	230.96	-0.1394	3.54	3.67	190.
27	246.01	-0.1207	3.36	3.47	-128.

COMMENTS-

Appendix Table 6.13   Results of test LS2-17

LEXAN SERIES 2 - TEST NUMBER 17 (LS2-17), 7/29/71
●●●

STRIKER VELOCITY (FT/SEC) = 534.1
STRIKER LENGTH (IN) = 0.995
TARGET LENGTH (IN) = 8.025
GRATING DISTANCE FROM IMPACT (IN) = 2.995
GRATING LENGTH (IN) = 0.0138
AMBIENT TEMPERATURE (DEG F) = 72.0
RESIDUAL STRAIN APPROX. FIVE MIN. AFTER TEST (%) = 0.0

DATA POINT	TIME (MICSEC)	SURF. ROT. (DEGREES)	EUL. STRAIN (PERCENT)	LAG. STRAIN (PERCENT)	AVG. STRAIN RATE(SEC-1)
1	0.0	0.0	0.0	0.0	0.
2	5.96	0.0	0.0	0.0	0.
3	11.92	0.0	0.0	0.0	0.
4	23.53	0.0	0.0	0.0	0.
5	29.87	0.0	0.0	0.0	0.
6	37.17	-0.0122	-0.09	-0.09	-123.
7	41.87	-0.0292	-0.25	-0.25	-339.
8	50.00	-0.1734	-0.89	-0.88	-778.
9	53.94	-0.2806	-1.37	-1.35	-1192.
10	61.04	-0.2862	-2.52	-2.46	-1564.
11	65.82	-0.2342	-3.15	-3.05	-1237.
12	70.37	-0.2190	-3.64	-3.51	-999.
13	75.94	-0.1967	-4.22	-4.05	-977.
14	80.30	-0.1445	-4.58	-4.38	-743.
15	89.66	-0.0852	-4.91	-4.68	-324.
16	95.39	0.0272	-4.88	-4.66	40.
17	102.26	0.1145	-4.59	-4.39	382.
18	105.43	0.1587	-4.37	-4.19	645.
19	110.28	0.1755	-4.02	-3.86	671.
20	118.58	0.2552	-3.11	-3.01	1030.
21	124.34	0.3407	-2.29	-2.24	1338.
22	130.76	0.4572	-1.07	-1.06	1835.
23	135.13	0.4135	-0.64	-0.63	1791.
24	141.53	-0.0321	0.00	0.00	761.
25	156.70	0.1459	-0.17	-0.17	-117.
26	160.79	0.0812	-0.17	-0.16	19.
27	165.06	-0.0869	-0.18	-0.18	-30.
28	168.73	-0.1989	-0.14	-0.14	95.
29	175.00	0.0694	-0.02	-0.02	202.
30	177.59	0.1694	-0.12	-0.12	-409.
31	182.06	0.0982	-0.01	-0.01	262.
32	188.44	0.0192	0.19	0.19	301.
33	194.94	0.0449	0.12	0.12	-104.
34	200.51	0.1766	0.09	0.09	-62.
35	205.67	0.0977	0.07	0.07	-26.
36	209.76	0.0014	0.09	0.09	35.
37	222.44	-0.0593	0.41	0.42	259.
38	231.26	-0.1056	0.65	0.66	274.
39	240.85	-0.1450	1.21	1.23	596.
40	245.86	-0.1734	1.57	1.60	740.

COMMENTS-

Appendix Table 6.14   Results of test LS2-18

LEXAN SERIES 2 - TEST NUMBER 18 (LS2-18), 7/30/71
●●●

STRIKER VELOCITY (FT/SEC) = 522.2
STRIKER LENGTH (IN) = 0.995
TARGET LENGTH (IN) = 7.999
GRATING DISTANCE FROM IMPACT (IN) = 3.008
GRATING LENGTH (IN) = 0.0146
AMBIENT TEMPERATURE (DEG F) = 72.0
RESIDUAL STRAIN APPROX, FIVE MIN, AFTER TEST (%) = 0.0

DATA POINT	TIME (MICSEC)	SURF. ROT. (DEGREES)	EUL. STRAIN (PERCENT)	LAG. STRAIN (PERCENT)	AVG. STRAIN RATE(SEC-1)
1	0.0	0.0	0.0	0.0	0.
2	2.06	0.0	0.0	0.0	0.
3	8.02	0.0	0.0	0.0	0.
4	11.07	0.0	0.0	0.0	0.
5	16.69	0.0	0.0	0.0	0.
6	21.58	0.0	0.0	0.0	0.
7	26.25	0.0	0.0	0.0	0.
8	36.95	0.0545	0.05	0.05	43.
9	47.20	-0.1381	-0.61	-0.60	-632.
10	52.70	-0.2481	-1.34	-1.32	-1311.
11	57.56	-0.2196	-1.99	-1.96	-1355.
12	62.51	-0.2605	-2.75	-2.67	-1393.
13	68.16	-0.2467	-3.42	-3.30	-1116.
14	72.86	-0.1949	-3.95	-3.80	-1049.
15	79.96	-0.1697	-4.48	-4.29	-691.
16	85.65	-0.1052	-4.73	-4.52	-404.
17	91.15	-0.0635	-4.82	-4.60	-144.
18	99.63	0.0761	-4.68	-4.47	149.
19	108.22	0.2037	-4.08	-3.92	635.
20	112.50	0.2275	-3.67	-3.54	902.
21	118.08	0.2816	-3.02	-2.93	1097.
22	121.93	0.3625	-2.43	-2.37	1440.
23	129.27	0.4850	-1.17	-1.16	1659.
24	135.38	0.3583	-0.32	-0.32	1368.
25	143.97	-0.1688	-0.05	-0.05	310.
26	149.39	-0.1076	-0.27	-0.27	-402.
27	154.93	0.1400	-0.35	-0.35	-158.
28	167.19	-0.2276	-0.14	-0.14	174.
29	172.84	-0.0834	-0.06	-0.06	132.
30	174.75	0.0453	-0.05	-0.05	81.
31	184.87	-0.0265	0.01	0.01	57.
32	187.50	-0.0310	0.13	0.13	451.
33	195.10	0.0654	0.05	0.05	-104.
34	206.82	0.0475	0.12	0.12	58.
35	214.42	-0.0326	0.14	0.14	25.
36	218.32	-0.0406	0.18	0.18	101.
37	225.84	-0.0617	0.44	0.44	345.
38	228.90	-0.0859	0.55	0.56	589.
39	230.77	-0.1053	0.65	0.65	509.
40	236.84	-0.1298	0.92	0.93	459.
41	241.12	-0.1575	1.21	1.23	694.
42	247.11	-0.1935	1.62	1.65	702.

COMMENTS-

Appendix Table 6.15 Results of test LS2-19

LEXAN SERIES 2 - TEST NUMBER 19 (LS2-19), 8/ 2/71
••

STRIKER VELOCITY (FT/SEC) = 540.5
STRIKER LENGTH (IN) = 0.992
TARGET LENGTH (IN) = 7.990
GRATING DISTANCE FROM IMPACT (IN) = 3.018
GRATING LENGTH (IN) = 0.0215
AMBIENT TEMPERATURE (DEG F) = 73.0
RESIDUAL STRAIN APPROX. FIVE MIN. AFTER TEST (%) = 0.0

DATA POINT	TIME (MICSEC)	SURF. ROT. (DEGREES)	EUL. STRAIN (PERCENT)	LAG. STRAIN (PERCENT)	AVG. STRAIN RATE(SEC-1)
1	0.0	0.0	0.0	0.0	0.
2	14.09	0.0	0.0	0.0	0.
3	20.46	0.0	0.0	0.0	0.
4	29.81	0.0	0.0	0.0	0.
5	36.65	0.0	0.0	0.0	0.
6	42.91	-0.0897	-0.41	-0.41	-656.
7	51.84	-0.2388	-1.31	-1.29	-985.
8	57.19	-0.2291	-2.02	-1.98	-1296.
9	64.40	-0.2256	-3.01	-2.92	-1304.
10	70.74	-0.1915	-3.68	-3.55	-984.
11	78.53	-0.2754	-3.86	-3.72	-218.
12	86.62	-0.1216	-4.82	-4.60	-1089.
13	91.70	-0.0501	-4.93	-4.70	-192.
14	98.22	0.0541	-4.87	-4.65	77.
15	103.00	0.1335	-4.55	-4.35	621.
16	107.84	0.1743	-4.29	-4.12	482.
17	115.29	0.1999	-3.69	-3.55	754.
18	122.73	0.2757	-2.76	-2.69	1162.
19	132.05	0.4195	-1.20	-1.19	1613.
20	138.46	0.1923	-0.26	-0.26	1446.
21	143.84	-0.0755	-0.22	-0.21	84.
22	153.81	0.0384	-0.39	-0.38	-170.
23	157.78	0.0911	-0.40	-0.40	-37.
24	166.82	-0.0731	-0.29	-0.29	124.
25	173.96	-0.1035	-0.15	-0.15	186.
26	182.13	0.1294	-0.09	-0.09	72.
27	189.65	0.0418	0.11	0.11	274.
28	195.65	0.0429	-0.01	-0.01	-205.
29	200.61	0.1294	0.08	0.08	180.
30	205.53	0.1030	0.04	0.04	-73.
31	210.38	-0.0309	0.11	0.11	137.
32	219.31	-0.0745	0.18	0.18	82.
33	226.26	-0.1118	0.44	0.45	382.
34	233.78	-0.1350	0.82	0.83	506.
35	241.84	-0.1576	1.31	1.33	620.
36	247.26	-0.1871	1.58	1.61	517.

COMMENTS-

Appendix Table 6.16   Results of test LS2-21

```
LEXAN  SERIES  2 - TEST  NUMBER 21 (LS2-21),  8/ 4/71
-------------------------------------------------------
```

STRIKER VELOCITY (FT/SEC) = 527.2
STRIKER LENGTH (IN) = 6.000
TARGET LENGTH (IN) = 2.904
GRATING DISTANCE FROM IMPACT (IN) = 1.382
GRATING LENGTH (IN) = 0.0177
AMBIENT TEMPERATURE (DEG F) = 71.0
RESIDUAL STRAIN APPROX. FIVE MIN. AFTER TEST (%) = -9.73

DATA POINT	TIME (MICSEC)	SURF. ROT. (DEGREES)	EUL. STRAIN (PERCENT)	LAG. STRAIN (PERCENT)	AVG. STRAIN RATE(SEC-1)
1	0.0	0.0	0.0	0.0	0.
2	3.55	0.0	0.0	0.0	0.
3	12.25	0.0	0.0	0.0	0.
4	23.40	-0.4780	-1.68	-1.65	-1483.
5	32.03	-0.4621	-3.23	-3.13	-1710.
6	36.92	-0.4252	-4.55	-4.17	-2138.
7	39.85	-0.3678	-4.89	-4.46	-1667.
8	44.44	-0.3497	-5.47	-5.19	-1143.
9	51.42	-0.2960	-6.23	-5.87	-976.
10	70.59	-0.2229	-7.46	-6.94	-558.
11	72.95	-0.1771	-7.75	-7.19	-1064.
12	74.94	-0.1449	-7.95	-7.37	-891.
13	80.32	-0.1067	-8.53	-7.86	-916.
14	88.03	-0.0292	-9.23	-8.45	-767.
15	97.50	0.0345	-10.22	-9.27	-867.
16	109.03	0.0724	-11.33	-10.18	-786.
17	115.10	0.0873	-12.05	-10.75	-943.
18	138.69	-0.0033	-14.23	-12.45	-722.
19	141.13	0.0008	-14.53	-12.54	-337.
20	146.02	-0.0298	-14.79	-12.89	-717.
21	149.45	-0.0587	-15.14	-13.15	-766.
22	151.86	-0.0701	-15.51	-13.28	-538.
23	162.05	-0.1582	-16.30	-14.01	-721.
24	166.02	-0.1736	-16.73	-14.33	-794.
25	167.74	-0.2084	-16.91	-14.46	-790.
26	172.44	-0.2555	-17.34	-14.78	-665.
27	177.47	-0.3074	-17.90	-15.18	-799.
28	183.16	-0.3900	-18.58	-15.67	-858.
29	186.18	-0.4035	-19.09	-16.03	-1202.
30	192.55	-0.5146	-19.79	-16.52	-765.
31	195.49	-0.4946	-19.79	-16.52	-14.
32	199.73	-0.6079	-20.66	-17.12	-1424.
33	204.16	-0.6693	-21.34	-17.59	-1045.
34	209.05	-0.8031	-22.31	-18.24	-1331.
35	211.49	-0.8360	-22.41	-18.31	-294.
36	214.47	-0.9040	-23.00	-18.70	-1309.
37	217.29	-0.9430	-23.15	-18.80	-341.
38	226.30	-1.1585	-24.16	-19.46	-739.

COMMENTS-SPECIMEN GLUED TO A 15 INCH STEEL BACK-UP BAR

Appendix Table 6.17   Results of test LS2-22

LEXAN SERIES 2 + TEST NUMBER 22 (LS2=22), A/ 6/71

STRIKER VELOCITY (FT/SEC) = 537.2
STRIKER LENGTH (IN) = 0.996
TARGET LENGTH (IN) = 2.898
GRATING DISTANCE FROM IMPACT (IN) = 2.135
GRATING LENGTH (IN) = 0.0134
AMBIENT TEMPERATURE (DEG F) = 72.0
RESIDUAL STRAIN APPROX. FIVE MIN. AFTER TEST (X) = 0.0

DATA POINT	TIME (MICSEC)	SURF. ROT. (DEGREES)	EUL. STRAIN (PERCENT)	LAG. STRAIN (PERCENT)	AVG. STRAIN RATE(SEC-1)
1	0.0	0.0	0.0	0.0	0.
2	4.70	0.0	0.0	0.0	0.
3	9.36	0.0	0.0	0.0	0.
4	11.65	0.0	0.0	0.0	0.
5	15.43	0.0	0.0	0.0	0.
6	18.95	0.0	0.0	0.0	0.
7	34.30	-0.1961	-1.01	-1.00	-649.
8	39.00	-0.3496	-1.73	-1.70	-1505.
9	44.20	-0.2950	-2.68	-2.61	-1740.
10	52.87	-0.2210	-4.32	-4.15	-1774.
11	61.16	-0.0098	-6.03	-5.69	-1858.
12	64.67	0.2742	-6.80	-6.37	-1942.
13	70.02	0.4759	-8.00	-7.41	-1942.
14	77.89	0.9453	-9.19	-8.42	-1287.
15	84.54	1.3612	-9.95	-9.05	-950.
16	92.98	1.7377	-10.12	-9.19	-163.
17	100.08	1.8353	-9.80	-8.93	369.
18	110.74	1.8269	-8.71	-8.01	861.
19	118.88	1.8181	-7.65	-7.11	1107.
20	130.91	1.5659	-5.88	-5.55	1295.
21	135.15	1.4615	-5.18	-4.92	1481.
22	144.13	1.2153	-3.98	-3.79	1263.
23	154.35	0.6840	-2.50	-2.44	1322.
24	162.96	0.4018	-1.69	-1.67	896.
25	171.25	0.1414	-1.33	-1.31	425.
26	177.90	0.1610	-0.92	-0.91	604.
27	181.99	0.0958	-0.53	-0.53	944.
28	187.83	0.0265	-0.11	-0.11	709.
29	197.53	-0.0214	0.68	0.69	823.
30	204.45	-0.0365	1.21	1.22	775.
31	212.28	-0.0697	1.60	1.65	517.
32	220.80	-0.0144	1.52	1.54	-344.
33	228.13	-0.0234	0.67	0.68	-899.
34	233.10	-0.0549	0.19	0.19	-986.
35	239.06	-0.0377	-0.42	-0.42	-1019.
36	243.60	0.1627	-0.69	-0.68	-580.
37	246.85	0.0377	-0.83	-0.82	-820.

COMMENTS-SPECIMEN GLUED TO A 15 INCH STEEL BACK-UP BAR

Appendix Table 6.18   Results of test LS2-23

LEXAN SERIES 2 - TEST NUMBER 23 (LS2-23), 8/10/71

STRIKER VELOCITY (FT/SEC) = 541.6
STRIKER LENGTH (IN) = 1.000
TARGET LENGTH (IN) = 2.899
GRATING DISTANCE FROM IMPACT (IN) = 2.151
GRATING LENGTH (IN) = 0.0154
AMBIENT TEMPERATURE (DEG F) = 72.0
RESIDUAL STRAIN APPROX. FIVE MIN. AFTER TEST (%) = 0.0

DATA POINT	TIME (MICSEC)	SURF. ROT. (DEGREES)	EUL. STRAIN (PERCENT)	LAG. STRAIN (PERCENT)	AVG. STRAIN RATE(SEC-1)
1	0.0	0.0	0.0	0.0	0.
2	2.18	0.0	0.0	0.0	0.
3	8.05	0.0	0.0	0.0	0.
4	15.19	0.0	0.0	0.0	0.
5	17.75	0.0	0.0	0.0	0.
6	25.99	0.0	0.0	0.0	0.
7	29.73	0.0	0.0	0.0	0.
8	35.61	0.0189	0.04	0.04	63.
9	44.19	-0.1681	-0.88	-0.87	-1061.
10	52.05	-0.3065	-2.19	-2.14	-1617.
11	54.46	-0.3046	-2.69	-2.62	-1957.
12	61.86	-0.2403	-4.12	-3.95	-1808.
13	65.45	-0.1373	-4.80	-4.58	-1746.
14	68.96	0.0326	-5.57	-5.27	-1973.
15	76.25	0.2541	-7.13	-6.65	-1892.
16	82.45	0.5274	-8.42	-7.77	-1809.
17	85.57	0.6381	-8.80	-8.09	-1089.
18	89.91	0.9540	-9.48	-8.66	-1242.
19	97.08	1.5928	-10.04	-9.12	-644.
20	104.79	1.7915	-10.20	-9.25	-166.
21	110.90	1.8972	-9.99	-9.08	284.
22	117.12	2.0158	-9.47	-8.65	685.
23	133.95	1.9940	-7.45	-6.93	1022.
24	141.77	1.8744	-6.53	-6.13	1028.
25	145.78	1.6934	-5.95	-5.61	1287.
26	152.76	1.6207	-4.88	-4.65	1375.
27	158.22	1.3758	-4.03	-3.87	1428.
28	163.45	1.0248	-3.17	-3.07	1540.
29	165.93	0.8709	-2.80	-2.73	1377.
30	172.07	0.4970	-1.98	-1.94	1284.
31	180.81	0.2933	-1.38	-1.36	658.
32	184.17	0.2738	-1.18	-1.17	574.
33	188.86	0.3935	-0.90	-0.89	599.
34	192.26	0.4011	-0.61	-0.61	832.
35	201.23	0.2578	0.07	0.07	758.
36	228.45	0.2054	1.41	1.43	889.
37	246.68	0.0575	-0.74	-0.73	-1218.

COMMENTS-SPECIMEN GLUED TO A 15 INCH STEEL BAR;RECORD STARTS 10

MICSEC TOO SOON.

Appendix Table 6.19   Results of test LS2-24

LEXAN SERIES 2 - TEST NUMBER 24 (LS2-24), 8/11/71
••

STRIKER VELOCITY (FT/SEC) = 541.4
STRIKER LENGTH (IN) = 4.005
TARGET LENGTH (IN) = 6.000
GRATING DISTANCE FROM IMPACT (IN) = 1.518
GRATING LENGTH (IN) = 0.0264
AMBIENT TEMPERATURE (DEG F) = 72.0
RESIDUAL STRAIN APPROX. FIVE MIN. AFTER TEST (%) = 0.0

DATA POINT	TIME (MICSEC)	SURF. ROT. (DEGREES)	EUL. STRAIN (PERCENT)	LAG. STRAIN (PERCENT)	AVG. STRAIN RATE(SEC-1)
1	0.0	0.0	0.0	0.0	0.
2	5.23	0.0	0.0	0.0	0.
3	10.57	0.0	0.0	0.0	0.
4	16.24	0.0	0.0	0.0	0.
5	18.74	-0.1932	-0.43	-0.43	-1735.
6	23.65	-0.2926	-0.96	-0.95	-1071.
7	28.86	-0.3480	-1.96	-1.93	-1858.
8	34.59	-0.4555	-2.99	-2.91	-1713.
9	42.49	-0.3703	-4.81	-4.59	-2132.
10	49.13	-0.3541	-5.55	-5.26	-1002.
11	53.18	-0.2757	-5.95	-5.62	-886.
12	56.42	-0.2595	-6.26	-5.89	-860.
13	59.06	-0.2769	-6.49	-6.10	-767.
14	68.68	-0.2510	-6.97	-6.52	-440.
15	75.82	-0.2623	-7.37	-6.87	-485.
16	81.50	-0.2718	-7.57	-7.04	-305.
17	87.42	-0.2965	-7.75	-7.20	-265.
18	95.93	-0.3123	-8.04	-7.44	-291.
19	102.77	-0.3287	-8.17	-7.55	-161.
20	112.59	-0.3767	-8.43	-7.78	-234.
21	119.14	-0.4065	-8.58	-7.90	-184.
22	124.26	-0.4206	-8.67	-7.98	-151.
23	131.17	-0.4546	-8.87	-8.15	-240.
24	144.42	-0.5000	-9.07	-8.31	-128.
25	152.09	-0.5573	-9.12	-8.35	-51.
26	157.20	-0.5818	-9.09	-8.33	45.
27	165.14	-0.6382	-9.04	-8.29	55.
28	172.97	-0.6892	-8.79	-8.08	268.
29	179.42	-0.7302	-8.47	-7.81	413.
30	183.51	-0.7749	-8.13	-7.52	706.
31	189.23	-0.8141	-7.60	-7.06	806.
32	193.70	-0.8575	-7.09	-6.62	995.
33	198.32	-0.8955	-6.61	-6.20	906.
34	204.73	-0.9307	-5.76	-5.44	1176.
35	213.44	-0.9623	-4.46	-4.27	1353.
36	220.12	-0.9920	-3.37	-3.26	1502.
37	236.80	-1.1350	0.46	0.46	2234.

COMMENTS-RESHOT OF TARGET USED IN LS2-8,GOOD IMPACT .

Appendix Table 6.20   Results of test LS2-25

LEXAN SERIES 2 - TEST NUMBER 25 (LS2-25), 8/11/71

STRIKER VELOCITY (FT/SEC) = 549.9
STRIKER LENGTH (IN) = 4.005
TARGET LENGTH (IN) = 5.994
GRATING DISTANCE FROM IMPACT (IN) = 1.525
GRATING LENGTH (IN) = 0.0224
AMBIENT TEMPERATURE (DEG F) = 72.0
RESIDUAL STRAIN APPROX. FIVE MIN. AFTER TEST (%) = 0.0

DATA POINT	TIME (MICSEC)	SURF. ROT. (DEGREES)	EUL. STRAIN (PERCENT)	LAG. STRAIN (PERCENT)	AVG. STRAIN RATE(SEC-1)
1	0.0	0.0	0.0	0.0	0.
2	5.76	0.0	0.0	0.0	0.
3	9.04	0.0	0.0	0.0	0.
4	12.17	0.0	0.0	0.0	0.
5	15.38	0.0	0.0	0.0	0.
6	17.59	-0.0027	-0.06	-0.06	-279.
7	22.94	-0.1674	-0.36	-0.36	-559.
8	28.55	-0.4199	-1.31	-1.29	-1656.
9	34.73	-0.3454	-2.27	-2.22	-1503.
10	38.43	-0.4705	-3.01	-2.93	-1908.
11	42.93	-0.4054	-4.12	-3.96	-2287.
12	48.43	-0.3457	-5.16	-4.91	-1733.
13	54.04	-0.3537	-5.67	-5.37	-825.
14	56.94	-0.2973	-6.03	-5.68	-1083.
15	60.60	-0.2635	-6.37	-5.98	-820.
16	65.49	-0.2825	-6.68	-6.26	-571.
17	71.21	-0.2392	-7.00	-6.54	-492.
18	84.61	-0.2651	-7.58	-7.05	-375.
19	88.06	-0.2826	-7.78	-7.22	-440.
20	91.67	-0.2723	-7.87	-7.29	-239.
21	93.61	-0.2694	-7.94	-7.35	-305.
22	100.79	-0.2991	-8.21	-7.59	-325.
23	112.39	-0.3328	-8.51	-7.84	-219.
24	117.92	-0.3584	-8.75	-8.05	-378.
25	125.25	-0.3787	-8.88	-8.16	-146.
26	137.54	-0.4292	-9.17	-8.40	-201.
27	140.32	-0.4545	-9.24	-8.46	-212.
28	151.58	-0.5076	-9.44	-8.63	-149.
29	157.46	-0.5361	-9.47	-8.65	-36.
30	159.52	-0.5399	-9.47	-8.65	-7.
31	166.73	-0.5789	-9.43	-8.62	47.
32	173.49	-0.6148	-9.28	-8.49	182.
33	181.80	-0.6688	-8.90	-8.17	388.
34	190.81	-0.7471	-7.98	-7.39	863.
35	196.73	-0.7985	-7.34	-6.84	944.
36	205.58	-0.8486	-6.22	-5.85	1112.
37	224.62	-0.9494	-3.24	-3.14	1426.
38	229.39	-1.0071	-2.39	-2.33	1684.
39	235.00	-1.0606	-1.13	-1.11	2176.
40	245.19	-0.9722	1.41	1.43	2498.
41	249.20	-0.8049	2.11	2.16	1810.

COMMENTS-RESHOT OF TARGET USED IN LS2-5.

Appendix Table 6.21   Results of test LS2-26

STRIKER VELOCITY (FT/SEC) = 533.4
STRIKER LENGTH (IN) = 3.995
TARGET LENGTH (IN) = 5.996
GRATING DISTANCE FROM IMPACT (IN) = 1.527
GRATING LENGTH (IN) = 0.0268
AMBIENT TEMPERATURE (DEG F) = 72.0
RESIDUAL STRAIN APPROX. FIVE MIN. AFTER TEST (%) = 0.0

DATA POINT	TIME (MICSEC)	SURF. ROT. (DEGREES)	EUL. STRAIN (PERCENT)	LAG. STRAIN (PERCENT)	AVG. STRAIN RATE(SEC-1)
1	0.0	0.0	0.0	0.0	0.
2	4.22	0.0	0.0	0.0	0.
3	6.24	0.0	0.0	0.0	0.
4	11.19	0.0	0.0	0.0	0.
5	16.52	0.0	0.0	0.0	0.
6	20.44	-0.0478	-0.14	-0.14	-354.
7	24.93	-0.3820	-1.13	-1.12	-2176.
8	29.04	-0.3423	-1.77	-1.73	-1504.
9	31.89	-0.3894	-2.33	-2.27	-1887.
10	34.98	-0.4491	-2.83	-2.76	-1567.
11	40.04	-0.3881	-4.04	-3.88	-2221.
12	52.41	-0.5054	-5.73	-5.42	-1245.
13	58.77	-0.2712	-6.30	-5.93	-798.
14	61.05	-0.2773	-6.48	-6.09	-708.
15	66.38	-0.2309	-6.69	-6.27	-335.
16	71.40	-0.2537	-6.88	-6.41	-274.
17	76.08	-0.2452	-7.21	-6.73	-683.
18	82.90	-0.2820	-7.43	-6.92	-279.
19	94.58	-0.2907	-7.81	-7.25	-288.
20	99.26	-0.3003	-7.97	-7.39	-295.
21	101.01	-0.3029	-8.03	-7.43	-279.
22	107.45	-0.3247	-8.12	-7.51	-118.
23	113.23	-0.3450	-8.24	-7.61	-179.
24	117.84	-0.3694	-8.39	-7.74	-264.
25	129.79	-0.4161	-8.66	-7.97	-197.
26	142.84	-0.4648	-8.95	-8.22	-187.
27	146.84	-0.4819	-8.97	-8.23	-40.
28	147.90	-0.4863	-8.87	-8.15	776.
29	153.23	-0.5234	-8.99	-8.25	-185.
30	155.90	-0.5315	-9.04	-8.29	-152.
31	161.72	-0.5696	-8.93	-8.20	152.
32	171.16	-0.6365	-8.73	-8.03	182.
33	175.99	-0.6542	-8.48	-7.82	436.
34	179.49	-0.6876	-8.29	-7.65	479.
35	183.57	-0.7438	-7.95	-7.37	698.
36	193.50	-0.8198	-6.88	-6.44	938.
37	198.83	-0.8575	-6.22	-5.86	1088.
38	205.38	-0.8877	-5.39	-5.11	1137.
39	212.04	-0.9055	-4.45	-4.26	1272.
40	231.22	-1.0877	-0.82	-0.81	1801.
41	233.20	-1.0995	-0.33	-0.32	2452.
42	234.64	-1.1028	0.07	0.07	2700.
43	236.32	-1.0959	0.43	0.43	2169.
44	248.46	-0.7287	2.54	2.60	1789.

COMMENTS-

Appendix Table 6.22   Results of test LS2-27

LEXAN SERIES 2 - TEST NUMBER 27 (LS2-27), 8/15/71
==

STRIKER VELOCITY (FT/SEC) = 541.8
STRIKER LENGTH (IN) = 0.996
TARGET LENGTH (IN) = 5.993
GRATING DISTANCE FROM IMPACT (IN) = 1.517
GRATING LENGTH (IN) = 0.0201
AMBIENT TEMPERATURE (DEG F) = 72.0
RESIDUAL STRAIN APPROX. FIVE MIN. AFTER TEST (%) = 0.0

DATA POINT	TIME (MICSEC)	SURF. ROT. (DEGREES)	EUL. STRAIN (PERCENT)	LAG. STRAIN (PERCENT)	AVG. STRAIN RATE(SEC-1)
1	0.0	0.0	0.0	0.0	0.
2	5.60	0.0	0.0	0.0	0.
3	9.86	0.0	0.0	0.0	0.
4	15.91	0.0	0.0	0.0	0.
5	18.16	-0.0692	-0.22	-0.22	-990.
6	24.98	-0.4257	-1.56	-1.54	-1928.
7	31.64	-0.4460	-2.68	-2.61	-1606.
8	36.63	-0.4214	-3.86	-3.72	-2232.
9	38.49	-0.4122	-4.17	-4.00	-1498.
10	49.53	-0.3671	-5.60	-5.30	-1180.
11	55.65	-0.2224	-5.96	-5.62	-527.
12	63.62	-0.0631	-5.86	-5.54	109.
13	70.44	0.0452	-5.36	-5.09	652.
14	76.60	0.1094	-4.75	-4.53	906.
15	86.27	0.1178	-3.40	-3.29	1282.
16	88.48	0.1696	-3.09	-2.99	1355.
17	103.45	0.0904	-0.71	-0.71	1528.
18	113.99	-0.2877	0.15	0.15	810.
19	117.00	-0.1522	0.21	0.22	226.
20	121.00	-0.0704	0.27	0.27	142.
21	125.19	0.0003	0.15	0.15	-279.
22	134.97	-0.0345	0.04	0.04	-118.
23	144.56	0.0970	-0.05	-0.05	-98.
24	153.66	-0.1059	0.08	0.08	152.
25	165.28	-0.0729	0.22	0.22	114.
26	172.05	-0.1610	0.40	0.41	280.
27	173.69	-0.1489	0.33	0.34	-432.
28	180.43	-0.2092	0.38	0.39	75.
29	183.17	-0.2128	0.54	0.55	589.
30	186.94	-0.2217	0.57	0.58	77.
31	193.18	-0.2744	0.95	0.96	613.
32	198.02	-0.2722	1.29	1.30	710.
33	200.84	-0.2984	1.41	1.44	473.
34	206.47	-0.3260	1.74	1.77	593.
35	217.70	-0.2991	2.44	2.51	655.
36	220.13	-0.3105	2.88	2.97	407.
37	239.86	-0.2866	3.03	3.12	139.
38	251.17	-0.3022	2.65	2.72	-353.

COMMENTS-

Appendix Table 6.23   Results of test LS2-28

```
LEXAN  SERIES  2 - TEST  NUMBER 28 (LS2-28),  8/16/71
•••••••••••••••••••••••••••••••••••••••••••••••••••
```

STRIKER VELOCITY (FT/SEC) = 548.8
STRIKER LENGTH (IN) = 3.995
TARGET LENGTH (IN) = 7.998
GRATING DISTANCE FROM IMPACT (IN) = 2.981
GRATING LENGTH (IN) = 0.0287
AMBIENT TEMPERATURE (DEG F) = 72.0
RESIDUAL STRAIN APPROX. FIVE MIN. AFTER TEST (%) = 0.0

DATA POINT	TIME (MICSEC)	SURF. ROT. (DEGREES)	EUL. STRAIN (PERCENT)	LAG. STRAIN (PERCENT)	AVG. STRAIN RATE(SEC-1)
1	0.0	0.0	0.0	0.0	0.
2	3.28	0.0	0.0	0.0	0.
3	8.97	0.0	0.0	0.0	0.
4	15.61	0.0	0.0	0.0	0.
5	19.13	0.0	0.0	0.0	0.
6	22.75	0.0	0.0	0.0	0.
7	27.22	0.0	0.0	0.0	0.
8	32.26	0.0	0.0	0.0	0.
9	37.75	-0.0763	-0.06	-0.06	-109.
10	40.12	0.0052	-0.03	-0.03	122.
11	46.27	-0.1466	-0.64	-0.64	-989.
12	51.88	-0.2748	-1.34	-1.32	-1223.
13	54.28	-0.2951	-1.55	-1.52	-821.
14	59.25	-0.2743	-2.45	-2.39	-1756.
15	62.91	-0.2392	-3.00	-2.92	-1427.
16	64.86	-0.2408	-3.18	-3.08	-840.
17	69.55	-0.2261	-3.75	-3.61	-1130.
18	73.18	-0.2061	-4.14	-3.97	-1001.
19	78.14	-0.2217	-4.62	-4.41	-886.
20	81.77	-0.1845	-4.91	-4.68	-724.
21	89.75	-0.1762	-5.39	-5.11	-544.
22	92.69	-0.1489	-5.57	-5.27	-561.
23	100.86	-0.1586	-6.01	-5.67	-483.
24	104.56	-0.1505	-6.10	-5.75	-224.
25	108.19	-0.1517	-6.23	-5.87	-314.
26	115.94	-0.1514	-6.57	-6.17	-389.
27	118.46	-0.1377	-6.65	-6.24	-281.
28	122.77	-0.1518	-6.80	-6.36	-292.
29	127.01	-0.1475	-6.91	-6.47	-239.
30	130.14	-0.1479	-6.96	-6.50	-119.
31	135.25	-0.1519	-7.18	-6.70	-385.
32	142.47	-0.1611	-7.37	-6.87	-234.
33	151.75	-0.1831	-7.58	-7.05	-195.
34	159.27	-0.1828	-7.74	-7.19	-182.
35	167.47	-0.1840	-7.87	-7.30	-134.
36	170.91	-0.1738	-7.93	-7.35	-150.
37	174.73	-0.1590	-7.90	-7.33	59.
38	180.15	-0.1413	-7.94	-7.36	-57.
39	187.55	-0.1015	-7.75	-7.19	225.
40	193.39	-0.0547	-7.61	-7.08	196.
41	200.61	-0.0440	-7.27	-6.78	412.
42	206.95	-0.0249	-7.00	-6.54	374.
43	217.83	-0.0025	-6.22	-5.86	627.
44	225.92	-0.0067	-5.56	-5.27	729.
45	234.66	0.0089	-4.74	-4.53	849.
46	244.28	-0.0006	-3.70	-3.57	997.

COMMENTS-

Appendix Table 6.24   Results of test LS2-29

LEXAN SERIES 2 - TEST NUMBER 29 (LS2-29), 8/17/71
•••

STRIKER VELOCITY (FT/SEC) = 543.9
STRIKER LENGTH (IN) = 3.982
TARGET LENGTH (IN) = 7.988
GRATING DISTANCE FROM IMPACT (IN) = 3.043
GRATING LENGTH (IN) = 0.0177
AMBIENT TEMPERATURE (DEG F) = 72.0
RESIDUAL STRAIN APPROX. FIVE MIN. AFTER TEST (%) = 0.0

DATA POINT	TIME (MICSEC)	SURF. ROT. (DEGREES)	EUL. STRAIN (PERCENT)	LAG. STRAIN (PERCENT)	AVG. STRAIN RATE(SEC-1)
1	0.0	0.0	0.0	0.0	0.
2	4.72	0.0	0.0	0.0	0.
3	7.81	0.0	0.0	0.0	0.
4	12.04	0.0	0.0	0.0	0.
5	19.16	0.0	0.0	0.0	0.
6	30.75	0.0	0.0	0.0	0.
7	41.64	0.0071	-0.19	-0.19	-176.
8	48.23	-0.126?	-0.82	-0.81	-935.
9	55.05	-0.2857	-1.64	-1.62	-1183.
10	63.21	-0.2591	-3.05	-2.99	-1683.
11	68.92	-0.2479	-3.73	-3.60	-1071.
12	70.86	-0.2333	-3.92	-3.77	-890.
13	78.64	-0.2272	-4.69	-4.48	-908.
14	85.49	-0.1976	-5.18	-4.93	-656.
15	88.85	-0.2000	-5.39	-5.11	-549.
16	104.81	-0.1819	-6.22	-5.86	-468.
17	110.45	-0.1895	-6.40	-6.01	-269.
18	117.99	-0.1862	-6.75	-6.33	-417.
19	131.48	-0.2291	-7.10	-6.63	-223.
20	135.56	-0.2552	-7.28	-6.78	-401.
21	139.86	-0.2640	-7.39	-6.88	-223.
22	144.74	-0.2895	-7.52	-7.00	-238.
23	151.98	-0.3275	-7.61	-7.07	-99.
24	154.11	-0.3332	-7.79	-7.23	-732.
25	158.72	-0.3286	-8.03	-7.43	-453.
26	163.48	-0.3206	-7.98	-7.39	86.
27	171.60	-0.3148	-8.28	-7.65	-314.
28	178.61	-0.2918	-8.21	-7.58	93.
29	188.13	-0.2557	-8.28	-7.65	-66.
30	189.62	-0.2448	-8.30	-7.66	-101.
31	195.60	-0.2172	-7.98	-7.39	447.
32	202.30	-0.2140	-7.55	-7.02	561.
33	205.05	-0.2193	-7.37	-6.87	557.
34	214.34	-0.2354	-6.84	-6.80	497.
35	221.51	-0.2274	-6.51	-5.94	652.
36	228.71	-0.2477	-5.66	-5.35	809.
37	233.47	-0.2570	-5.33	-5.06	609.
38	236.78	-0.2543	-4.94	-4.70	1081.
39	240.52	-0.2554	-4.54	-4.34	965.
40	247.79	-0.2839	-3.78	-3.65	960.

COMMENTS-

Appendix Table 6.25   Results of test LS2-30

```
LEXAN  SERIES  2 - TEST  NUMBER 30 (LS2-30),  8/18/71
=======================================================

STRIKER VELOCITY (FT/SEC) =  696.6
STRIKER LENGTH (IN) = 1.000
TARGET LENGTH (IN) = 5.740
GRATING  DISTANCE FROM IMPACT (IN) = 0.251
GRATING LENGTH (IN) = 0.0244
AMBIENT TEMPERATURE (DEG F) = 72.0
RESIDUAL STRAIN APPROX. FIVE MIN. AFTER TEST (%) = -0.68
```

DATA POINT	TIME (MICSEC)	SURF. ROT. (DEGREES)	EUL. STRAIN (PERCENT)	LAG. STRAIN (PERCENT)	AVG. STRAIN RATE(SEC-1)
1	0.0	0.0	0.0	0.0	0.
2	1.37	-0.0331	-0.15	-0.15	-1092.
3	2.59	-0.0378	-0.18	-0.18	-241.
4	7.02	-2.6175	-5.95	-5.61	-12280.
5	9.76	-2.8571	-6.72	-6.30	-2496.
6	11.40	-2.8484	-7.54	-7.01	-4363.
7	12.74	-2.9518	-8.37	-7.73	-5347.
8	15.52	-3.2288	-9.84	-8.96	-4433.
9	18.23	-3.4080	-11.01	-9.91	-3522.
10	23.53	-3.8240	-13.46	-11.87	-3684.
11	33.06	-4.1129	-15.24	-13.23	-1428.
12	38.40	-4.0865	-15.24	-13.23	1.
13	44.51	-3.9980	-15.37	-13.32	-158.
14	48.74	-3.8641	-14.68	-12.80	1231.
15	53.93	-3.7641	-13.53	-11.92	1711.
16	60.07	-3.6875	-12.58	-11.02	1466.
17	62.28	-3.7196	-11.98	-10.70	1432.
18	68.57	-3.8443	-11.04	-9.94	1205.
19	74.90	-4.0213	-9.92	-9.02	1449.
20	78.07	-4.0648	-9.56	-8.72	949.
21	81.57	-4.2445	-9.24	-8.46	749.
22	84.78	-4.2861	-8.84	-8.12	1060.
23	90.88	-4.4738	-8.29	-7.66	760.
24	94.43	-4.5084	-8.04	-7.44	618.
25	98.70	-4.5544	-7.74	-7.18	597.
26	105.85	-4.6839	-7.32	-6.82	700.
27	108.38	-4.7117	-7.10	-6.63	416.
28	111.36	-4.6237	-6.64	-6.22	1374.
29	123.26	-4.4638	-6.03	-5.69	453.
30	128.52	-4.3616	-5.58	-5.29	755.
31	136.87	-4.1935	-5.20	-4.94	412.
32	146.37	-4.1219	-4.89	-4.67	294.
33	152.32	-4.0419	-5.37	-5.10	-724.
34	161.62	-3.8601	-4.76	-4.55	591.
35	168.18	-3.7745	-4.53	-4.34	318.
36	176.99	-3.5373	-4.28	-4.10	269.
37	186.79	-3.3563	-4.01	-3.85	253.
38	190.30	-3.3291	-4.03	-3.88	-65.
39	192.74	-3.3087	-3.99	-3.83	166.
40	195.41	-3.2883	-3.94	-3.79	152.
41	200.29	-3.2385	-3.72	-3.58	433.
42	206.05	-3.2816	-3.51	-3.39	329.
43	214.56	-3.3270	-3.18	-3.09	362.
44	227.07	-3.1750	-3.10	-3.00	66.
45	243.05	-2.9661	-3.10	-3.00	-1.

COMMENTS-

Appendix Table 6.26   Results of test LS2-31

LEXAN SERIES 2 - TEST NUMBER 31 (LS2-31), 8/18/71
●●

STRIKER VELOCITY (FT/SEC) = 655.9
STRIKER LENGTH (IN) = 0.998
TARGET LENGTH (IN) = 5.945
GRATING DISTANCE FROM IMPACT (IN) = 0.253
GRATING LENGTH (IN) = 0.0173
AMBIENT TEMPERATURE (DEG F) = 72.0
RESIDUAL STRAIN APPROX. FIVE MIN. AFTER TEST (%) = -0.18

DATA POINT	TIME (MICSEC)	SURF. ROT. (DEGREES)	EUL. STRAIN (PERCENT)	LAG. STRAIN (PERCENT)	AVG. STRAIN RATE(SEC-1)
1	0.0	0.0	0.0	0.0	0.
2	0.95	0.0	0.0	0.0	0.
3	3.62	-0.0459	-0.26	-0.26	-955.
4	6.48	-1.9212	-4.98	-4.74	-15694.
5	8.08	-2.2462	-6.10	-5.75	-6273.
6	11.48	-2.7895	-7.31	-6.81	-5135.
7	14.99	-2.9864	-8.79	-8.08	-3614.
8	18.00	-3.5385	-10.46	-9.47	-4622.
9	20.63	-3.4335	-11.14	-10.02	-2076.
10	30.39	-3.7249	-13.82	-12.14	-2170.
11	34.48	-3.6267	-13.65	-12.01	316.
12	42.10	-3.4833	-13.91	-12.21	-267.
13	49.01	-3.3065	-13.38	-11.80	596.
14	52.32	-3.2145	-12.71	-11.28	1586.
15	56.71	-3.0431	-11.52	-10.33	2148.
16	59.53	-2.9443	-11.10	-9.99	1228.
17	64.64	-3.0185	-10.11	-9.18	1574.
18	67.69	-2.9817	-9.57	-8.74	1458.
19	73.57	-3.2130	-8.69	-8.00	1763.
20	80.70	-3.3903	-7.57	-7.03	1350.
21	86.42	-3.5874	-7.03	-6.56	821.
22	93.63	-3.6299	-6.29	-5.92	895.
23	96.45	-3.6655	-6.10	-5.75	596.
24	98.89	-3.6616	-6.01	-5.67	346.
25	103.96	-3.6217	-5.71	-5.40	524.
26	108.54	-3.5316	-5.42	-5.14	563.
27	115.13	-3.2742	-4.93	-4.69	680.
28	123.11	-2.9593	-4.35	-4.17	661.
29	128.18	-2.7390	-4.08	-3.92	401.
30	134.20	-2.5839	-3.84	-3.70	368.
31	139.50	-2.3562	-3.71	-3.57	282.
32	143.51	-2.3080	-3.70	-3.57	9.
33	148.92	-2.1633	-3.33	-3.22	648.
34	159.49	-1.9854	-3.08	-2.99	220.
35	166.66	-1.8514	-3.05	-2.96	34.
36	173.41	-1.7458	-2.90	-2.81	220.
37	175.01	-1.7084	-2.85	-2.78	240.
38	181.57	-1.6711	-2.89	-2.81	-46.
39	184.89	-1.6138	-2.78	-2.71	297.
40	192.55	-1.4908	-2.50	-2.44	349.
41	199.07	-1.4149	-2.34	-2.29	230.
42	208.04	-1.3986	-2.01	-1.97	354.
43	223.10	-1.3912	-1.71	-1.68	196.
44	228.93	-1.3289	-1.50	-1.48	339.
45	240.15	-1.2322	-1.63	-1.61	-115.
46	245.60	-1.1795	-1.70	-1.67	-117.
47	251.93	-1.1135	-1.74	-1.71	-60.

COMMENTS-

Appendix Table 6.27   Results of test LS2-36

LEXAN SERIES 2 - TEST NUMBER 36 (LS2-36), 8/22/71

STRIKER VELOCITY (FT/SEC) = 611.6
STRIKER LENGTH (IN) = 0.990
TARGET LENGTH (IN) = 6.749
GRATING DISTANCE FROM IMPACT (IN) = 0.288
GRATING LENGTH (IN) = 0.0165
AMBIENT TEMPERATURE (DEG F) = 72.0
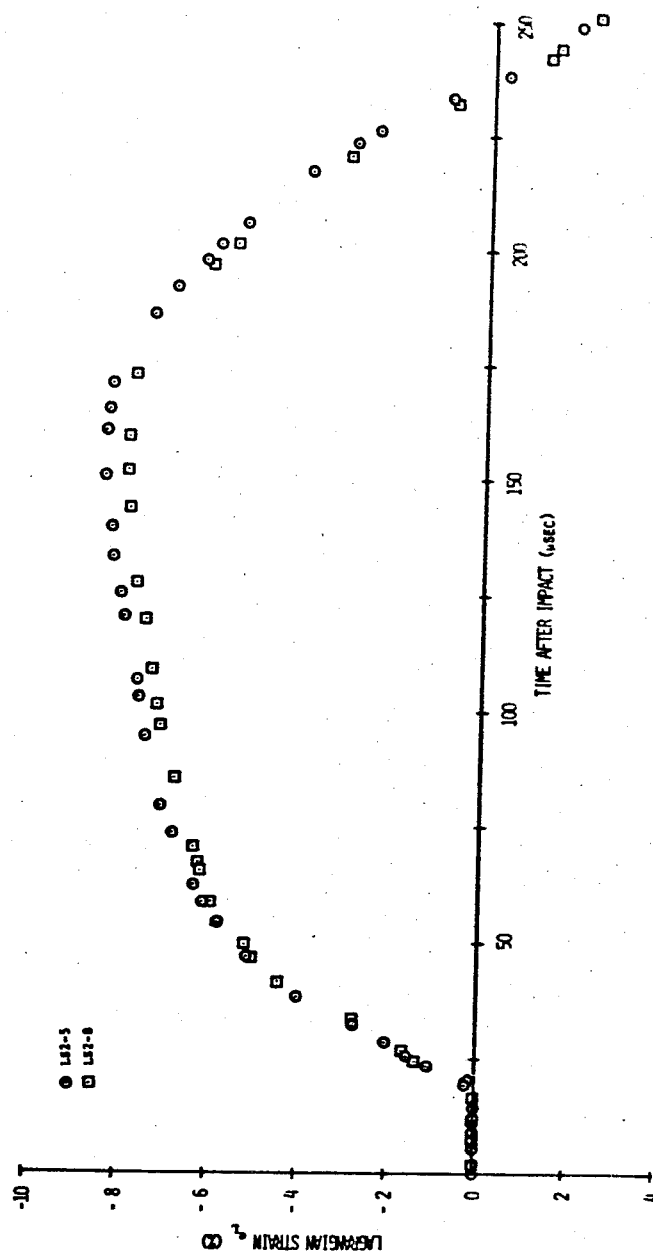RESIDUAL STRAIN APPROX. FIVE MIN. AFTER TEST (%) = 0.0

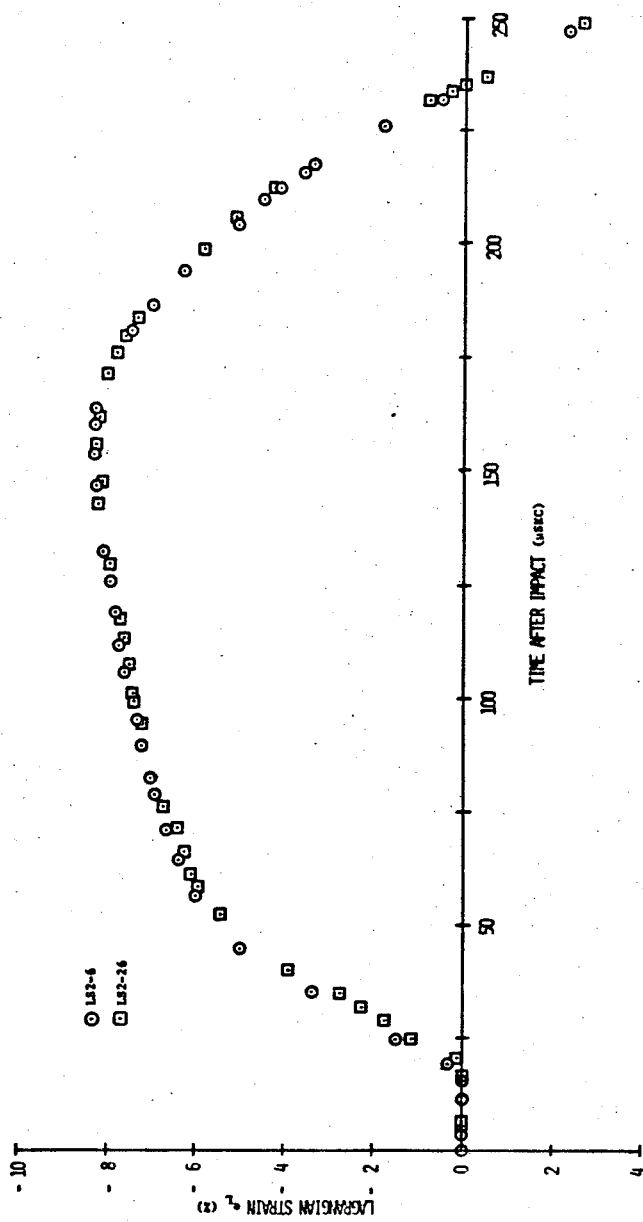| DATA POINT	TIME (MICSEC)	SURF. ROT. (DEGREES)	EUL. STRAIN (PERCENT)	LAG. STRAIN (PERCENT)	AVG. STRAIN RATE(SEC-1)
1	0.0	0.0	0.0	0.0	0.
2	8.00	-2.2485	-6.48	-6.08	-7607.
3	13.52	-2.2369	-8.55	-7.88	-3204.
4	20.15	-2.1990	-10.39	-9.42	-2323.
5	23.00	-2.0665	-11.03	-9.98	-1830.
6	94.80	-0.6565	-1.57	-1.54	1183.
7	97.92	-0.6248	-1.38	-1.36	568.
8	106.03	-0.3303	-0.60	-0.67	850.
9	113.31	-0.3076	-0.61	-0.61	90.
10	140.46	-0.4487	-0.60	-0.59	5.
11	154.90	-0.4574	-0.58	-0.58	11.
12	160.23	-0.4632	-0.58	-0.58	-0.
13	172.61	-0.4718	-0.57	-0.56	13.
14	178.78	-0.4603	-0.57	-0.56	0.
15	191.31	-0.4603	-0.57	-0.56	0.
16	197.09	-0.4574	-0.55	-0.55	29.
17	203.84	-0.5036	-0.52	-0.51	47.
18	218.00	-0.5614	-0.42	-0.42	69.

COMMENTS-RECORD INCOMPLETE,DIDN'T GET MAX. STRAIN,SKIP IN
           RECORD.

6.2   Summary of Pertinent Experimental Conditions
   and Plots of Strain-Time Histories for Lexan
      Series 2 (LS2) Tests

Appendix Table 6.28 Summary of experimental conditions

Test	Striker velocity (ft/sec)	Striker length (in)	Target length (in)	Grating position (in)	Grating length (in)	Ambient temperature (°F)	Residual e_L (percent)	Comments
LS2-5	545.3	3.997	5.994	1.525	0.0224	72	0	-
LS2-8	540.5	4.000	6.000	1.518	0.0264	72	0	Aberrant surface rotation
LS2-6	526.3	4.000	5.994	1.518	0.0224	72	0	-
LS2-26	533.4	3.995	5.996	1.527	0.0268	72	0	-
LS2-11	549.5	3.971	5.994	2.290	0.0134	72	0	-
LS2-12	551.6	3.977	6.023	2.279	0.0233	73	0	-
LS2-28	548.8	3.995	7.998	2.981	0.0287	72	0	-
LS2-29	543.9	3.982	7.988	3.043	0.0177	72	0	-
LS2-25	549.9	4.005	5.994	1.525	0.0224	72	0	Reshot of specimen of LS2-5
LS2-24	541.4	4.005	6.000	1.518	0.0264	72	0	Reshot of specimen of LS2-8
LS2-13	533.0	1.001	5.994	1.517	0.0114	73	0	-
LS2-27	541.8	0.996	5.993	1.517	0.0201	72	0	-
LS2-15	529.9	1.004	5.985	2.265	0.0272	72	0	-
LS2-16	533.9	0.994	5.990	2.243	0.0134	73	0	-
LS2-17	534.1	0.995	8.025	2.995	0.0138	72	0	-
LS2-19	540.5	0.992	7.990	3.018	0.0213	73	0	-
LS2-18	522.2	0.995	7.999	3.008	0.0146	72	0	-
LS2-3	548.0	1.25	6.0	0.254	0.0244	82	0	-
LS2-36	611.6	0.994	6.749	0.244	0.0165	72	0	Incomplete; skip in record
LS2-31	655.9	0.998	5.945	0.253	0.0173	72	-0.14	-
LS2-30	696.6	1.000	5.740	0.251	0.0244	72	-0.68	-
LS2-22	537.2	0.996	2.898	2.135	0.0134	72	0	Specimen glued to steel back-up bar
LS2-23	541.6	1.000	2.899	2.151	0.0154	72	0	Specimen glued to steel back-up bar; record starts 10 μsec too soon
LS2-21	527.2	6.000	2.904	1.382	0.0177	71	-9.73	Specimen glued to steel back-up bar

Appendix Figure 6.1 Strain e_L versus time after impact for tests LS2-5 and LS2-8
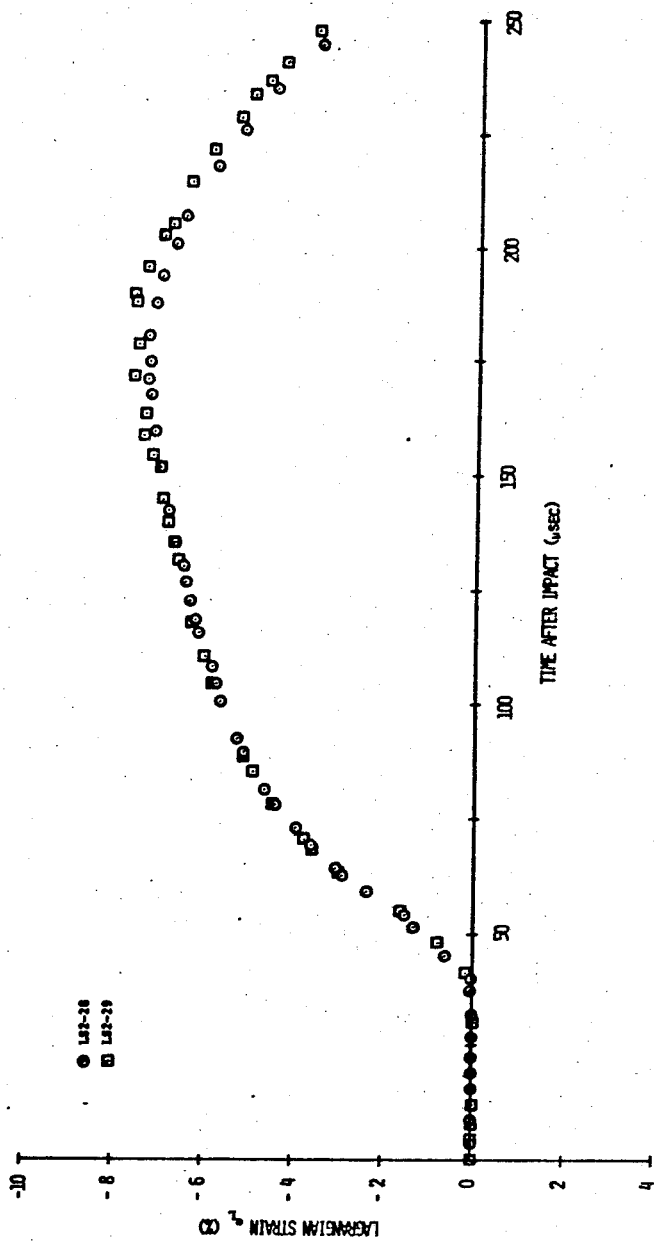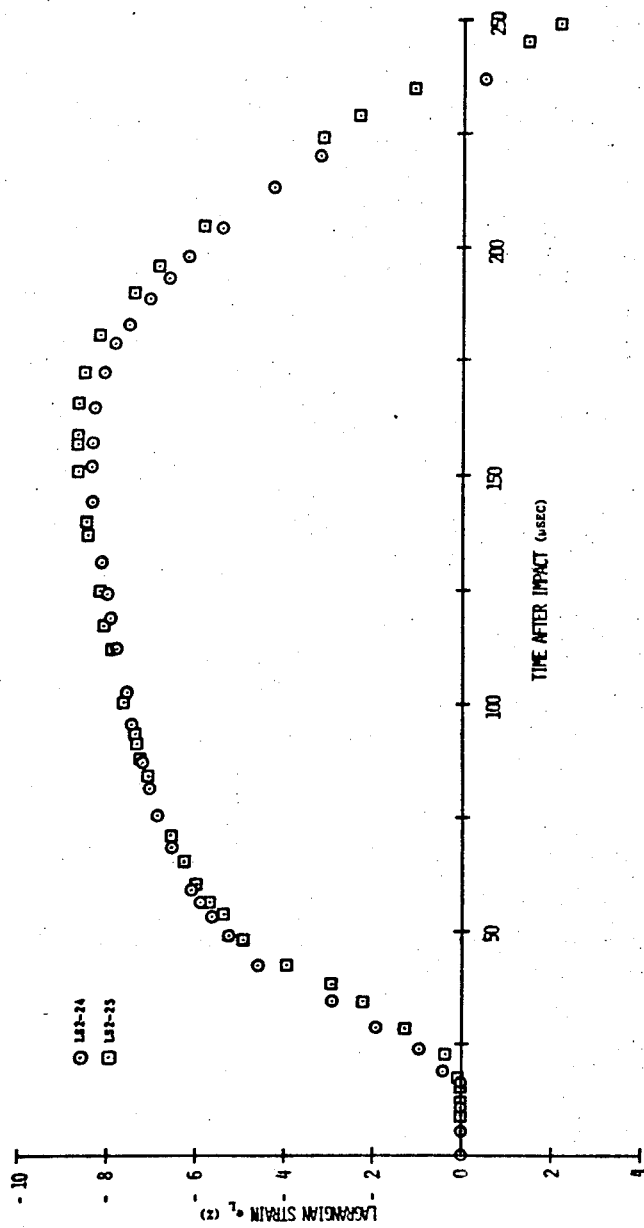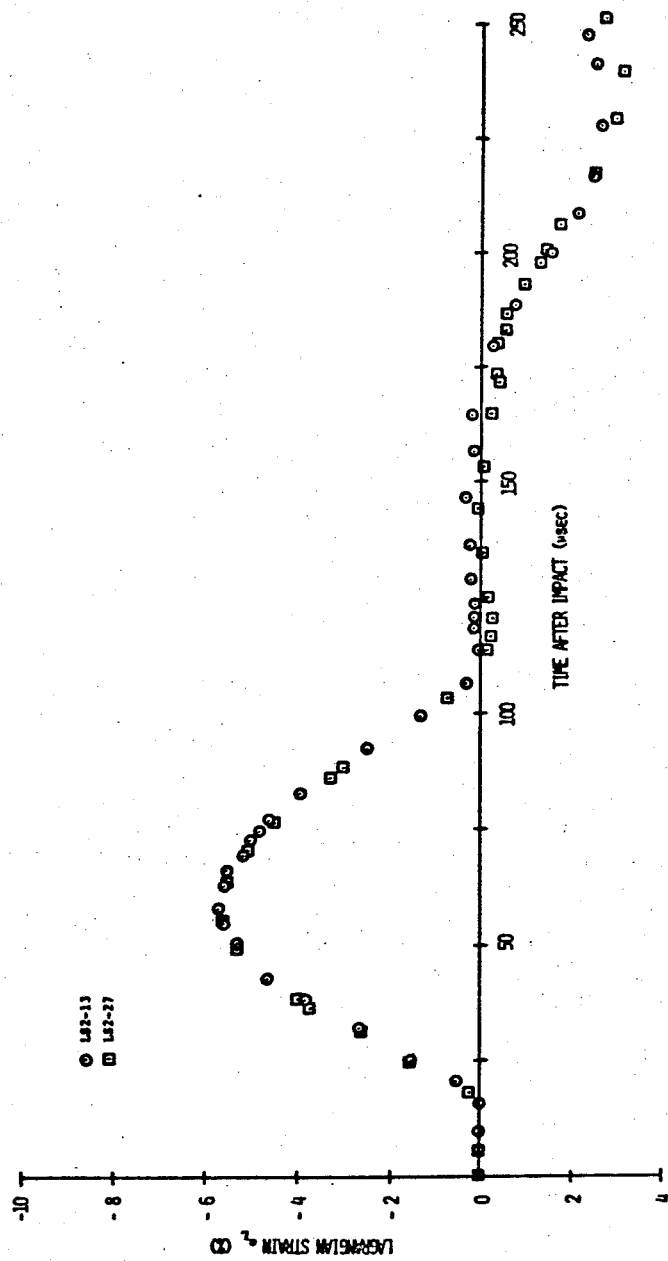
127

Appendix Figure 6.2   Strain e_L versus time after impact for tests LS2-6 and LS2-26

129
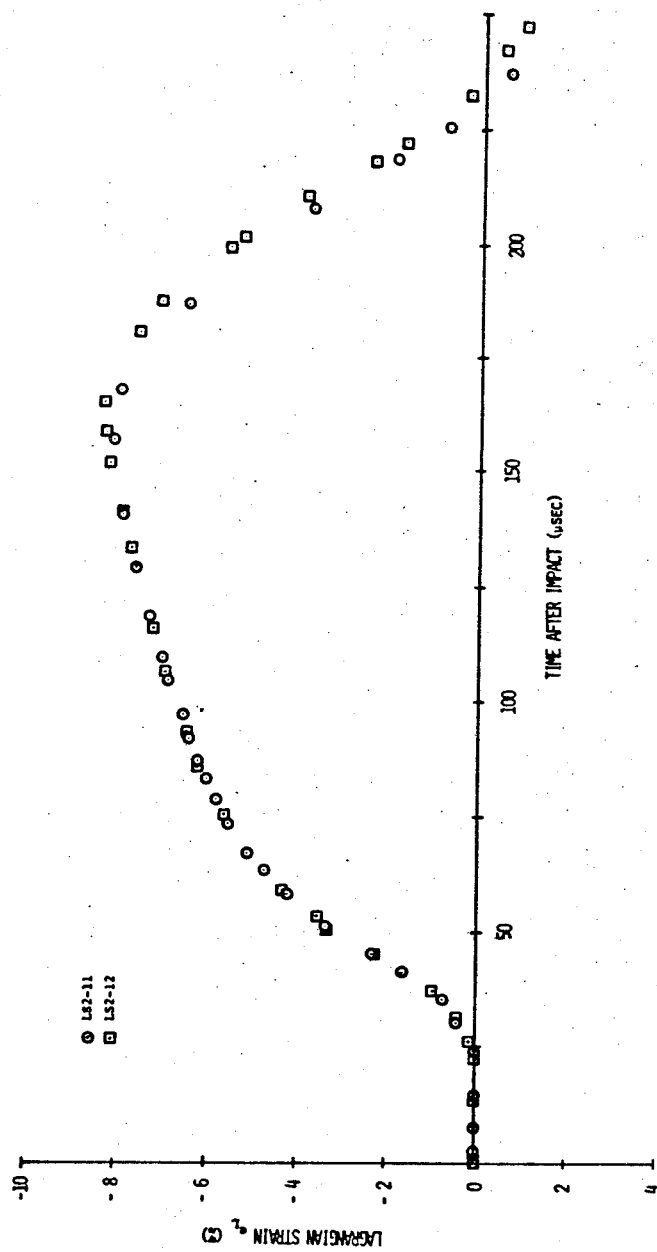
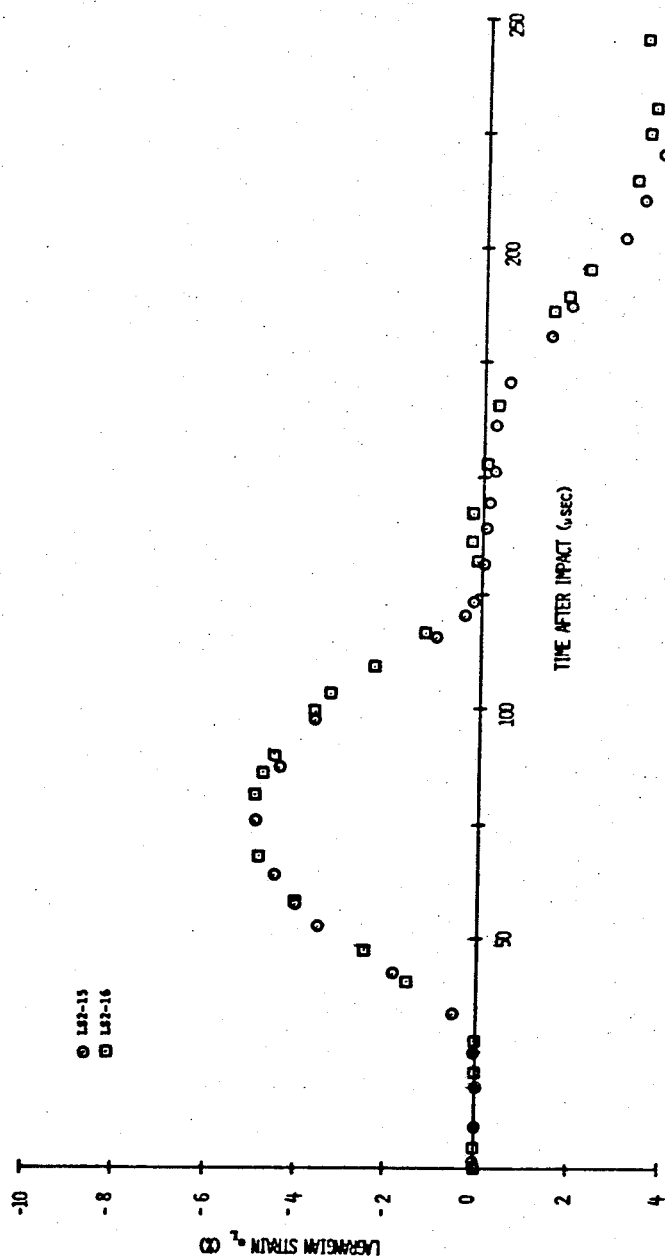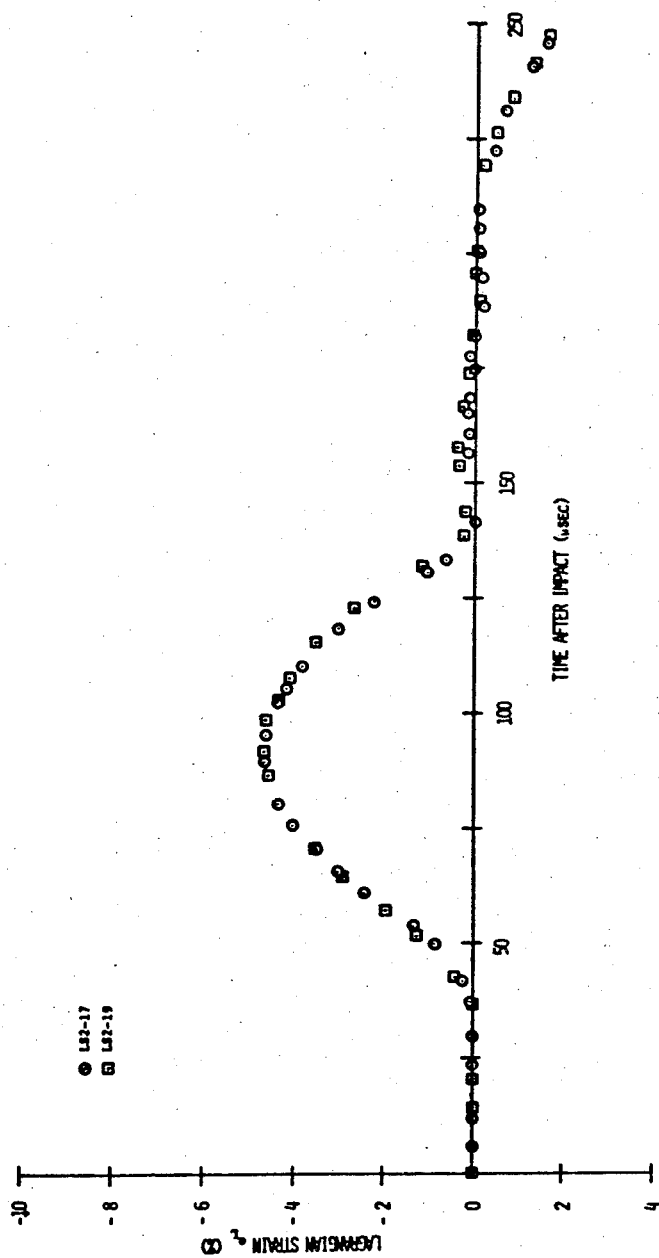Appendix Figure 6.3 Strain e_L versus time after impact for tests LS2-11 and LS2-12

130

TIME AFTER IMPACT (µsec)

LAGRANGIAN STRAIN e_L (%)

LS2-28
LS2-29

Appendix Figure 6.4   Strain e_L versus time after impact for tests LS2-28 and LS2-29

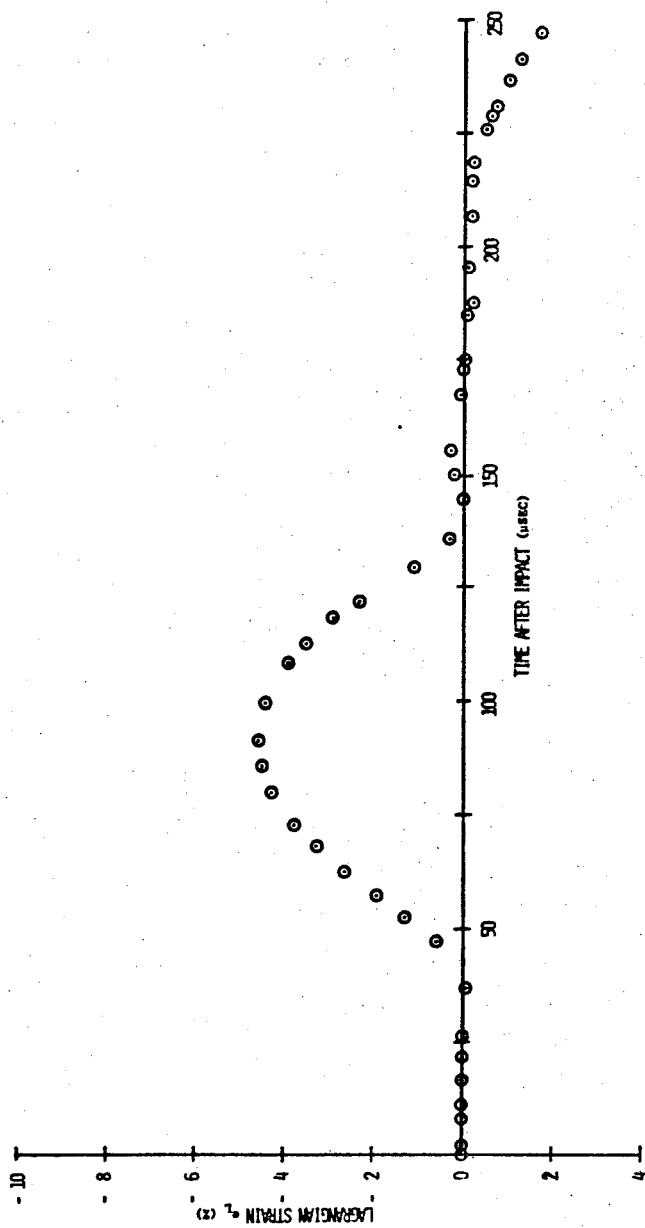Appendix Figure 6.5   Strain e_L versus time after impact for tests LS2-24 and LS2-25

131

Appendix Figure 6.6   Strain e_L versus time after impact for tests LS2-13 and LS2-27
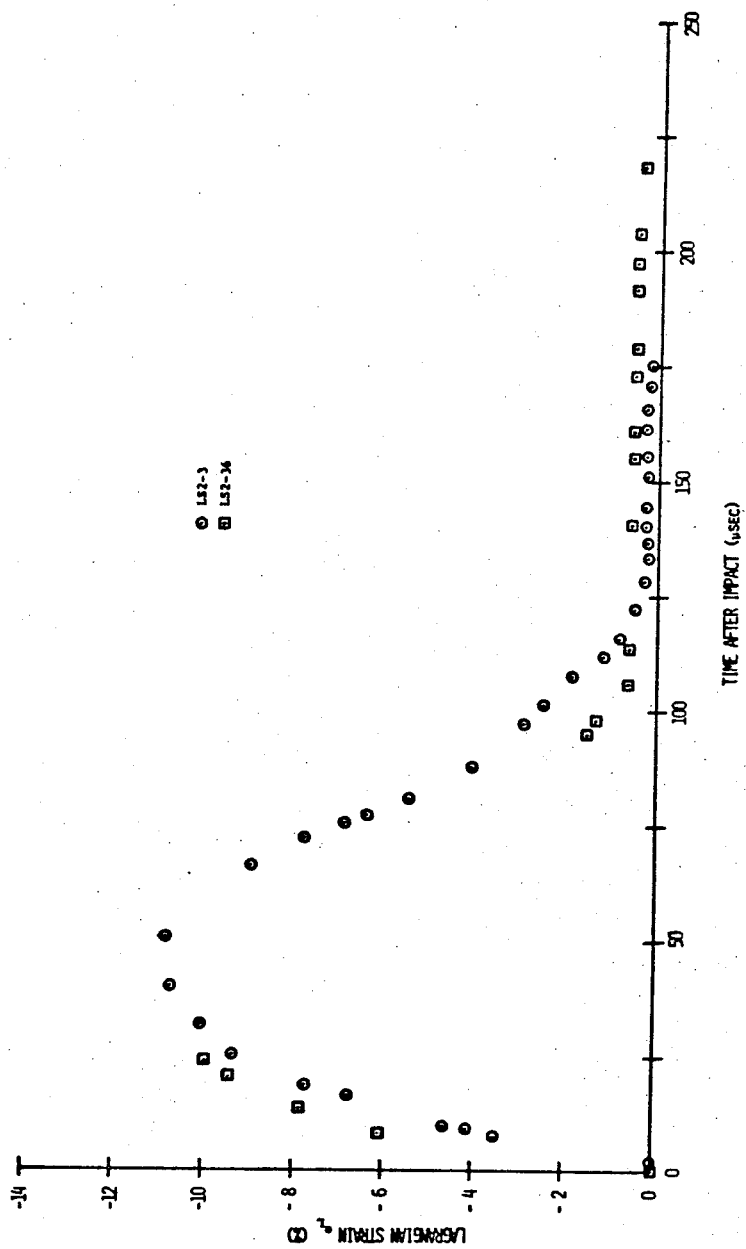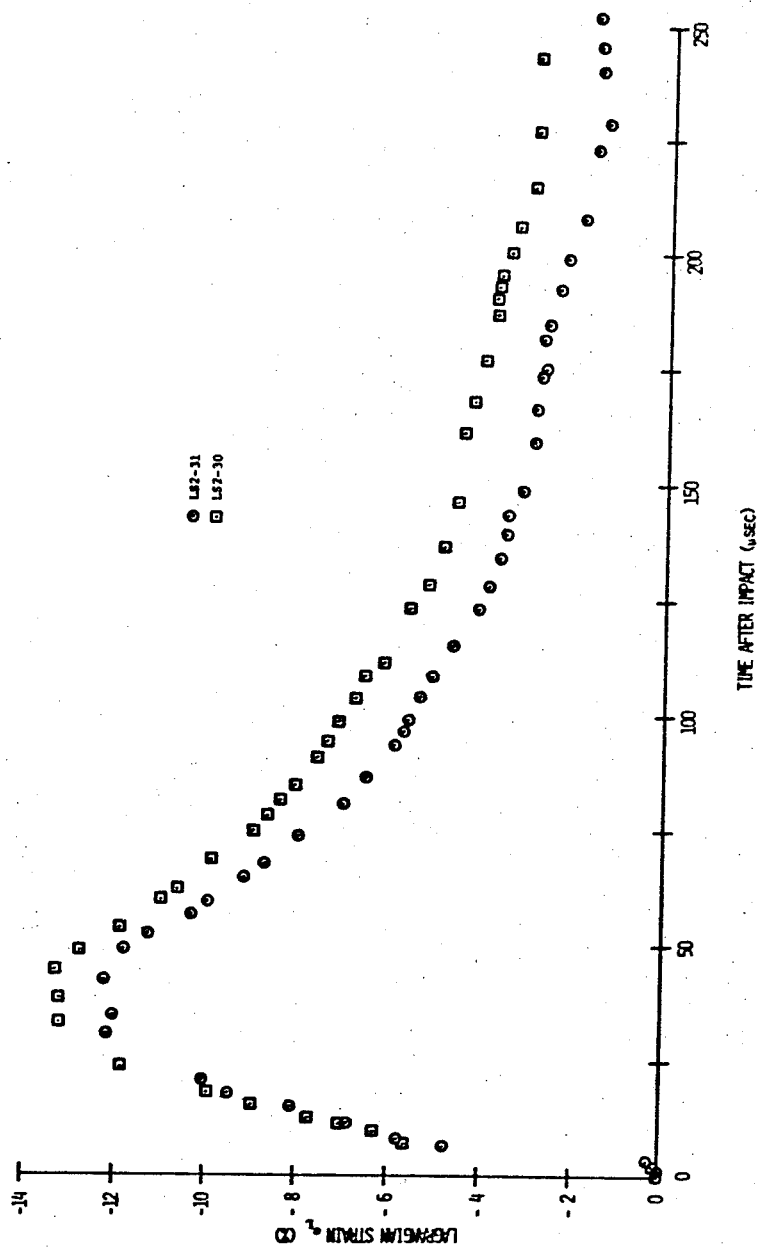
132

Appendix Figure 6.7   Strain e_L versus time after impact for tests LS2-15 and LS2-16

Appendix Figure 6.8   Strain e_L versus time after impact for tests LS2-17 and LS2-19

134

Appendix Figure 6.9   Strain e_L versus time after impact for test LS2-18

136

TIME AFTER IMPACT (μsec)

LAGRANGIAN STRAIN e_L (%)

Appendix Figure 6.10   Strain e_L versus time after impact for tests LS2-3 and LS2-36

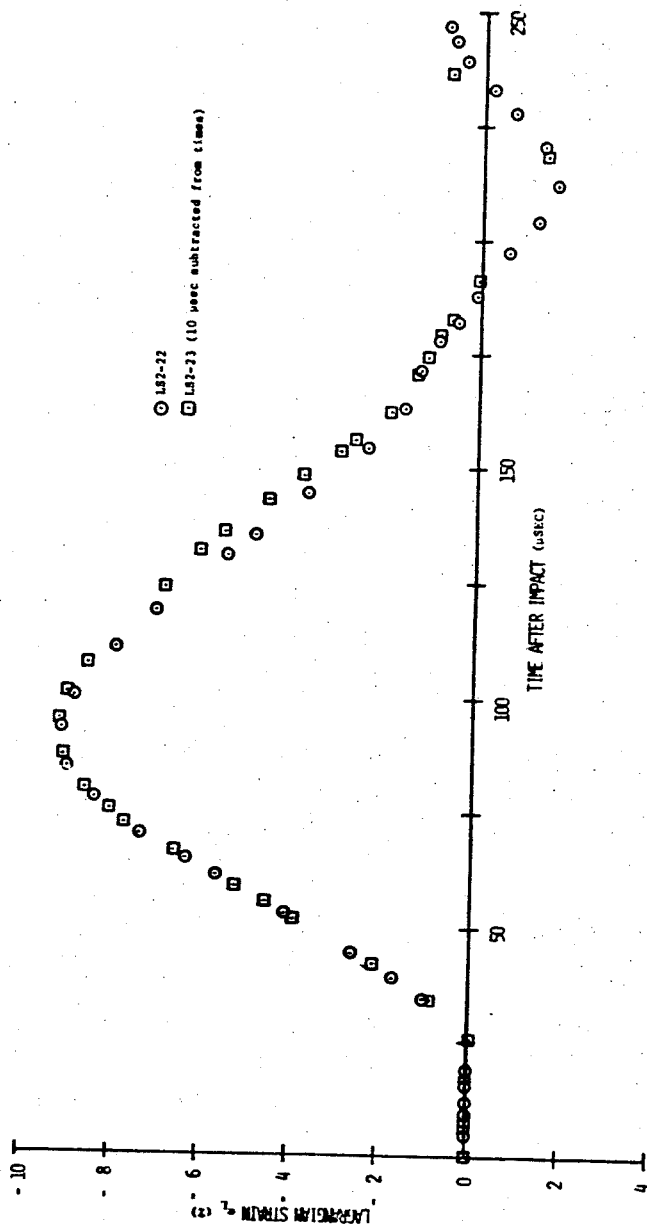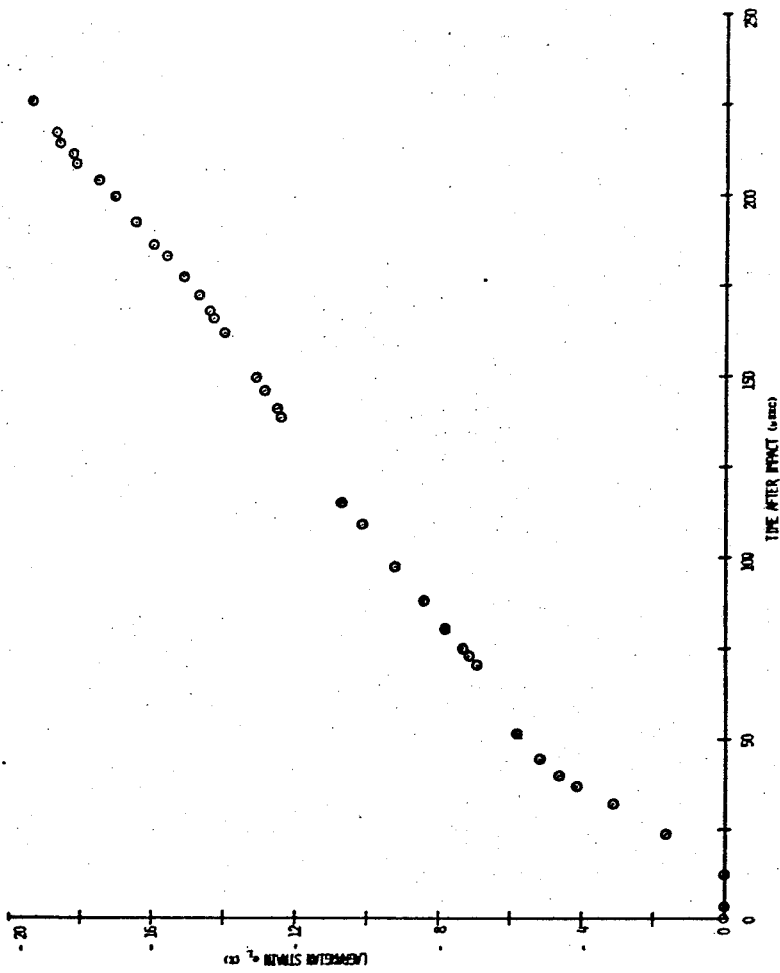Appendix Figure 6.11   Strain e_L versus time after impact for tests LS2-31 and LS2-30

Appendix Figure 6.12   Strain e_L versus time after impact for tests LS2-22 and LS2-23

138

Appendix Figure 6.13   Strain e_L versus time after impact for test LS2-21

6.3   List of Symbols

c	wave speed
c_d	dilatational wave speed
c_r	rod wave speed
c_s	shear wave speed
d	groove spacing of a diffraction grating ($d \approx 1/m$)
d_o	initial groove spacing of a diffraction grating
E	Young's modulus
e	engineering strain
e_E	Eulerian strain
e_L	Lagrangian ("engineering") strain
G	Shearing modulus = Lamé constant
i	angle between the normal to the diffraction grating plane and the incident light beam
i_o	initial angle between the normal to the diffraction grating plane and the incident light beam
$\pm k$	orders of interference of the diffracted beams observed during a test (k a positive integer)
m	number of grooves (lines) per unit length of a diffraction grating ($m = 1/d$)
m_o	initial number of grooves (lines) per unit length of a diffraction grating
n	order of interference associated with a particular diffracted beam; may have positive, negative, or zero integral values
P_o	initial compressed-gas reservoir pressure
R	rod radius
r	radial coordinate
t	time
u_r	radial displacement

V_s striker velocity just prior to impact

W_s striker mass

X grating distance from impact site

x axial coordinate

α sum of the initial diffraction angle and the angular displacement for $+k^{th}$ diffracted order

β sum of the initial diffraction angle and the angular displacement for $-k^{th}$ diffracted order

θ_n angle between the normal to the diffraction grating plane and the nth order diffracted beam

θ_{no} initial angle between the normal to the diffraction grating plane and the nth order diffracted beam

$\theta_{\pm k}$ angles between the normal to the diffraction grating plane and the $\pm k^{th}$ order diffracted beams

$\theta_{\pm ko}$ initial angles between the normal to the diffraction grating plane and the $\pm k^{th}$ order diffracted beams

λ wavelength of collimated monochromatic light incident on a diffraction grating

λ Lamé constant

μ 10^{-6}

ν Poisson's ratio

ρ density

σ engineering stress

ψ_n angular displacement of the nth order diffracted beam

$\psi_{\pm k}$ angular displacements of the $\pm k^{th}$ order diffracted beams

ω angle of rotation of the diffraction grating plane